

Aus dem Institut für Chirurgische Forschung
der Ludwig-Maximilians-Universität München

Vorstand: Prof. Dr. Markus Sperandio



**Von erhöhter Schubspannung bis hin zur Rekrutierung von Leukozyten:
Mechanistische Einsichten in die Arteriogenese**

Dissertation
zum Erwerb des Doktorgrades der Medizin
an der Medizinischen Fakultät
der Ludwig-Maximilians-Universität zu München

vorgelegt von

Manuel Lasch

aus Augsburg

2020

Mit Genehmigung der Medizinischen Fakultät
der Universität München

Berichterstatter: Priv. Doz. Dr. E. Deindl

Mitberichterstatter: Priv. Doz. Dr. C. Nußbaum

Prof. Dr. B. Heindl

Prof. Dr. G. Enders

Dekan: Prof. Dr. med. dent. Reinhard Hickel

Tag der mündlichen Prüfung: 03.12.2020

*Meiner Familie, insbesondere
meiner Hanni Oma und Sarah*

Ich erkläre hiermit an Eides statt, dass ich die vorliegende Dissertation mit dem Titel:

**„Von erhöhter Schubspannung bis hin zur Rekrutierung von Leukozyten:
Mechanistische Einsichten in die Arteriogenese“**

selbstständig verfasst, mich außer der angegebenen keiner weiteren Hilfsmittel bedient und alle Erkenntnisse, die aus dem Schrifttum ganz oder annähernd übernommen sind, als solche kenntlich gemacht und nach ihrer Herkunft unter Bezeichnung der Fundstelle einzeln nachgewiesen habe.

Ich erkläre des Weiteren, dass die hier vorgelegte Dissertation nicht in gleicher oder in ähnlicher Form bei einer anderen Stelle zur Erlangung eines akademischen Grades eingereicht wurde.

München, den 29.04.2020

Manuel Lasch

Ort, Datum

Unterschrift Doktorand

Inhaltsverzeichnis

I. Abkürzungsverzeichnis	6
II. Publikationsliste	8
III. Bestätigung der Ko-Autoren	10
IV. Einleitung.....	10
1. Arteriogenese – Allgemeines	10
2. Abgrenzung der Arteriogenese von der Angiogenese	11
3. Allgemeiner Ablauf der Arteriogenese	12
4. Leukozytenrekrutierung während der Arteriogenese.....	13
5. Von Willebrand Faktor und Plättchen-Neutrophilen-Aggregatbildung in der Arteriogenese	13
6. Initierung der Arteriogenese durch erhöhte Schubspannung.....	14
7. Mausmodell der peripheren Arteriogenese.....	15
V. Zielsetzung und Eigenanteil der Veröffentlichungen	17
1. Zielsetzung.....	17
2. Eigenanteil Veröffentlichung 1 (Perivascular mast cells govern shear stress-induced arteriogenesis by orchestrating leukocyte function).....	17
3. Eigenanteil Veröffentlichung 2 (Extracellular RNA released due to shear stress controls natural bypass growth by mediating mechanotransduction in mice).....	18
VI. Zusammenfassung.....	20
VII. Summary.....	22
VIII. Literaturverzeichnis	25
IX. Veröffentlichung 1	28
X. Veröffentlichung 2	52
XI. Danksagung	75
XII. Abbildungsverzeichnis.....	76

I. Abkürzungsverzeichnis

ATP	Adenosintriphosphat
C48/80	„compound 48/80“
DNA	„deoxyribonucleic acid“
DNase	Desoxyribonuklease
EC	„endothelial cell“
EGF	„epidermal growth factor“
eRNA	„extracellular ribonucleic acid“
FACS	„fluorescence activated cell sorting“
FAL	Femoralarterienligatur
FGF-2	„fibroblast growth factor-2“
FSS	„fluid shear stress“/Schubspannung
GM-CSF	„granulocyte-macrophage colony-stimulating factor“
GPIba	„glycoprotein I b α“
HIF-1α	„hypoxia-inducible factor-1 α“
ICAM-1	„intercellular adhesion molecule-1“
MMP	„matrix metalloproteinase“
MCP-1	„monocyte chemoattractant protein-1“
NRP-1	„neuropilin-1“
pAVK	Periphere arterielle Verschlusskrankheit
PECAM-1	„platelet endothelial cell adhesion molecule-1“
PDGFβ	„platelet derived growth factor β“
PLGF	„placental growth factor“
RNA	„ribonucleic acid“
RNase	Ribonuklease

ROS	„reactive oxygen species“
SMC	„smooth muscle cell“
TNF α	„tumor necrosis factor α “
VCAM-1	„vascular cell adhesion molecule-1“
VE-Cadherin	„vascular endothelial cell cadherin“
VEGF	„vascular endothelial growth factor“
VEGFR2	„vascular endothelial growth factor receptor 2“
vWF	von Willebrand Faktor
WPB	„Weibel-Palade Bodies“

II. Publikationsliste

Originalartikel:

Lasch, M., Caballero-Martinez, A., Kumaraswami, K., Meister, S., Ishikawa-Ankerhold, H., Deindl, E. (2020). Contribution of the potassium channels KV1.3 and KCa3.1 to smooth muscle cell proliferation in growing collateral arteries. *Cells*, 9(4), 913.

Lasch, M., Kleinert, E. C., Meister, S., Kumaraswami, K., Buchheim, J. I., Grantzow, T., Fleming, I., Randi, A. M., Sperandio, M., Preissner K. T. & Deindl, E. (2019). Extracellular RNA released due to shear stress controls natural bypass growth by mediating mechanotransduction in mice. *Blood*, 134(17), 1469-1479.

Thulasingam, S., Krishnasamy, S., Raj, C., **Lasch, M.**, Vedantham, S., & Deindl, E. (2019). Insulin Treatment Forces Arteriogenesis in Diabetes Mellitus by Upregulation of the Early Growth Response-1 (Egr-1) Pathway in Mice. *International Journal of Molecular Sciences*, 20(13), 3320.

Elsemüller, A. K., Tomalla, V., Gärtner, U., Troidl, K., Jeratsch, S., Graumann, J., Baal, N., Hackstein, H., **Lasch, M.**, Deindl, E., Preissner, K. T., & Fischer S. (2019). Characterization of mast cell-derived rRNA-containing microvesicles and their inflammatory impact on endothelial cells. *The FASEB Journal*, 33(4), 5457-5467.

Lasch, M., Nekolla, K., Klemm, A. H., Buchheim, J. I., Pohl, U., Dietzel, S., & Deindl, E. (2019). Estimating hemodynamic shear stress in murine peripheral collateral arteries by two-photon line scanning. *Molecular and Cellular Biochemistry*, 453(1-2), 41-51.

Lautz, T., **Lasch, M.**, Borgolte, J., Troidl, K., Pagel, J. I., Caballero-Martinez, A., Kleinert, E. C., Walzog, B., & Deindl, E. (2018). Midkine Controls Arteriogenesis by Regulating the Bioavailability of Vascular Endothelial Growth Factor A and the Expression of Nitric Oxide Synthase 1 and 3. *EBioMedicine*, 27, 237-246.

Chillo, O., Kleinert, E. C., Lautz, T., **Lasch, M.**, Pagel, J. I., Heun, Y., Kurz, A. R., Assmann, G., Rehberg, M., Kanse, S. M., Nieswandt, B., Walzog, B., Reichel, C. A., Mannell, H., Preissner, K. T., & Deindl, E. (2016). Perivascular mast cells govern shear stress-induced arteriogenesis by orchestrating leukocyte function. *Cell Reports*, 16(8), 2197-2207.

Lasch, M., Caballero-Martinez, A., Troidl, K., Schloegl, I., Lautz, T., & Deindl, E. (2016). Arginase inhibition attenuates arteriogenesis and interferes with M2 macrophage accumulation. *Laboratory Investigation*, 96(8), 830-838.

Kongressbeiträge:

Lasch M., Kleinert E.C., Lautz T., Caballero-Martinez A., Deindl E. (2016). Extracellular RNA Degradation as well as VEGF Receptor Inhibition Counteracts Arteriogenesis by Interfering with Mast Cell Degranulation. *13th International Conference on Innate Immunity Rhodos, Griechenland*

III. Bestätigung der Ko-Autoren

Die Bestätigungen der Ko-Autoren sind vollständig im beigefügten Promotionsantrag zu finden.

IV. Einleitung

1. Arteriogenese – Allgemeines

Kardiovaskuläre Erkrankungen, wie das akute Koronarsyndrom, die periphere arterielle Verschlusskrankheit (pAVK) und der ischämische Insult stellen seit vielen Jahren die führende Todesursache in der westlichen Welt dar. Insgesamt machte der Komplex dieser gefäßverschließenden Krankheiten im Jahre 2017 30% der Todesfälle aus [1]. Therapeutisch liegen je nach Krankheitsstadium meist invasive Methoden, wie die perkutane Intervention und Revaskularisation mittels Stents, sowie eine Operation durch Bypass-Chirurgie vor. Es ist bereits bekannt, dass der Körper die Fähigkeit besitzt, eigenständig Kollateralkreisläufe um ein verschlossenes Gefäß auszubilden. Dieser Prozess wird als Arteriogenese bezeichnet [2]. Als therapeutische Option wird diese jedoch bisher, aufgrund der unzureichend erforschten pathophysiologischen Mechanismen, kaum genutzt. Intensive Forschungsarbeiten der letzten Jahre konnten zeigen, dass während der Arteriogenese durch gesteigerten Blutfluss in bereits präexistenten Arteriolen die Schubspannung („fluid shear stress“, (FSS)) erhöht wird und im Verlauf eine lokale Inflammation auftritt [3, 4]. Hierbei handelt es sich um einen multifaktoriellen Prozess, bei dem Leukozyten, insbesondere Monozyten, rekrutiert werden, die anschließend eine Vielzahl von Zytokinen bereitstellen, welche die Proliferation von Endothelzellen („endothelial cells“, (ECs)) und glatten Gefäßmuskelzellen („smooth muscle cells“, (SMCs)) stimulieren [5]. Die Erforschung des Prozesses der Arteriogenese kann somit wichtige Angriffspunkte zur alternativen Therapie von Gefäßverschlüssen gegenüber interventionellen Verfahren, welche häufig bei multi-morbid Patienten schwer einsetzbar sind, liefern.

2. Abgrenzung der Arteriogenese von der Angiogenese

Der akute oder chronische Verschluss eines arteriellen Gefäßes, meist ausgelöst durch Arteriosklerose [6], stellt neben Prozessen der Wundheilung [7] und des Tumorwachstums [8] die Voraussetzung für den Prozess einer Kapillarsprossung (Angiogenese) oder des Wachstums bereits bestehender Kollateralkreisläufe (Arteriogenese) dar. Das Gewebegebiet stromabwärts/distal eines verschlossenen Gefäßes wird nicht mehr ausreichend mit Sauerstoff und Nährstoffen versorgt, wodurch eine Ischämie in jenem distalen Areal provoziert wird. Diese Ischämie initiiert die Gefäß- und Kapillar-Neubildung, welche als Angiogenese bezeichnet wird [9]. Der Prozess der Angiogenese ist abhängig von erhöhten Mengen des Transkriptionsfaktor „hypoxia-inducible factor-1 α“ (HIF-1 α) [10] sowie von VEGF, den „vascular endothelial growth factor“, welcher dabei vermehrt von Leukozyten freigesetzt wird [11] (Abbildung 1A). Die VEGF-Familie unterteilt sich in unterschiedliche Wachstumsfaktoren: VEGFA, VEGFB, VEGFC, VEGFD, VEGFE und „placental growth factor“ (PLGF) [12].

Die Arteriogenese hingegen ist Hypoxie-unabhängig und nicht assoziiert mit HIF-1α oder einer erhöhten lokalen Expression von VEGF [13, 14]. Im Bereich der bereits vorhandenen Kollateralarterien entsteht keine Sauerstoffunterversorgung, jedoch erhöht sich durch den arteriellen Verschluss der Blutfluss signifikant innerhalb der Kollateralen, was zu einer erhöhten Schubspannung führt. Im Verlauf bewirkt dies ein Wachstum der Kollateralen, die sogenannte Arteriogenese [4] (Abbildung 1B). Es ist beschrieben, dass der Prozess der Aktivierung und Initiierung der Arteriogenese durch erhöhten FSS ausgelöst wird [15], welche Mechanismen hierbei jedoch ablaufen ist bisher nicht bekannt und war Thema dieser Forschungsarbeit.

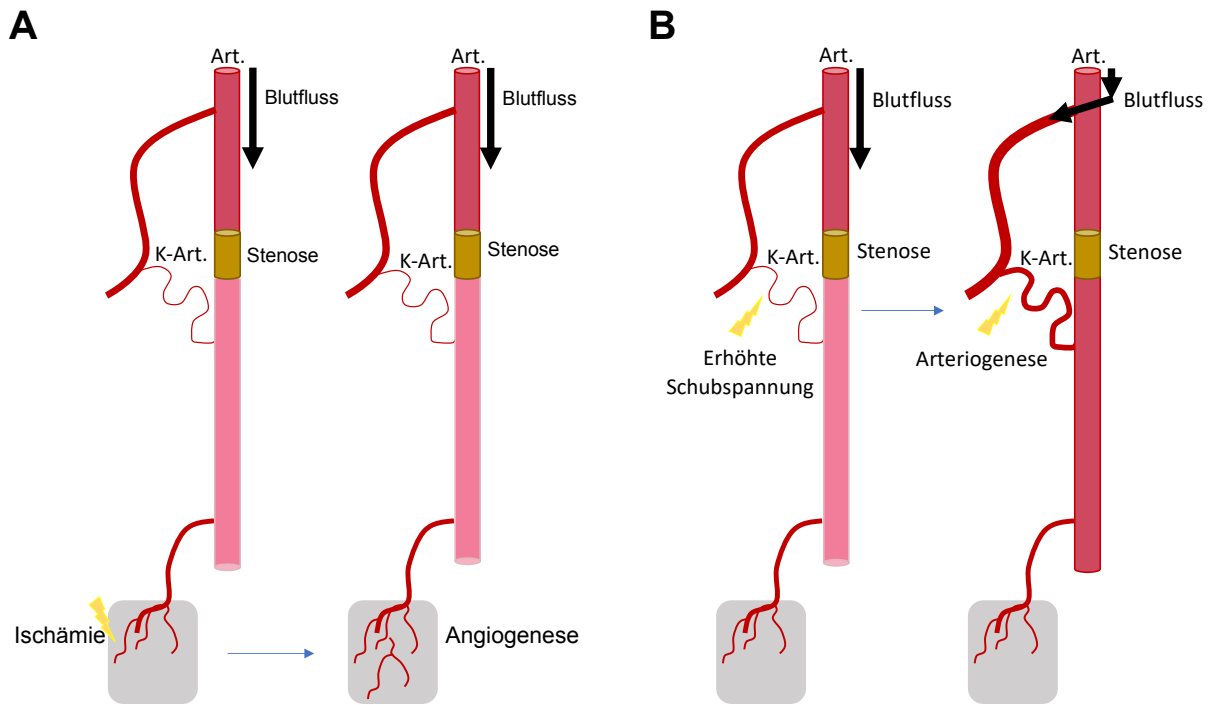


Abbildung 1: Angiogenese und Arteriogenese

(A) Nach Verschluss einer blutführenden Arterie (Art.) kommt es aufgrund der, distal des Verschlusses entstehenden, Ischämie zur Kapillarsprossung (Angiogenese). (B) Durch die Stenosierung eines arteriellen Gefäßes (Art.) entsteht in präexistenten Kollateralkreisläufen (K-Art.) eine erhöhte Schubspannung, welche das Wachstum dieser präexistenten Kollateralen, die sogenannte Arteriogenese, stimuliert.

3. Allgemeiner Ablauf der Arteriogenese

Die Arteriogenese kann in 4 Phasen gegliedert werden: die initiale Phase (0-24 Stunden nach Verschluss des arteriellen Gefäßes), die proliferative Phase (2-7 Tage nach Gefäßverschluss), die synthetische Phase (8-14 Tage nach Verschluss) und die Reifungsphase (15-21 Tage nach Gefäßverschluss) [16, 17]. Die hier vorliegende Arbeit konzentriert sich vor allem auf die initiale Phase, in welcher die Endothelzellen zur Expression von Adhäsionsmolekülen wie „intercellular adhesion molecule-1“ (ICAM-1) und „vascular cell adhesion molecule-1“ (VCAM-1) stimuliert werden und Leukozyten adhärieren, sowie auf die proliferative Phase. In dieser Phase weisen Endothelzellen und glatte Gefäßmuskelzellen eine maximale mitotische Aktivität auf. Hierbei spielt Synectin, das mit „neuropilin-1“ (NRP-1) interagiert, eine wichtige Rolle [18, 19]. Als Modulator des „vascular endothelial growth factor receptor 2“ (VEGFR2) Singaltransduktionswegs nimmt NRP-1, als VEGFR2-Co-Rezeptor, einen hohen Stellenwert in der Aktivierung des VEGFR2 und somit bei der Arteriogenese ein [20].

Die letzte Phase der Arteriogenese ist durch eine erhöhte proteolytische Aktivität der Leukozyten, sowie eine geringere Migrationsrate gekennzeichnet [16].

4. Leukozytenrekrutierung während der Arteriogenese

Bereits in früheren Studien konnte gezeigt werden, dass die Arteriogenese als inflammatorischer Prozess stark von der Rekrutierung und Aktivierung von Leukozyten, insbesondere Monozyten, abhängig ist [21]. Nach Extravasation in das sogenannte perivaskuläre Gewebe präexistenter Kollateralen und Differenzierung von Monozyten zu Makrophagen liefern diese wichtige Zytokine wie „monocyte chemoattractant protein-1“ (MCP-1) oder Wachstumsfaktoren wie „fibroblast growth factor-2“ (FGF-2) und „matrix-metalloproteinases“ (MMPs) [5, 22]. Als weitere Immunzellpopulation im perivaskulären Bereich präexistenter Kollateralen wurden Mastzellen beschrieben [23], welche ebenfalls vasoaktive Wachstumsfaktoren wie VEGF, FGF-2, „platelet derived growth factor β“ (PDGFβ), „epidermal growth factor“ (EGF), Interleukine, „granulocyte-macrophage colony-stimulating factor“ (GM-CSF), „tumor necrosis factor α“ (TNFα) oder MMPs freisetzen können [24, 25].

Es ist bereits bekannt, dass einige dieser Substanzen am arteriellen Gefäßumbau/Gefäßwachstum beteiligt sind [26, 27]. Dass Mastzellen und auch neutrophile Granulozyten eine mögliche Funktion während der Arteriogenese ausüben und wichtig für eine Rekrutierung von Monozyten sind, wurde bereits 2010 vermutet [28], jedoch nie *in vivo* untersucht und war Bestandteil dieser Forschungsarbeit.

5. Von Willebrand Faktor und Plättchen-Neutrophilen-Aggregatbildung in der Arteriogenese

Von Willebrand Faktor (vWF) ist ein multimerisches Glykoprotein, welches im Blutplasma, in der subendothelialen Matrix oder in Speicherorganellen in Endothelzellen („Weibel-Palade-Bodies“, WPB) und Plättchen (Alpha-Granula) vorkommt [29]. Es wird konstitutiv in den Blutkreislauf freigesetzt, kann jedoch auch in Endothelzellen gespeichert werden und zügig aus WPB nach Stimulation freigesetzt werden [30]. vWF vermittelt die Adhäsion von Plättchen und agiert als Transportprotein für Faktor VIII [31]. vWF spielt somit eine essentielle Rolle während der Blutgerinnung und ist unter anderem in die Ausbildung von akuten koronaren Thrombosen involviert

[32]. Bei Patienten mit bereits präexistenten kardiovaskulären Erkrankungen kann er als klinischer Marker für das Risiko eines akuten Koronarsyndroms dienen [32]. Des Weiteren spielt vWF eine wichtige Rolle bei der Regulation inflammatorischer Prozesse durch die Modulation der Adhäsion von Leukozyten [33, 34] und stellt einen der Hauptliganden des „glycoprotein Iba“- (GPIb α)-Rezeptors, einem Oberflächenrezeptor auf Plättchen, dar. Eine durch diesen Rezeptor vermittelte Aktivierung der Plättchen und damit verbundene Wechselwirkung von Plättchen mit dem Kollateralendothel, sowie Plättchen-Neutrophilen-Aggregatbildung und die Extravasation von Leukozyten während der Arteriogenese konnte bereits gezeigt werden [35]. Eine mögliche Relevanz von vWF selbst im Rahmen der Arteriogenese war jedoch bislang noch nicht erforscht worden und sollte im Rahmen der hier vorliegenden Arbeit ebenfalls untersucht werden.

6. Initiierung der Arteriogenese durch erhöhte Schubspannung

Eine Aktivierung der Endothelzellen durch erhöhten FSS stellt die Initiierung der Arteriogenese dar [15, 21]. Es gibt bereits Ergebnisse aus *in vitro*-Studien, die einen komplexen Ablauf des Prozesses beschreiben. Hierbei ist ein mechanosensorischer Komplex identifiziert worden, der aus dem „platelet endothelial cell adhesion molecule“ (PECAM-1), dem „vascular endothelial cell cadherin“ (VE-Cadherin) und dem VEGFR2 besteht. Diese *in vitro* generierten Ergebnisse wurden bereits in Aorten von Mäusen an Stellen mit gestörtem Blutfluss und daraus resultierender Leukozytenrekrutierung und Atherosklerose bestätigt [36]. Der Mechanismus der Mechanoperzeption von Endothelzellen während der Arteriogenese ist jedoch noch unzureichend erforscht und untersucht [37]. Andere Forschungsarbeiten haben zeigen können, dass Endothelzellen als Antwort auf eine erhöhte Schubspannung Adenosintriphosphat (ATP) freisetzen können, welches die Gq- und G11-Proteingekoppelten Purinorezeptoren (P2Y2) aktiviert, welche wiederum für eine Thyrosinphosphorylierung von PECAM-1 wichtig sind [38]. Anschließend wird durch die Komplexbildung von PECAM-1 mit VE-Cadherin der VEGFR2 rekrutiert. Obwohl eine direkte Blockierung des VEGFR2 oder eine Applikation von Antikörpern gegen VEGFA, den Liganden von VEGFR2, die Arteriogenese stark beeinträchtigt, wird der Prozess durch eine zusätzliche Applikation von VEGFA nur geringfügig bis gar nicht gefördert [14]. Eine Stimulation des VEGFR2-Signalwegs ist somit für die regelhafte

Initiierung der Arteriogenese nötig und wird durch den nontyrosinkinase Co-Rezeptor NRP-1 vermittelt [19]. Dieser ist in der Lage, die VEGFA165 Isoform des VEGFA zu binden und somit die lokale Plasmakonzentration und damit die Bindung von VEGFA an VEGFR2 zu fördern [39-41]. Über die NRP-1 gekoppelte Aktivierung von VEGFR2 gibt es bereits Hinweise aus *in vitro* Daten, dass hierbei Heparin sowie „extracellular ribonucleic acid“ (eRNA) eine wichtige Rolle spielen [42]. RNA selbst ist ein Ribonukleotid, das aus vier unterschiedlichen Nucleosidmonophosphaten aufgebaut ist und meist in Einzelstrangform vorliegt, im Gegensatz zu in Doppelstrangform vorliegender „deoxyribonucleic acid“ (DNA) [43]. Dass RNA, welche unter anderem durch Tumorzellen oder im Rahmen einer Gewebeschädigung freigesetzt werden kann [44], keine chemische Reaktivität aufweist, jedoch verschiedene biologische Reaktionen stimulieren kann, wurde bereits von Fischer et al. postuliert [45]. Ein durch eRNA vermittelter Effekt auf das angeborene Immunsystem und ein Zusammenhang mit der Bildung von Thrombosen wurde bereits mehrfach beschrieben [44]. Konkret konnte der Einfluss von eRNA auf die Adhäsion und Transmigration von Leukozyten aus den Gefäßen in einem *in vivo*-Mausmodell am M. cremaster gezeigt werden [46]. Der Einfluss von eRNA auf den Prozess der Arteriogenese war zu Beginn meiner Arbeit weitgehend unbekannt. Ziel meiner Forschungsarbeit war zu analysieren, ob und, wenn ja, inwiefern eRNA einen Einfluss auf die Vermittlung des mechanischen Reizes, der erhöhten Schubspannung, bezüglich der Immunzellrekrutierung und -aktivierung, welche die essentielle Grundlage für den Ablauf der Arteriogenese darstellt, hat.

7. Mausmodell der peripheren Arteriogenese

Um das Wachstum von Kollateralen zu untersuchen wird das Modell nach Limbourg et al. am häufigsten verwendet [47]. Hierbei wird insbesondere die Ähnlichkeit von muriner und humaner arterieller Versorgung des Beins genutzt. Die A. femoralis stellt die hauptsächlich versorgende Arterie der unteren Extremität dar. Distal des Leistenbands geht die A. epigastrica caudalis und die A. profunda femoris ab. Die bereits präexistenten Kollateralen zwischen A. profunda femoris und A. femoralis werden innerhalb dieses Modells untersucht. Sie verlaufen parallel zu Fasern der Adduktorenmuskulatur des Oberschenkels. Auf der rechten Hinterlaufseite erfolgt direkt distal des Abgangs der A. profunda femoris die Unterbindung der A. femoralis

(FAL) mit Hilfe einer chirurgischen Gefäßligatur. Zur Kontrolle wird auf der linken Seite eine Scheinoperation ohne Ligatur durchgeführt, um einen möglichen Einfluss des Fremdmaterials, sowie des operativen Eingriffs als solchen auszuschließen. Der Erfolg der Operation wird mittels Laser-Doppler-Imaging (LDI) unmittelbar postoperativ verifiziert. Hierbei wird die Durchblutung der Pfoten gemessen, welche direkt nach Ligatur stark eingeschränkt ist. Zur besseren Vergleichbarkeit der Ergebnisse zwischen den verschiedenen Mäusen wird das Verhältnis der Durchblutung des ligierten Hinterlaufs zur schein-operierten Gegenseite bestimmt. Zur detaillierteren Analyse der Arteriogenese wurden neben der LDI Methode weitere histologische und molekularbiologische Analysen nach erfolgter Gewebeentnahme zu definierten Zeitpunkten durchgeführt.

V. Zielsetzung und Eigenanteil der Veröffentlichungen

1. Zielsetzung

Die vorliegende Arbeit konzentriert sich insbesondere auf den Mechanismus der Initiierung der Arteriogenese. Im Detail soll analysiert werden, wie eine erhöhte Schubspannung innerhalb der Kollateralarterien zur Rekrutierung und Aktivierung von Leukozyten und Mastzellen führt, welche essentiell für eine Proliferation von Endothelzellen und glatten Gefäßmuskelzellen ist.

2. Eigenanteil Veröffentlichung 1 (Perivascular mast cells govern shear stress-induced arteriogenesis by orchestrating leukocyte function)

Mein Anteil an dieser Originalarbeit bestand in der Erforschung der Rolle neutrophiler Granulozyten im Rahmen der Arteriogenese und die damit verbundene Aktivierung/Degranulation von perivaskulären Mastzellen *in vivo*.

Hierbei wurde oben beschriebenes Mausmodell genutzt wobei die unilaterale Ligatur der A. femoralis durchgeführt wurde und anschließend die distale Durchblutung der Hinterbeine mit der LDI Methode zu unterschiedlichen Zeitpunkten (vor Ligatur, nach Ligatur, Tag 3, Tag 7) gemessen wurde. Dies geschah in mehreren Mausgruppen mit unterschiedlichen Behandlungen. Um die allgemeine Beteiligung neutrophiler Granulozyten während der Arteriogenese zu untersuchen, wurden die Tiere mit dem Ziel der Depletion der neutrophilen Granulozyten mit einem Anti-Ly6G-Antikörper (1A8) intraperitoneal behandelt. Dabei zeigte sich an Tag 3 und Tag 7 eine signifikant schlechtere Durchblutung der Hinterbeine nach Depletion der neutrophilen Granulozyten. Zur detaillierteren Analyse der Auswirkung der 1A8-Antikörperbehandlung wurde an Tag 1 nach Ligatur die Degranulation/Aktivierung von perivaskulären Mastzellen untersucht, bei deren Auswertung ich ebenfalls beteiligt war. Da hierbei eine verringerte Mastzelldegranulation nach Behandlung mit dem Antikörper 1A8 festgestellt werden konnte, wurde weiterführend analysiert ob durch eine erhöhte Stimulation der Mastzellen zur Degranulation mittels „compound 48/80“ (C48/80), einem selektiven Mastzellaktivator, der Effekt der Neutrophilendepletion aufgehoben werden konnte. Hierfür wurde eine zweite Mausgruppe mit 1A8 und

C48/80 in Kombination behandelt und erneut die Durchblutung der Hinterbeine mittels LDI Methode gemessen.

Weiterführend bestand meine Aufgabe für diese Veröffentlichung darin, mehrere Abbildungen für die Publikation zu erstellen und den Revision-Prozess zu unterstützen.

3. Eigenanteil Veröffentlichung 2 (Extracellular RNA released due to shear stress controls natural bypass growth by mediating mechanotransduction in mice)

Der an dieser Forschungsarbeit geleistete Eigenanteil bestand insbesondere in der Erforschung, wie der gesteigerte mechanische Reiz, die erhöhte intravaskuläre Schubspannung, in biologische Signaltransduktionskaskaden umgesetzt wird und dies zur Aktivierung des Gefäßendothels mit nachfolgender Mastzellaktivierung und Leukozytenrekrutierung führt.

Für die *in vivo* durchgeführten Versuche wurde erneut das Mausmodell der peripheren Arteriogenese verwendet. Nach unterschiedlicher Behandlung der Mäuse u.a. mit Semaxanib (VEGFR2-Blocker) oder RNase A/humaner aktiver RNase1 (Degradierung der eRNA) wurde zunächst der Effekt der Behandlung zu unterschiedlichen Zeitpunkten durch die Analyse der peripheren Durchblutung mittels LDI-Methode gemessen. Zur weiteren Evaluation des Behandlungseffekts wurde 7 Tage nach FAL über eine Immunfluoreszenz-BrdU-Färbung die Proliferation der ECs und SMCs untersucht und mittels Giemsa-Färbung der Gefäßdurchmesser berechnet. Zusätzlich wurde ebenfalls 7 Tage nach FAL die Anzahl der rekrutierten, perivaskulären Makrophagen mittels Immunfluoreszenzfärbung analysiert und quantifiziert.

Des Weiteren wurde die Aktivierung/Degranulation perivaskulärer Mastzellen zu verschiedenen Zeitpunkten mittels Giemsa-Färbung untersucht. Darüber hinaus wurden FACS-Analysen des Vollbluts der Mäuse 24 h nach FAL im Hinblick auf die Bildung von Plättchen-Neutrophilen-Aggregaten durchgeführt. Mittels Immunfluoreszenzfärbungen gelang der Nachweis von freigesetztem vWF auf dem Gefäßendothel 2 h nach Ligatur der Femoralarterie. Zuletzt wurde bereits 30 min nach FAL Immunfluoreszenzfärbungen zur Darstellung von aktiv sezernierter eRNA im Bereich der Kollateralarterien angefertigt.

Die Niederschrift von Teilen des Manuskripts, des Material- und Methodenteils, sowie die Anfertigung aller Abbildungen und die Durchführung des Revisionsprozesses gehörte ebenfalls zu meinem Aufgabenbereich.

VI. Zusammenfassung

Im Bereich kardiovaskulärer Erkrankungen, wie der koronaren Herzkrankheit oder der peripheren arteriellen Verschlusskrankheit, bestehen aktuell fast ausschließlich interventionelle Therapiemöglichkeiten wie die perkutane transluminale (Coronar)-Angioplastie oder die Bypasschirurgie. Dabei besitzt der menschliche Organismus die Fähigkeit ein stenosiertes oder verschlossenes Blutgefäß durch einen mehrstufigen Prozess des Wachstums von präexistenten Kollateralarterien zu kompensieren.

Die Extravasation von Leukozyten in das sogenannte perivaskuläre Gewebe sowie die Proliferation von Endothelzellen und glatten Gefäßmuskelzellen stellen wichtige Schritte während des, als Arteriogenese bezeichneten, Prozesses dar.

In dieser Arbeit konnte *in vivo* gezeigt werden, dass extrazelluläre RNA nach Verschluss eines arteriellen Gefäßes als Folge einer erhöhten Schubspannung in den Kollateralgefäßeln aktiv freigesetzt wird. Zusätzlich konnte *in vitro* gezeigt werden, dass eRNA von Schubspannung-ausgesetzten Endothelzellen aktiv freigesetzt worden ist. Die freigesetzte eRNA ist essentiell für eine verstärkte VEGFA vermittelte Aktivierung des VEGFR2/NRP-1-Rezeptorkomplexes. Eine Aktivierung dieses Rezeptorkomplexes resultiert in einer aktiven Freisetzung von vWF aus den WPB nach intraluminal, welcher mittels Immunfluoreszenzfärbung in der frühen Phase der Arteriogenese (2 h nach Ligatur) nachgewiesen werden konnte (siehe dazu auch die Graphik in Abbildung 2). Da vWF einen Hauptligand des GPIba Plättchenrezeptors darstellt [35], kommt es nach Freisetzung des vWF zu einer Aktivierung der Plättchen und einer Ausbildung von Plättchen-Neutrophilen-Aggregaten (24 h nach Ligatur), welche mittels FACS Analyse nachgewiesen werden konnten. Weiter konnte gezeigt werden, dass die Ausbildung dieser Komplexe essentiell für eine Aktivierung und Extravasation der neutrophilen Granulozyten ist. Nach Extravasation der neutrophilen Granulozyten aktivieren diese mittels „reactive oxygen species“ (ROS) die perivaskulären Mastzellen, welche degranulieren und über die Sezernierung von Zytokinen und Wachstumsfaktoren weitere Immunzellen wie Monozyten rekrutieren und das Wachstum der ECs und SMCs stimulieren (Abbildung 3). Eine Blockade/Inhibition dieser, zuvor nur in Teilen oder gar nicht bekannten, erstmalig zusammengefügten Abläufe an unterschiedlichen Stellen wie z.B. VEGFR2/eRNA mittels RNase A/VEGFR2-Blocker, neutrophile Granulozyten mittels Depletion durch

1A8, Mastzellen mittels Cromolyn oder die Verwendung von vWF-defizienten Mäusen führte jeweils zu einer signifikanten Verschlechterung der Arteriogenese.

Anhand dieser Ergebnisse kann zusammengefasst geschlussfolgert werden, dass eRNA, welche durch einen erhöhten FSS aktiv aus ECs freigesetzt wird, einen maßgeblichen Faktor in der Vermittlung der Mechanotransduktion darstellt und die entscheidende inflammatorische Reaktion initiiert, welche anschließend die Arteriogenese stimuliert. Dieses neu gewonnene Wissen könnte in Zukunft dafür verwendet werden, neue medikamentöse Angriffspunkte zur Behandlung von stenosierenden Herz-Kreislauf-Erkrankungen zu etablieren. Von diesen konservativen Therapiealternativen würden vor allem multimorbide Patienten, welche für eine interventionelle Therapie nicht mehr in Frage kommen, profitieren, wodurch ein entscheidender Beitrag zur Reduktion der Mortalität kardiovaskulärer Erkrankungen geleistet werden könnte.

VII. Summary

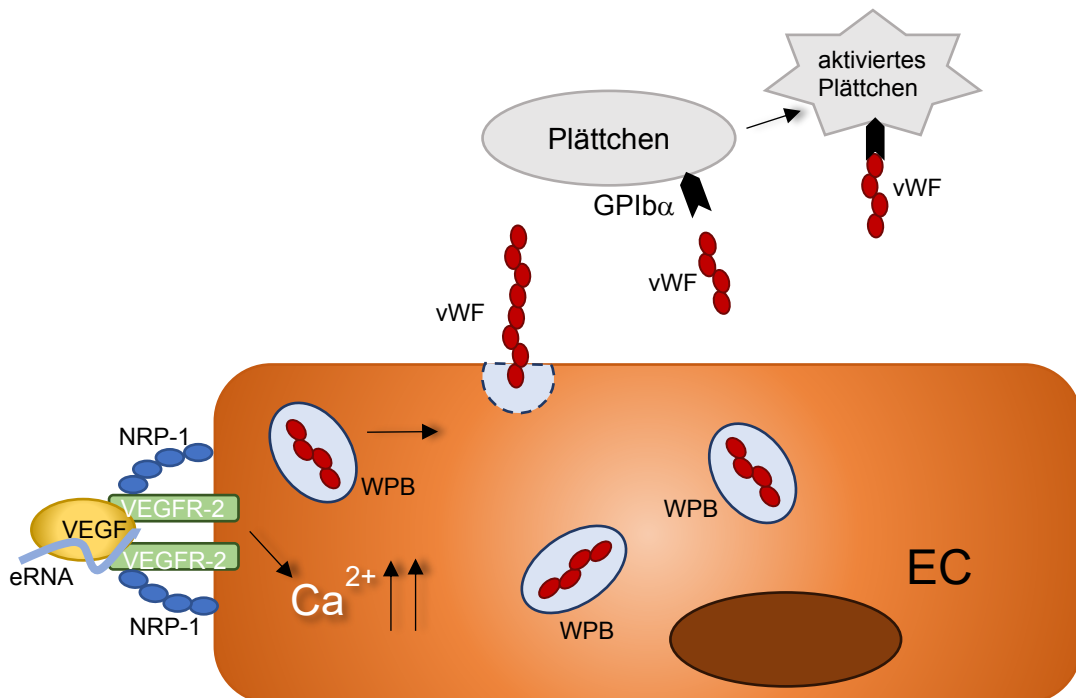
In case of cardiovascular diseases, such as myocardial infarction or peripheral artery disease, there are almost exclusively interventional therapy options such as percutaneous transluminal (coronary) angioplasty or bypass surgery. Interestingly, the human organism has the ability to compensate a stenosed or closed artery through a multi-step growth process of preexisting collateral arteries, called arteriogenesis.

The extravasation of leukocytes in the perivascular space as well as the proliferation of endothelial cells and smooth muscle cells represent important steps in this process. In this project I have shown by means of *in vivo* analyses that extracellular RNA is actively released after the occlusion of an arterial vessel as a result of an increased FSS in the preexisting collateral arteries. In addition, it was shown *in vitro* that eRNA is actively released from shear stress-exposed endothelial cells. The released eRNA is essential for an enhanced activation of the VEGFR2/NRP-1 receptor complex by VEGFA. The activation of this receptor complex results in an active release of vWF from WPB, which was demonstrated by immunofluorescence staining of tissue samples isolated at an early phase of arteriogenesis (2 h after ligation, see also the graphic of Figure 2). vWF is a major ligand of the GPIba platelet receptor [35]. Accordingly, platelets were activated by released vWF and platelet-neutrophil aggregates were formed as shown by FACS analyses (24 h after induction of arteriogenesis by femoral artery ligation). Furthermore, it was shown that the formation of these aggregates is essential for the activation and extravasation of neutrophil granulocytes. After extravasation, these neutrophils activate the perivascular mast cells by producing and releasing reactive oxygen species (ROS). Mast cells in turn degranulate and recruit additional immune cells such as monocytes via the secretion of cytokines and growth factors, and stimulate the growth of ECs and SMCs (Figure 3). A blockade/inhibition of individual steps of these processes (previously only partially or not at all known) e.g. VEGFR2/eRNA using RNase A/VEGFR2 blocker, neutrophils using 1A8, mast cells using cromolyn or the use of vWF-deficient mice resulted always in a significant deterioration of arteriogenesis.

Based on these results, it can be concluded that eRNA, which is actively released from ECs by an increased FSS, is a decisive factor in mediating mechanotransduction and initiates the relevant inflammatory reaction, which subsequently stimulates

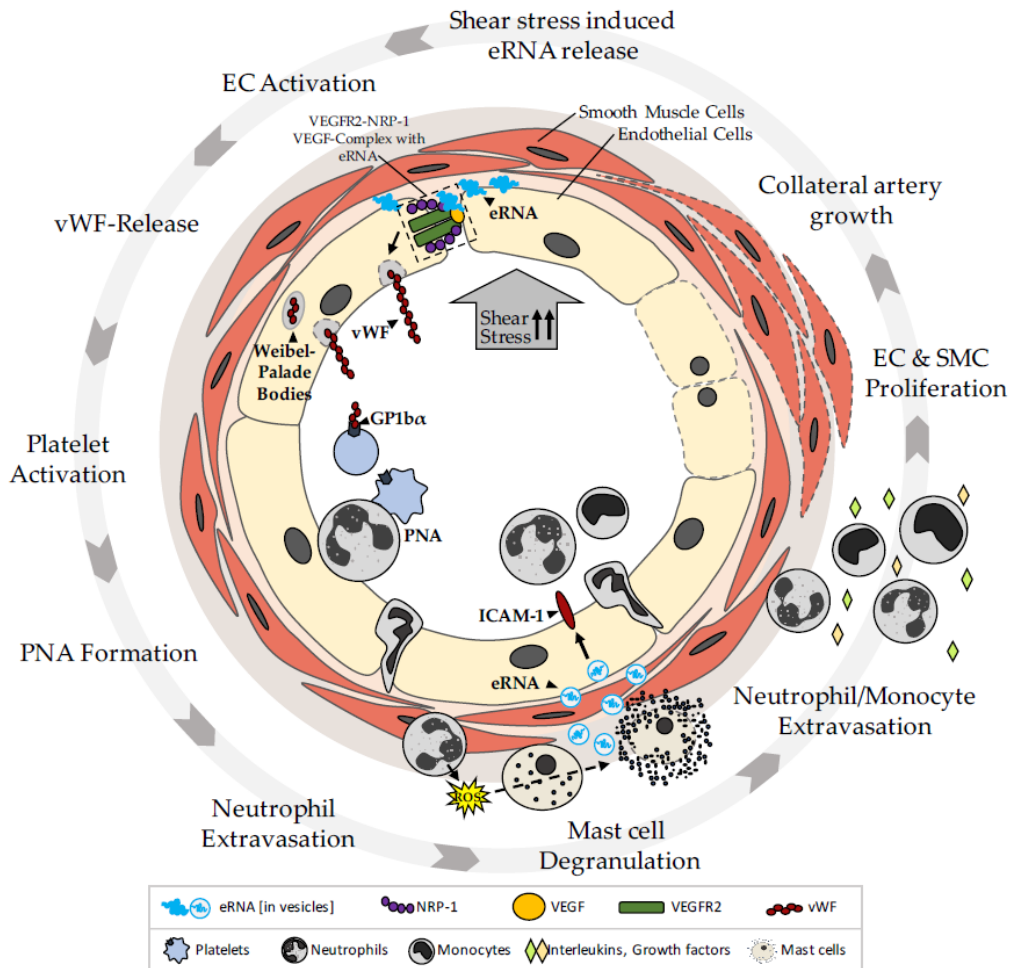
arteriogenesis. This newly acquired knowledge may be useful to identify prospective drug targets for the treatment of cardiovascular diseases in the future.

Particularly multimorbid patients, incapable of undergoing interventional therapy, would benefit from new conservative therapy options, which ultimately, could make a decisive contribution to reducing the mortality of cardiovascular diseases.



Abbildung/Figure 2: Freisetzung von vWF

Nach Aktivierung des „vascular endothelial growth factor receptor 2“ / „neuropilin-1“ (VEGFR2/NRP-1) Rezeptorkomplexes auf „endothelial cells“ (ECs) durch „vascular endothelial growth factor“ (VEGF) und „extracellular ribonucleic acid“ (eRNA) kommt es zu einer Kalziumionenerhöhung (Ca^{2+}) intrazellulär, welche eine aktive Exozytose der „Weibel-Palade Bodies“ (WPB) triggert, worauf der darin enthaltene von Willebrand Faktor (vWF) nach intraluminal freigesetzt wird. Der freigesetzte vWF aktiviert anschließend unter Bindung an den „glycoprotein Ib α “- (GPIb α)-Rezeptor die Plättchen.



**Abbildung/Figure 3 (aus Kluever et al. [48]):
Der Kreislauf der Arteriogenese**

Nach Stenosierung einer blutversorgenden Arterie erhöht sich der „fluid shear stress“ (FSS) in präexistenten Kollateralarterien. Daraufhin folgt eine aktive Freisetzung von „extracellular ribonucleic acid“ (eRNA), welche zusammen mit „vascular endothelial growth factor“ (VEGF) den Rezeptorkomplex aus „vascular endothelial growth factor receptor 2“ (VEGFR2) und „neuropilin-1“ (NRP-1) aktiviert. Die Rezeptoraktivierung resultiert in ein Freisetzen von von Willebrand Faktor (vWF) aus „Weibel-Palade Bodies“ (WBP), welcher zur Aktivierung der Plättchen führt und die Bildung von „platelet-neutrophil aggregates“ (PNA) triggert. Die PNA sind essentiell für perivaskuläre Mastzellaktivierung und die daraufhin folgende Rekrutierung von Leukozyten. Die rekrutierten Leukozyten fördern über Zytokine die „endothelial cell“ (EC)- und „smooth muscle cell“ (SMC)-Proliferation, bis die Kollateralarterien eine ausreichende Größe erreicht haben und die distale Durchblutung normalisiert wurde.

VIII. Literaturverzeichnis

1. Roth, G.A., et al., *Global, regional, and national age-sex-specific mortality for 282 causes of death in 195 countries and territories, 1980–2017: a systematic analysis for the Global Burden of Disease Study 2017*. The Lancet, 2018. **392**(10159): p. 1736-1788.
2. Carmeliet, P., et al., *Abnormal blood vessel development and lethality in embryos lacking a single VEGF allele*. Nature, 1996. **380**(6573): p. 435-439.
3. Deindl, E. and W. Schaper, *The art of arteriogenesis*. Cell biochemistry and biophysics, 2005. **43**(1): p. 1-15.
4. Pipp, F., et al., *Elevated fluid shear stress enhances postocclusive collateral artery growth and gene expression in the pig hind limb*. Arteriosclerosis, thrombosis, and vascular biology, 2004. **24**(9): p. 1664-1668.
5. Arras, M., et al., *Monocyte activation in angiogenesis and collateral growth in the rabbit hindlimb*. The Journal of clinical investigation, 1998. **101**(1): p. 40-50.
6. Gisterå, A. and G.K. Hansson, *The immunology of atherosclerosis*. Nature Reviews Nephrology, 2017. **13**(6): p. 368.
7. Tonnesen, M.G., et al., *Angiogenesis in wound healing*. Journal of Investigative Dermatology Symposium Proceedings. 2000. **5**(1): p.40-46.
8. Folkman, J., *Angiogenesis in cancer, vascular, rheumatoid and other disease*. Nature medicine, 1995. **1**(1): p. 27-30.
9. Risau, W., *Mechanisms of angiogenesis*. Nature, 1997. **386**(6626): p. 671-674.
10. Semenza, G.L., et al., *Transcriptional regulation of genes encoding glycolytic enzymes by hypoxia-inducible factor 1*. Journal of biological chemistry, 1994. **269**(38): p. 23757-23763.
11. Scapini, P., et al., *CXCL1/macrophage inflammatory protein-2-induced angiogenesis in vivo is mediated by neutrophil-derived vascular endothelial growth factor-A*. The Journal of Immunology, 2004. **172**(8): p. 5034-5040.
12. Plate, K.H., et al., *Vascular endothelial growth factor and glioma angiogenesis: coordinate induction of VEGF receptors, distribution of VEGF protein and possible in vivo regulatory mechanisms*. International journal of cancer, 1994. **59**(4): p. 520-529.
13. Deindl, E., et al., *Role of ischemia and of hypoxia-inducible genes in arteriogenesis after femoral artery occlusion in the rabbit*. Circulation research, 2001. **89**(9): p. 779-786.
14. Lautz, T., et al., *Midkine Controls Arteriogenesis by Regulating the Bioavailability of Vascular Endothelial Growth Factor A and the Expression of Nitric Oxide Synthase 1 and 3*. EBioMedicine, 2018. **27**: p. 237-246.
15. Lasch, M., et al., *Estimating hemodynamic shear stress in murine peripheral collateral arteries by two-photon line scanning*. Mol Cell Biochem, 2019. **453**(1-2): p. 41-51.
16. Scholz, D., et al., *Ultrastructure and molecular histology of rabbit hind-limb collateral artery growth (arteriogenesis)*. Virchows Archiv, 2000. **436**(3): p. 257-270.
17. Ito, W.D., et al., *Angiogenesis but not collateral growth is associated with ischemia after femoral artery occlusion*. American Journal of Physiology-Heart and Circulatory Physiology, 1997. **273**(3): p. H1255-H1265.

18. Cai, H. and R.R. Reed, *Cloning and characterization of neuropilin-1-interacting protein: a PSD-95/Dlg/ZO-1 domain-containing protein that interacts with the cytoplasmic domain of neuropilin-1*. Journal of Neuroscience, 1999. **19**(15): p. 6519-6527.
19. Lanahan, A., et al., *The neuropilin 1 cytoplasmic domain is required for VEGF-A-dependent arteriogenesis*. Developmental cell, 2013. **25**(2): p. 156-168.
20. Kofler, N.M. and M. Simons, *Angiogenesis versus arteriogenesis: neuropilin 1 modulation of VEGF signaling*. F1000prime reports, 2015. **7**.
21. Heil, M., et al., *Blood monocyte concentration is critical for enhancement of collateral artery growth*. American Journal of Physiology-Heart and Circulatory Physiology, 2002. **283**(6): p. H2411-H2419.
22. Deindl, E., et al., *Involvement of the fibroblast growth factor system in adaptive and chemokine-induced arteriogenesis*. Circulation research, 2003. **92**(5): p. 561-568.
23. Wolf, C., et al., *Vascular remodeling and altered protein expression during growth of coronary collateral arteries*. Journal of molecular and cellular cardiology, 1998. **30**(11): p. 2291-2305.
24. Hiromatsu, Y. and S. Toda, *Mast cells and angiogenesis*. Microscopy research and technique, 2003. **60**(1): p. 64-69.
25. Rao, K.N. and M.A. Brown, *Mast cells: multifaceted immune cells with diverse roles in health and disease*. Annals of the New York Academy of Sciences, 2008. **1143**(1): p. 83-104.
26. Ito, W.D., et al., *Monocyte chemotactic protein-1 increases collateral and peripheral conductance after femoral artery occlusion*. Circulation research, 1997. **80**(6): p. 829-837.
27. Cao, R., et al., *Angiogenic synergism, vascular stability and improvement of hind-limb ischemia by a combination of PDGF-BB and FGF-2*. Nature medicine, 2003. **9**(5): p. 604-613.
28. Meisner, J.K. and R.J. Price, *Spatial and temporal coordination of bone marrow-derived cell activity during arteriogenesis: regulation of the endogenous response and therapeutic implications*. Microcirculation, 2010. **17**(8): p. 583-599.
29. Lenting, P.J., et al., *von Willebrand factor biosynthesis, secretion, and clearance: connecting the far ends*. Blood, The Journal of the American Society of Hematology, 2015. **125**(13): p. 2019-2028.
30. Sporn, L.A., et al., *Inducible secretion of large, biologically potent von Willebrand factor multimers*. Cell, 1986. **46**(2): p. 185-190.
31. Huang, J., et al., *Integrin av β 3 on human endothelial cells binds von Willebrand factor strings under fluid shear stress*. Blood, The Journal of the American Society of Hematology, 2009. **113**(7): p. 1589-1597.
32. Spiel, A.O., et al., *von Willebrand factor in cardiovascular disease: focus on acute coronary syndromes*. Circulation, 2008. **117**(11): p. 1449-1459.
33. Denis, C.V., et al., *Defect in regulated secretion of P-selectin affects leukocyte recruitment in von Willebrand factor-deficient mice*. Proceedings of the National Academy of Sciences, 2001. **98**(7): p. 4072-4077.
34. Pendu, R., et al., *P-selectin glycoprotein ligand 1 and β 2-integrins cooperate in the adhesion of leukocytes to von Willebrand factor*. Blood, 2006. **108**(12): p. 3746-3752.
35. Chandraratne, S., et al., *Critical role of platelet glycoprotein iba in arterial remodeling*. Arteriosclerosis, thrombosis, and vascular biology, 2015. **35**(3): p. 589-597.

36. Tzima, E., et al., *A mechanosensory complex that mediates the endothelial cell response to fluid shear stress*. Nature, 2005. **437**(7057): p. 426-431.
37. Givens, C. and E. Tzima, *Endothelial mechanosignaling: does one sensor fit all?* Antioxidants & redox signaling, 2016. **25**(7): p. 373-388.
38. Wang, S., et al., *P2Y 2 and G q/G 11 control blood pressure by mediating endothelial mechanotransduction*. The Journal of clinical investigation, 2015. **125**(8): p. 3077-3086.
39. Koch, S., *Neuropilin signalling in angiogenesis*. Biochemical Society Transactions, 2012. **40**(1): p. 20-25
40. Koch, S., et al., *Signal transduction by vascular endothelial growth factor receptors*. Biochemical journal, 2011. **437**(2): p. 169-183.
41. Sorkin, A. and M. Von Zastrow, *Endocytosis and signalling: intertwining molecular networks*. Nature reviews Molecular cell biology, 2009. **10**(9): p. 609-622.
42. Fischer, S., et al., *Signaling mechanism of extracellular RNA in endothelial cells*. The FASEB Journal, 2009. **23**(7): p. 2100-2109.
43. Portin, P., *The birth and development of the DNA theory of inheritance: sixty years since the discovery of the structure of DNA*. Journal of genetics, 2014. **93**(1): p. 293-302.
44. Fischer, S. and K. Preissner, *Extracellular nucleic acids as novel alarm signals in the vascular system*. Hämostaseologie, 2013. **33**(01): p. 37-42.
45. García-Olmo, D.C. and R. Ruiz-Piqueras, *Circulating nucleic acids in plasma and serum (CNAPS) and its relation to stem cells and cancer metastasis: state of the issue*. Histology and histopathology, 2004. **19**(2): p. 575-583.
46. Fischer, S., et al., *Extracellular RNA promotes leukocyte recruitment in the vascular system by mobilising proinflammatory cytokines*. Thrombosis and haemostasis, 2012. **108**(10): p. 730-741.
47. Limbourg, A., et al., *Evaluation of postnatal arteriogenesis and angiogenesis in a mouse model of hind-limb ischemia*. Nature protocols, 2009. **4**(12): p. 1737-1746.
48. Kluever, A.-K., et al., *The Extraordinary Role of Extracellular RNA in Arteriogenesis, the Growth of Collateral Arteries*. International Journal of Molecular Sciences, 2019. **20**(24): p. 6177.

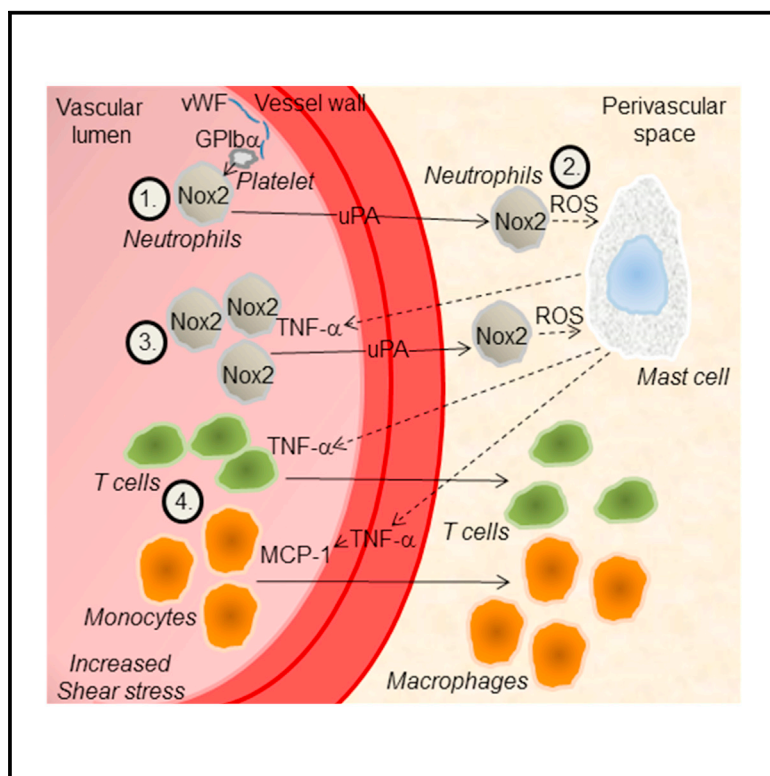
IX. Veröffentlichung 1

Chillo, O., Kleinert, E. C., Lautz, T., **Lasch, M.**, Pagel, J. I., Heun, Y., Kurz, A. R., Assmann, G., Rehberg, M., Kanse, S. M., Nieswandt, B., Walzog, B., Reichel, C. A., Mannell, H., Preissner, K. T., & Deindl, E. (2016). Perivascular mast cells govern shear stress-induced arteriogenesis by orchestrating leukocyte function. *Cell Reports*, 16(8), 2197-2207.

<https://doi.org/10.1016/j.celrep.2016.07.040>

Perivascular Mast Cells Govern Shear Stress-Induced Arteriogenesis by Orchestrating Leukocyte Function

Graphical Abstract



Authors

Omary Chillo, Eike Christian Kleinert,
Thomas Lautz, ..., Hanna Mannell,
Klaus T. Preissner, Elisabeth Deindl

Correspondence

elisabeth.deindl@med.uni-muenchen.de

In Brief

Increased fluid shear stress is the triggering force for the growth of natural bypasses. How this mechanical load is translated into collateral artery growth is an enigma. Chillo et al. find that mast cell activation governs arteriogenesis by orchestrating leukocyte function.

Highlights

- Arteriogenesis is mediated by coordinated action of innate immune cells
- Mast cells orchestrate leukocyte function in arteriogenesis
- Platelet GPIba is decisive for shear stress-provoked mast cell activation
- Shear stress-induced mast cell activation is mediated by neutrophil-derived ROS

Perivascular Mast Cells Govern Shear Stress-Induced Arteriogenesis by Orchestrating Leukocyte Function

Omary Chillo,¹ Eike Christian Kleinert,¹ Thomas Lautz,¹ Manuel Lasch,¹ Judith-Irina Pagel,^{1,2} Yvonn Heun,¹ Kerstin Troidl,³ Silvia Fischer,⁴ Amelia Caballero-Martinez,¹ Annika Mauer,^{1,4} Angela R.M. Kurz,¹ Gerald Assmann,⁵ Markus Rehberg,⁶ Sandip M. Kanse,⁷ Bernhard Nieswandt,⁸ Barbara Walzog,¹ Christoph A. Reichel,^{1,9} Hanna Mannell,¹ Klaus T. Preissner,⁴ and Elisabeth Deindl^{1,10,*}

¹Walter-Brendel-Centre of Experimental Medicine, Ludwig-Maximilians-Universität (LMU) Munich, 81377 Munich, Germany

²Hospital of the University of Munich, Department of Anesthesiology, LMU Munich, 81377 Munich, Germany

³Division of Arteriogenesis Research, Max Planck Institute for Heart and Lung Research, 61231 Bad Nauheim, Germany

⁴Institute for Biochemistry, Medical School, Justus-Liebig-Universität, 35392 Giessen, Germany

⁵Institute of Pathology, LMU Munich, 81377 Munich, Germany

⁶Institute for Stroke and Dementia Research, LMU Munich, 81377 Munich, Germany

⁷Institute of Basic Medical Sciences, University of Oslo, 0372 Oslo, Norway

⁸Institute of Experimental Biomedicine, University Hospital and Rudolf Virchow Center, University of Würzburg, 97080 Würzburg, Germany

⁹Hospital of the University of Munich, Department of Otorhinolaryngology, Head and Neck Surgery, LMU Munich, 81377 Munich, Germany

¹⁰Lead Contact

*Correspondence: elisabeth.deindl@med.uni-muenchen.de

<http://dx.doi.org/10.1016/j.celrep.2016.07.040>

SUMMARY

The body has the capacity to compensate for an occluded artery by creating a natural bypass upon increased fluid shear stress. How this mechanical force is translated into collateral artery growth (arteriogenesis) is unresolved. We show that extravasation of neutrophils mediated by the platelet receptor GPIb α and uPA results in Nox2-derived reactive oxygen radicals, which activate perivascular mast cells. These c-kit $^+$ /CXCR-4 $^+$ cells stimulate arteriogenesis by recruiting additional neutrophils as well as growth-promoting monocytes and T cells. Additionally, mast cells may directly contribute to vascular remodeling and vascular cell proliferation through increased MMP activity and by supplying growth-promoting factors. Boosting mast cell recruitment and activation effectively promotes arteriogenesis, thereby protecting tissue from severe ischemic damage. We thus find that perivascular mast cells are central regulators of shear stress-induced arteriogenesis by orchestrating leukocyte function and growth factor/cytokine release, thus providing a therapeutic target for treatment of vascular occlusive diseases.

INTRODUCTION

Arteries transport oxygenated blood from the heart to every individual organ of the body. Accordingly, occlusion of a major

artery by thrombus formation or stenosis results in substantially reduced perfusion of distal organs, leading to ischemic damage or even necrosis of the affected tissue. Current options to treat vascular occlusive diseases such as myocardial infarction, stroke, or peripheral artery disease are percutaneous transluminal angioplasty (PTA) or bypass surgery. However, the body can create natural bypasses from pre-existing arteriolar anastomoses. This so-called arteriogenesis constitutes a tissue and even life-saving process, as it can compensate for the loss of a major peripheral or coronary artery. Promoting arteriogenesis in ischemia-related diseases may present a non-invasive alternative therapeutic approach to established clinical interventions.

Arteriogenesis is a complex, multi-factorial process (Deindl and Schaper, 2005) that involves the proliferation of endothelial cells (ECs) and smooth muscle cells (SMCs) as well as the recruitment of leukocytes, especially monocytes, which provide a variety of growth-promoting factors to the growing blood vessel (Arras et al., 1998). It is, therefore, not surprising that the therapeutic use of single growth factors or cytokines to support arteriogenesis did not meet expectations in clinical studies. To effectively promote arteriogenesis in patients, it is important to identify the molecular mechanisms naturally triggering the process of collateral artery growth.

Mast cells reside in the perivascular space of arteries (Wolf et al., 1998) and produce several vasoactive substances and growth factors (Hiromatsu and Toda, 2003; Rao and Brown, 2008), some of which have been described to contribute to arterial remodeling (Cao et al., 2003; Ito et al., 1997). The functional role of these c-kit $^+$ /CXCR4 $^+$ cells in arteriogenesis is currently unclear. Moreover, how fluid shear stress, which is the driving force for arteriogenesis (Pipp et al., 2004) and is sensed directly by vascular ECs, is translated into the activation of perivascular mast cells remains unresolved. Here we dissect the underlying



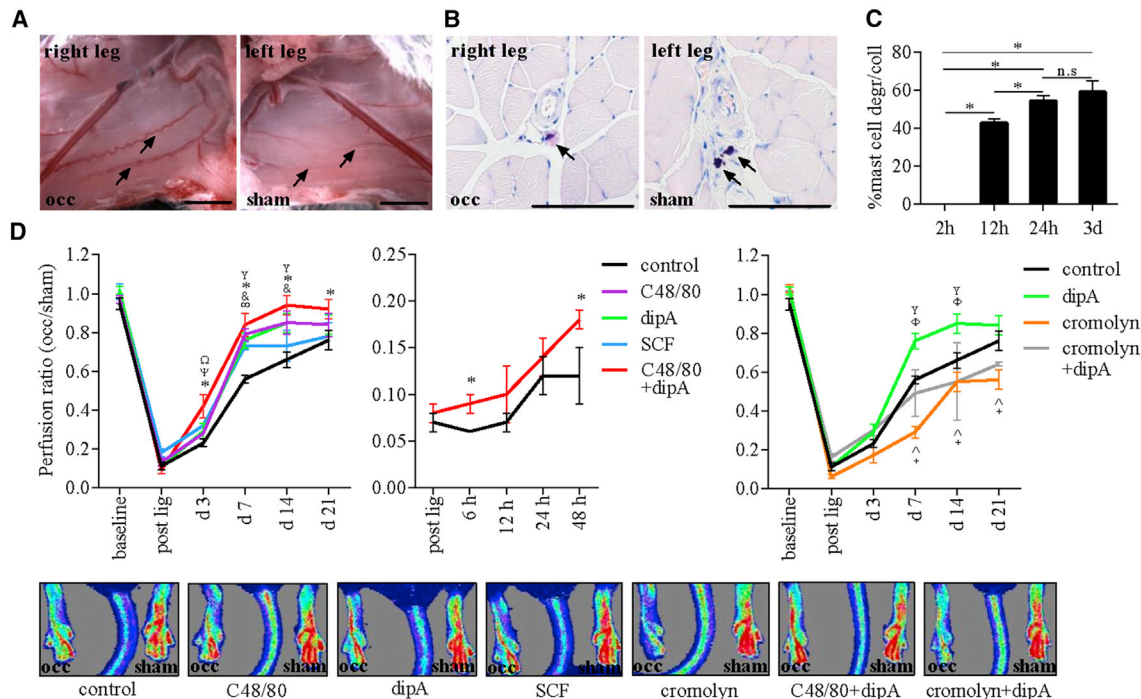


Figure 1. Collateral Artery Growth Is Fostered by Activated Mast Cells

(A) Photographs of superficial collateral arteries (arrows) in the medial adductor hindlimb region of a mouse. Right: pre-existing collaterals on the left sham-operated leg are observed as thin vessels running in straight line. Left: grown collateral arteries of the occluded right leg (occ) have drastically increased in diameter and appear in a typical corkscrew formation. Pictures were taken 21 days after the surgical procedure. Scale bar, 1 mm; n = 3.

(B) Representative Giemsa staining reveals mast cell degranulation next to growing collaterals (arrow left), whereas sham operation had no effect on mast cells (arrows right). Pictures were taken 3 days after the surgical procedure. Scale bar, 100 μm; n = 6.

(C) Mast cell degranulation is shown per collateral 2 hr, 12 hr, 24 hr, and 3 days after fal (n = 4 animals with four collaterals/time point; *p ≤ 0.05 from two-way ANOVA with Newman-Keuls test).

(D) Laser Doppler perfusion measurements of wild-type mice following fal (right leg) and sham operation (left leg). Upper panels: perfusion was calculated by means of laser Doppler right-to-left ratios before, immediately after, and at 6, 12, 24, and 48 hr (middle panel) or at days 3, 7, 14, and 21 after the surgical procedure (right and left panels). Color-coded lines indicate treatment of mice (control = saline). Control and internal control (dipA) of the right plot are identical to that of the left plot. Statistical analysis (p ≤ 0.05) was performed between different groups (n = 6 per group) using repeated-measures two-way ANOVA with subsequent multiple comparisons by Bonferroni test (^aC48/80 versus control; ^bdipA versus control; ^cSCF versus control; ^dC48/80 + dipA versus control; ^eC48/80 + dipA versus dipA; ^fC48/80 + dipA versus C48/80; ^gcromolyn versus control; ^hcromolyn versus dipA; and ⁱcromolyn + dipA versus dipA). Lower panels: representative flow images of day 7 are shown.

Data are means ± SEM. See also Figure S1.

mechanisms, finding a decisive role for platelets and neutrophils in this process. In particular we find that platelet receptor GPIbα-dependent and urokinase plasminogen activator (uPA)-mediated extravasation of neutrophils culminates in mast cell activation by reactive oxygen species (ROS) produced by neutrophil-expressed Nox2. Furthermore, following natural or pharmacological activation, we find that mast cells promote arteriogenesis by creating an inflammatory microenvironment essential for the recruitment of growth-promoting leukocytes. Thus, mast cells might represent a therapeutic target for the treatment of vascular occlusive diseases.

RESULTS

Mast Cell Activation Fosters Experimental Arteriogenesis

To study the functional impact of mast cells in arteriogenesis, we used an experimental murine hindlimb model in which

femoral artery ligation (fal) resulted in collateral artery growth in the upper leg (Figure 1A) (Limbourg et al., 2009). Our results showed that, upon fal, mast cells located in the perivascular space of collaterals became activated and gradually but specifically degranulated (Figures 1B and 1C). Moreover, treatment of mice with the mast cell activator Compound 48/80 (C48/80); the c-kit ligand stem cell factor (SCF), which triggers mast cell maturation and recruitment (Oliveira and Lukacs, 2003); or diprotin A (dipA) (for protocols, see Figure 7 and *Supplemental Experimental Procedures*), respectively, significantly enhanced perfusion recovery upon fal (Figure 1D). DipA treatment, inhibiting dipeptidylpeptidase IV (DPPIV) activity and, thereby, retarding stroma cell-derived factor-1 (SDF-1 α) degradation (Zaruba et al., 2009), resulted in an increased level of SDF-1 α (Figure S1A) and drastically increased the number of c-kit $^+$ cells (Figure S1B). In accordance with previous findings (McGowen et al., 2009), C48/80 treatment provoked enhanced mast cell degranulation, culminating in a

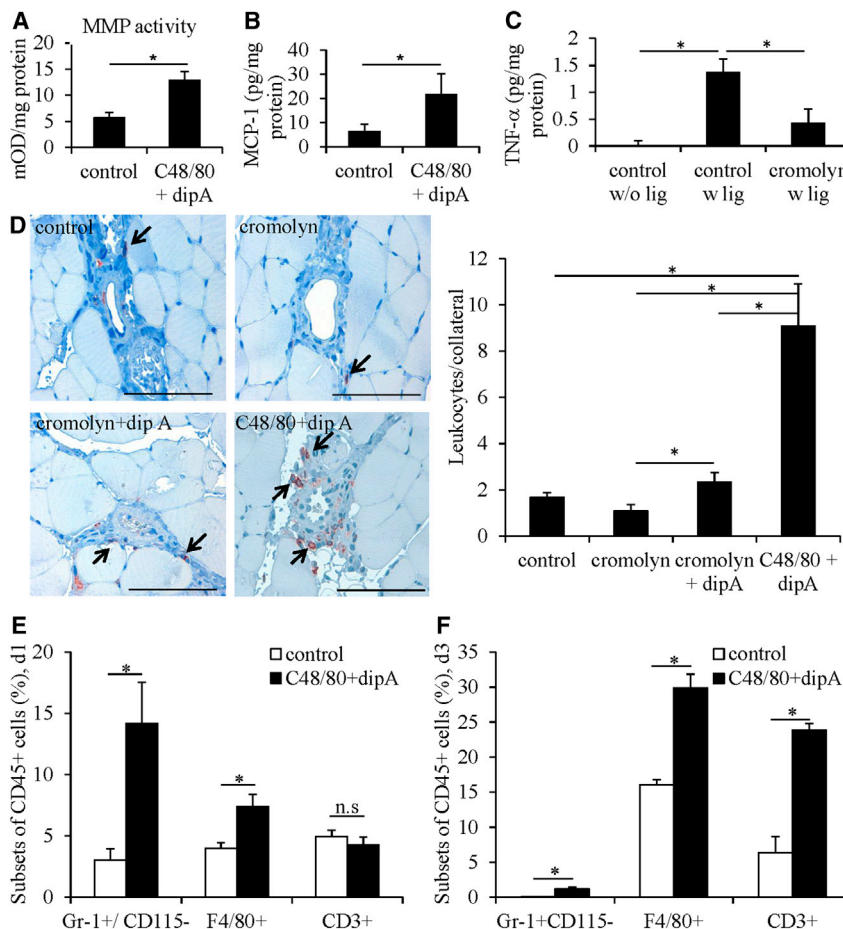


Figure 2. C48/80 + DipA Treatment Fosters Leukocyte Recruitment

(A) Proteolytic activity of matrix metalloproteinases (MMPs) was measured in collaterals of mice 24 hr after fal and saline (control) or C48/80 + dipA treatment ($n = 3$).

(B) MCP-1 protein levels were measured in collaterals of mice treated with saline (control) or C48/80 + dipA 24 hr after fal ($n = 3$).

(C) TNF- α levels were measured in plasma of mice without fal (control w/o lig) or 24 hr after fal and saline (control w lig) or cromolyn treatment (cromolyn w lig) ($n = 3$ per group).

(D) Left: representative immunostaining showing CD45-positive cells (arrows) in the perivascular region of collaterals of saline- (control), cromolyn-, cromolyn + dipA-, and C48/80 + dipA-treated animals 3 days after fal. Right: quantitative analysis is shown. Scale bars, 100 μ m; $n = 4$ animals with four collaterals each.

(E and F) Quantitative analyses by flow cytometry of CD45 $^+$ /CD11b $^+$ /Gr-1 $^+$ /CD115 $^-$, CD45 $^+$ /CD11b $^+$ /F4/80 $^+$, and CD45 $^+$ /CD3 $^+$ cells in adductor muscles of mice at day 1 (E) and day 3 (F) after fal and saline (control, open bars) or C48/80 + dipA (filled bars) treatment ($n = 6$ per group; * $p \leq 0.05$ in (C) and (D) from two-way ANOVA with Newman-Keuls test).

Data are means \pm SEM. See also Figures S2 and S3.

drastic reduction in the numbers of detectable mast cells in the vicinity of collateral arteries ($93\% \pm 4.6\%$ reduction, $p < 0.05$). Combined administration of C48/80 and dipA further increased perfusion recovery, reaching significant values already 6 hr after fal (Figure 1D), whereas combined treatment of mice with C48/80, dipA, and SCF showed no further additive effect (Figure S1C).

Simultaneous treatment of mice with dipA and the mast cell stabilizer cromolyn was performed to exclude the possibility that the positive effect of dipA was not mainly due to the mobilization of other bone marrow-derived cells also expressing the SDF-1 α receptor CXCR-4 (e.g., monocytes and stem cells). Cromolyn treatment abolished the stimulating effect of dipA and impaired perfusion recovery (Figure 1D) to a similar extent as observed with single cromolyn treatment (Figure 1D), indicating that the majority of recruited cells were indeed mast cells that promoted arteriogenesis by their degranulation products. Cromolyn treatment also blocked the positive effect of C48/80 (Figure S1D).

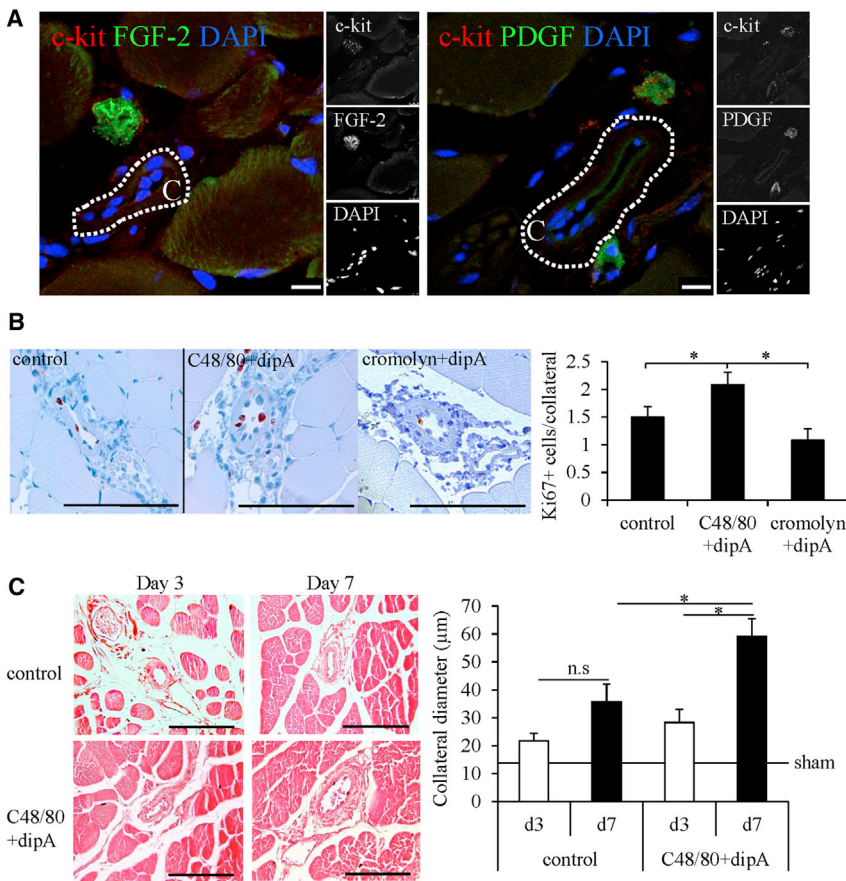
Mast cell-deficient Mcpt5-Cre $^+$ R-DTA mice showed no reduced perfusion recovery upon the induction of arteriogenesis. Intriguingly, these mice responded neither to cromolyn nor to C48/80 treatment (Figure S1E). These data indicate that these transgenic mice were capable of compensating the lack of

mast cells in arteriogenesis; yet, cromolyn as well as C48/80, specifically influenced the action of mast cells or, if at all, did not influence decisively other cells or off targets relevant for the process of collateral artery growth in wild-type mice.

Combined Treatment of Mice with C48/80 and DipA Promotes Leukocyte Recruitment and Vascular Cell Proliferation

Matrix metalloproteinases (MMPs), which are well described to be activated by mast cell-derived proteases (Kovanen, 2007), degrade and remove basement membrane proteins around SMCs (Rudijanto, 2007) and have been shown to promote vascular remodeling in the context of arteriogenesis (Cai et al., 2000). In growing collaterals of mice treated with C48/80 + dipA, we found significantly increased MMP activity compared to saline-treated controls (Figure 2A).

MCP-1 and tumor necrosis factor α (TNF- α) are two cytokines previously reported to be of major relevance for leukocyte recruitment in the process of arteriogenesis (Grundmann et al., 2005; Ito et al., 1997). Here mice treated with C48/80 + dipA showed significantly increased mRNA and protein levels of MCP-1 compared to saline-treated controls (Figures 2B and S2). In contrast, cromolyn treatment strongly reduced the plasma level of TNF- α as compared to saline-treated controls (Figure 2C), indicating that mast cells play a major role in providing this cytokine being relevant for leukocyte recruitment (Malaviya et al., 1996).



Immunohistological analyses of the adductor muscle revealed significantly increased numbers of CD45⁺ (pan leukocyte marker) cells in the perivascular space of C48/80 + dipA-treated mice (Figure 2D). Subset analyses of recruited CD45⁺ cells by flow cytometry showed significantly increased levels of neutrophils (Gr-1⁺/CD115⁻) and macrophages (F4/80⁺) at day 1 after fal (Figures 2E and S3A) and neutrophils, macrophages, and T cells (CD3⁺) at day 3 after fal (Figures 2F and S3B). The latter represents a subset of leukocytes previously described to invade tissue in a TNF- α -dependent manner (Maggi et al., 2013) and to be involved in arteriogenesis (Stabile et al., 2006). Regarding the recruitment of subsets of CD45⁺ cells at day 1 and day 3 after fal, a similar although less drastic effect was observed in mice treated with C48/80 alone (Figures S3C and S3D).

Treatment of primary vascular ECs and SMCs with conditioned medium of activated mast cells increased their proliferation rate (Figure S4). Moreover, fibroblast growth factor (FGF)-2 and platelet-derived growth factor (PDGF)-BB was found in mast cells located in close proximity to collateral arteries (Figure 3A). A combined administration of both growth factors previously has been described to enhance arteriogenesis (Cao et al., 2003). Mice treated with combined C48/80 + dipA revealed an increased number of Ki67⁺ (cell proliferation marker) vascular cells in collateral arteries (Figure 3B), which was associated with an increased luminal diameter of these

Figure 3. Mast Cells Promote Vascular Cell Proliferation and Vessel Growth

(A) Representative fluorescent immunohistological pictures of collaterals of mice 2 hr after fal. c-kit⁺ cells in close proximity to collaterals (marked by dotted lines) stain positive for FGF-2 and PDGF-BB. Scale bar, 10 μ m; n = 6 slices from three individual experiments.

(B) Left: representative immunostaining showing Ki67⁺ cells (stained in brown) in collaterals of mice treated with saline (control), C48/80 + dipA, or cromolyn + dipA 3 days after fal. Right: quantitative analysis is shown. Scale bar, 100 μ m; n = 3 animals with four collaterals each.

(C) Left: representative HE staining documenting collaterals of mice treated with saline (control) or C48/80 + dipA at day 3 or 7 after fal. Right: chart shows inside luminal diameter of collaterals of mice treated with saline (control) or C48/80 + dipA at day 3 and 7 after fal or sham operation.

Scale bar, 100 μ m; n = 3 animals with three collaterals each; *p \leq 0.05 (B and C) from two-way ANOVA with Newman-Keuls test. Data are means \pm SEM. See also Figure S4.

blood vessels (Figure 3C). In contrast, combined treatment with cromolyn + dipA reduced the number of Ki67⁺ vascular cells (Figure 3B). Altogether these data suggest that mast cells promote vascular cell proliferation, not only indirectly by promoting leukocyte recruitment supplying growth-promoting factors

but also by themselves representing a source of vascular growth factors.

Boosting Mast Cell Recruitment and Activation Protects Tissue from Damage by Fostering Arteriogenesis

Upon ligation of the femoral artery in the upper leg, the resulting reduced perfusion of the lower leg was associated with ischemic damage, provoking increased infiltration of leukocytes and capillary sprouting (angiogenesis). Both processes are necessary for removing fibrotic and necrotic tissue. Since our data demonstrate that combined treatment of mice with C48/80 + dipA significantly increased perfusion recovery already 6 hr after fal (Figure 1D), we hypothesized that this is associated with reduced damage of the distal calf muscle (Figure S5). Histological analysis of the gastrocnemius muscle revealed almost negligible ischemic tissue damage in mice treated with C48/80 + dipA (Figure 4A). This was associated with (1) a significantly reduced infiltration of leukocytes (CD45⁺ cells) (Figure 4B) as well as (2) a diminished capillary sprouting, as shown by the reduced number of Ki67⁺ ECs (Figure 4C) and a reduced capillary-to-muscle fiber ratio (Figure S6). Interestingly, neither fal nor local application of C48/80 in the upper leg resulted in mast cell degranulation in the ipsilateral lower leg (M. gastrocnemius) (Figure 4D) or in the contralateral upper or lower leg (data not shown). These data indicate that local application of C48/80 in the upper leg did not result in systemic effects of the agent. Additionally, the

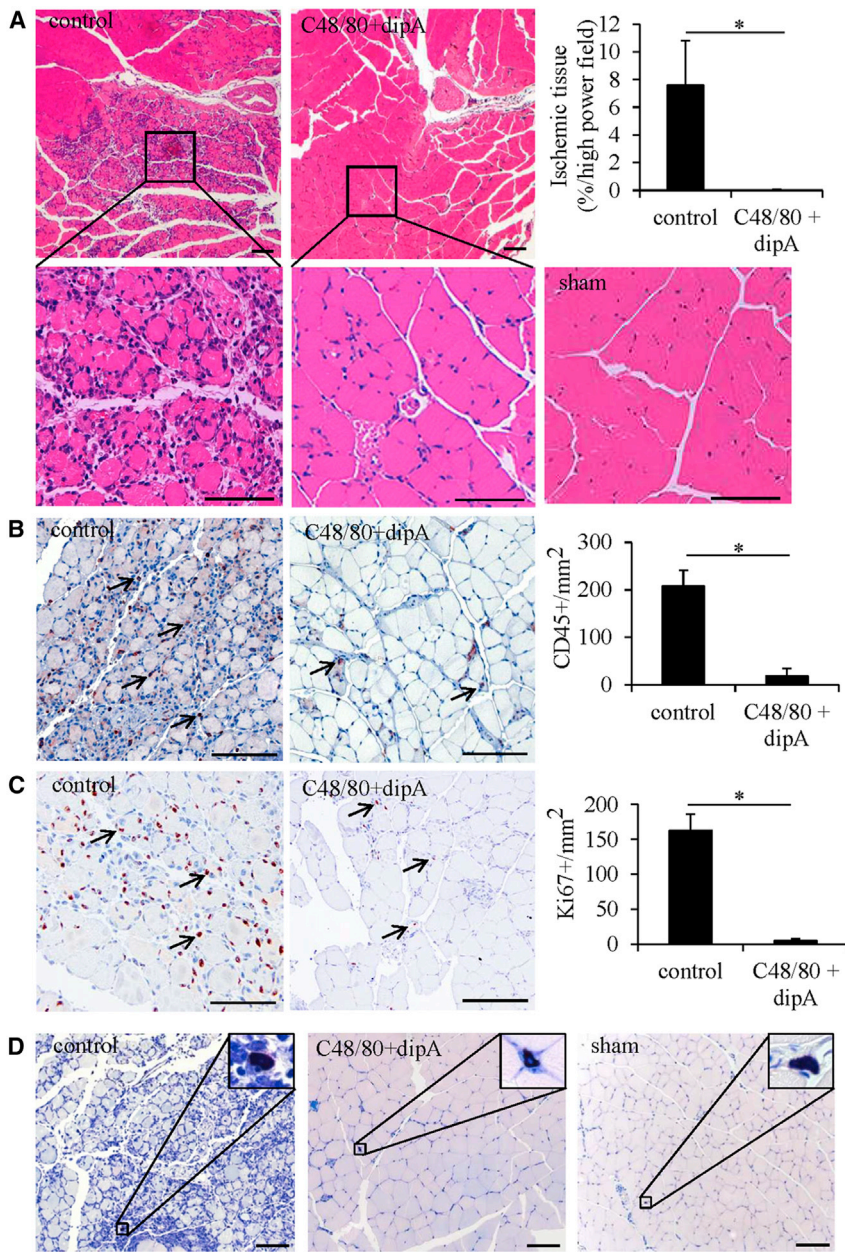


Figure 4. Effective Arteriogenesis Protects Tissue from Severe Ischemic Damage

(A) Representative HE staining of gastrocnemius muscles 3 days after fal (control) or sham operation or 3 days after fal and C48/80 + dipA treatment in different magnifications. Scale bar, 100 μ m. Bar graph represents ischemic tissue in the M. gastrocnemius in percentage of high-power field.

(B) Left: representative pictures of immunostaining show reduced infiltration of leukocytes (CD45⁺ cells, arrows, stained in brown) in the M. gastrocnemius of mice treated with C48/80 + dipA compared to saline- (control) treated mice 3 days after fal. Scale bar, 100 μ m. Right: quantitative analysis is shown.

(C) Left: following fal, representative pictures document Ki67-positive capillaries (arrows, stained in brown) in the M. gastrocnemius of saline- (control) or C48/80-treated mice 3 days after fal. Scale bar, 100 μ m. Right: number of Ki67-positive capillaries was quantified.

(D) Representative Giemsa staining of the M. gastrocnemius of mice treated with saline (control) or C48/80 + dipA 3 days after fal or sham operation. Insets show magnifications of mast cells.

Scale bar, 100 μ m; n = 3 in triplicates (A–D). Data are means \pm SEM. See also Figures S5 and S6.

receptor (Sadler, 2002), we hypothesized that platelets or platelet-dependent reactions may be involved in transmitting molecular signals from the vascular lumen to the perivascular space.

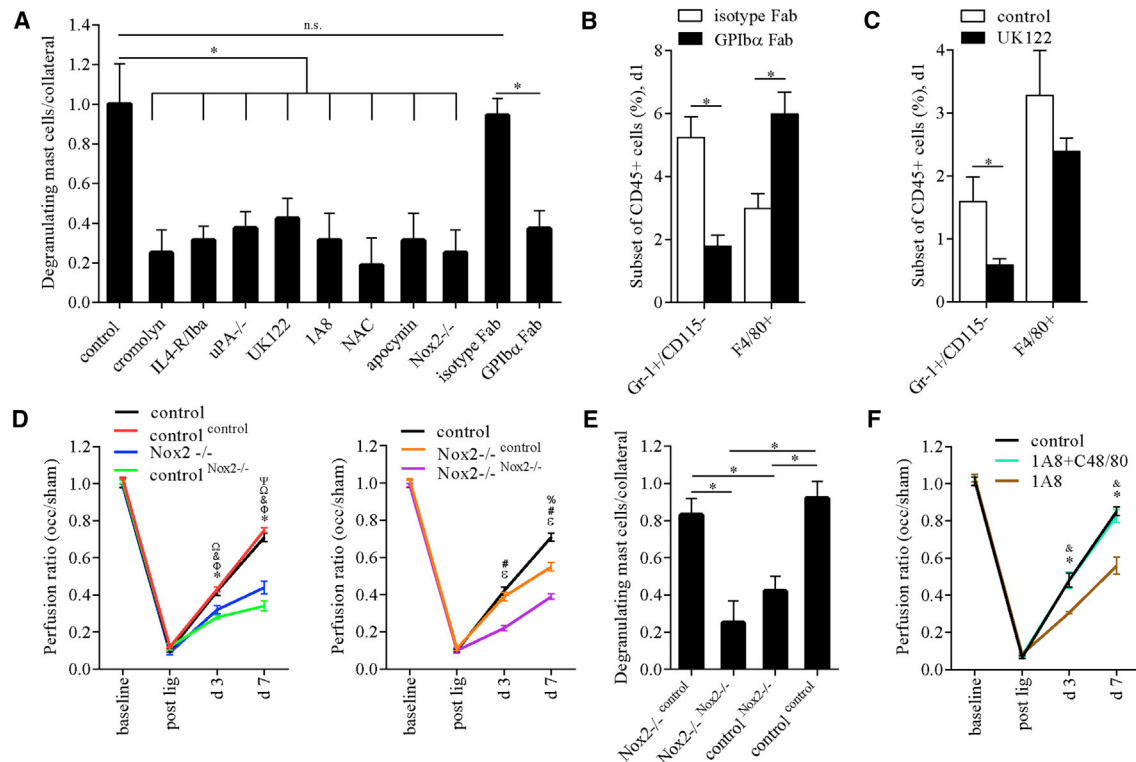
Interestingly, blockage of the platelet receptor GPIb α as well as genetic ablation of the ectodomain of GPIb α in transgenic IL4-R/Iba mice inhibited mast cell degranulation to a similar extent as cromolyn treatment (Figure 5A). Similarly, uPA deficiency or the inhibition of uPA proteolytic activity by the administration of UK122 significantly diminished mast cell degranulation (Figure 5A).

We have shown previously that uPA deficiency (but not uPA receptor or tissue plasminogen activator deficiency) is associated with a reduced perfusion recovery upon fal, which was due to reduced leukocyte infiltration (day 3 after fal) (Deindl et al., 2003). Recently, we observed a reduced reperfusion recovery upon fal when blocking the GPIb α receptor using a Fab fragment. Furthermore, the same effect was seen in GPIb α receptor-deficient IL4-R/Iba mice. Of note, our results evidenced that the GPIb α receptor is essential in arteriogenesis for (1) transient platelet interaction with collateral endothelium, (2) differential expression of vascular uPA (day 1 after fal), (3) platelet-neutrophil aggregate (PNA) formation (day 1 after fal), and (4) extravasation of leukocytes (3 days after fal) (Chandraratne et al., 2015). Furthermore, in a model of hepatic ischemia reperfusion injury, we found endothelial-derived uPA to be essential for intravascular adherence of neutrophils. Moreover,

data suggest that protection of tissue from ischemic damage was a result of arteriogenesis in the upper leg, but not due to degranulation of mast cells in the lower leg.

Perivascular Mast Cells Are Activated by a Cascade of Platelet- and Neutrophil-Dependent Reactions

Fluid shear stress, which is the driving force behind arteriogenesis, can only be sensed directly by vascular ECs, but not by perivascular cells. Hence, we asked which factors or cells may be responsible for mast cell degranulation during the initial phase of arteriogenesis. As platelets are sensors of fluid shear stress and can adhere to endothelial von Willebrand factor (vWF) under conditions of increased fluid shear stress through platelet GPIb α

**Figure 5. Mast Cells Are Activated by Neutrophil-Derived ROS**

(A) Degranulated mast cells in the perivascular space of collaterals 1 day after fal in control mice or in mice treated with cromolyn to stabilize mast cells; UK122 (uPA inhibition); 1A8 (neutrophil-depleting agent); N-acetylcysteine (NAC, ROS scavenger); apocynin (NADPH oxidase inhibitor); GPIb α -blocking Fab fragment; isotype Fab fragment; and in mice deficient for platelet receptor GPIb α (IL4-R/Iba mice), uPA, or Nox2, respectively, are shown (n = 4 animals with two collaterals each).

(B and C) Flow cytometry analysis of CD45 $^{+}$ /CD11b $^{+}$ /Gr-1 $^{+}$ /CD115 $^{-}$ and CD45 $^{+}$ /CD11b $^{+}$ /F4/80 $^{+}$ cells in adductor muscles of animals treated with GPIb α -blocking Fab fragment or isotype Fab fragment (B) or uPA inhibitor UK122 or control group (C) at day 1 after fal is shown (n = 4).

(D) Laser Doppler perfusion measurements of (left panel) wild-type mice (control), Nox2-deficient mice (Nox2 $^{-/-}$), wild-type mice reconstituted with bone marrow from wild-type mice (control $^{\text{control}}$), and wild-type mice reconstituted with bone marrow from Nox2-deficient mice (control $^{\text{Nox2}^{-/-}}$) and (right panel) wild-type mice (control), Nox2-deficient mice reconstituted with bone marrow from Nox2-deficient mice (Nox2 $^{-/-}$), and Nox2-deficient mice reconstituted with bone marrow from wild-type mice (Nox2 $^{-/-}$ control) after the induction of arteriogenesis (right leg) or sham operation (left leg) at the indicated time points after the surgical procedure. Color-coded lines indicate different groups. The controls of the left and right plot are identical. Statistical analysis (p ≤ 0.05) was as follows: *Nox2 $^{-/-}$ versus control; $^{\text{b}}\text{control}^{\text{Nox2}^{-/-}}$ versus control; $^{\text{a}}\text{Nox2}^{-/-}$ versus control $^{\text{control}}$, $^{\text{c}}\text{control}^{\text{Nox2}^{-/-}}$ versus control $^{\text{control}}$, $^{\text{d}}\text{control}^{\text{Nox2}^{-/-}}$ versus Nox2 $^{-/-}$; $^{\text{e}}\text{Nox2}^{-/-}$ versus control $^{\text{Nox2}^{-/-}}$; $^{\text{f}}\text{Nox2}^{-/-}$ versus Nox2 $^{-/-}$ control; and $^{\text{g}}\text{Nox2}^{-/-}$ control versus control (n = 5 per group).

(E) Degranulated mast cells in the perivascular space of growing collaterals 1 day after fal in Nox2 $^{-/-}$ control, Nox2 $^{-/-}$ Nox2 $^{-/-}$, control $^{\text{Nox2}^{-/-}}$, and control $^{\text{control}}$ mice are shown (n = 6 slices from three individual animals with two collaterals each).

(F) Laser Doppler perfusion measurements of saline- (control), 1A8-, or 1A8 + C48/80-treated wild-type mice following fal (right leg) and sham operation (left leg) (n = 6 per group). Statistical analysis (p ≤ 0.05) was as follows: $^{\text{a}}\text{control}$ versus 1A8 and $^{\text{b}}\text{1A8+C48/80}$ versus 1A8.

Data are means ± SEM. Significances (*p ≤ 0.05) in (A) and (E) were from two-way ANOVA with Newman-Keuls test, and significances in (D) and (F) were from repeated-measures two-way ANOVA with subsequent multiple comparisons by Bonferroni test. See also Figure S7.

neutrophil-derived uPA was critical for subsequent paracellular transmigration of neutrophils and, hence, extravasation (Reichel et al., 2011). We therefore hypothesized that neutrophils also may play a role in arteriogenesis and may represent the missing link in mast cell activation. Indeed, inhibition of GPIb α receptor or uPA activity resulted not only in reduced mast cell activation but also in diminished neutrophil infiltration at day 1 after fal, as assessed by flow cytometry (Figures 5B and 5C).

To analyze the functional relevance of neutrophils and PNA formation in more detail, we performed in vitro studies using isolated platelets and neutrophils. We found that PNA formation is a prerequisite for surface expression of uPA on neutrophils as well

as for extracellular superoxide anion formation (Figures S7A–S7D). P-selectin deficiency on platelets as well as deficiency of its ligand PSGL-1 on neutrophils interfered with PNA formation and diminished uPA surface expression (Figures S7A–S7C). In addition, P-selectin deficiency of platelets prevented superoxide anion formation (Figure S7D), accounting for the relevance of platelet P-selectin for the production of neutrophil-derived ROS (Page and Pitchford, 2013). Finally, extracellular ROS production was absent when using Nox2-deficient neutrophils for PNA formation, indicating that neutrophils are the source of superoxide anions (Figure S7D). A proposed model for neutrophil activation during arteriogenesis is shown in Figure S7E.

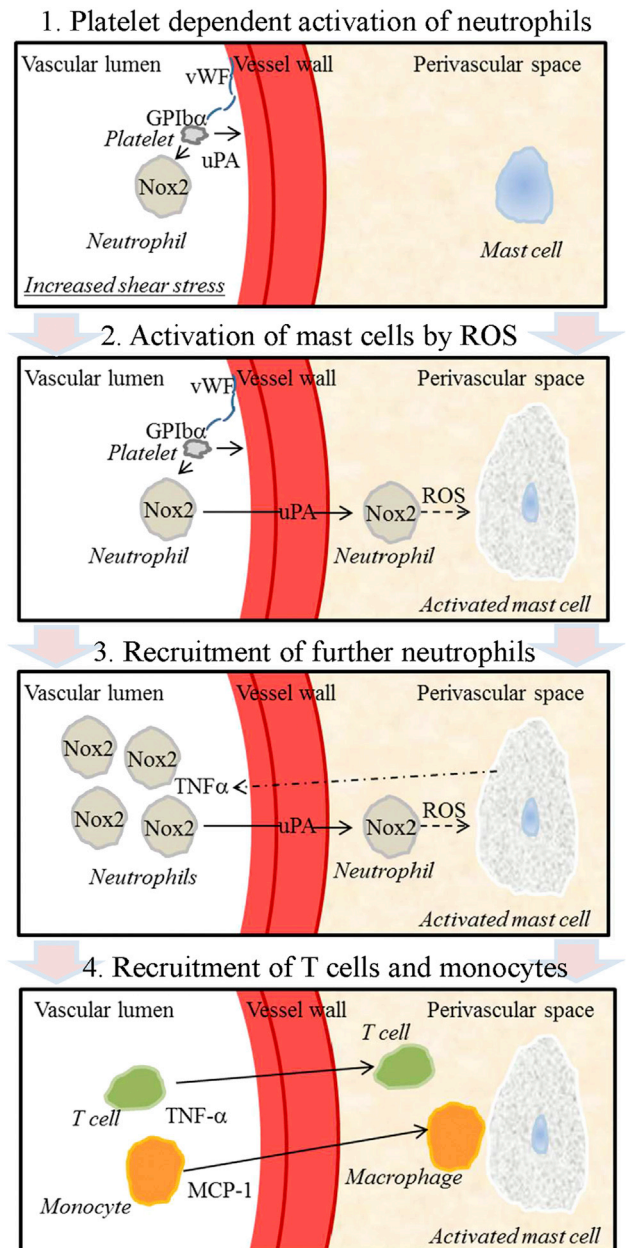


Figure 6. Proposed Model for the Central Role of Mast Cells in Arteriogenesis

Step 1. Upon occlusion of a main artery, increased fluid shear stress in collateral arteries initiates GPIb α -dependent PNA formation, which results in the activation of neutrophils. Step 2. After uPA-mediated extravasation of neutrophils, Nox2-derived superoxide anions (ROS) induce mast cell degranulation. Step 3. TNF- α promotes further neutrophil extravasation in a positive feedback loop. Step 4. TNF- α supports T cell extravasation and MCP-1 attracts monocytes, which mature to macrophages and supply the growing vessel with growth factors and cytokines. See also Figure S7E.

To assess whether Nox2-derived ROS from neutrophils are relevant for mast cell degranulation during arteriogenesis, we performed further *in vivo* analyses. Indeed, our results showed

that depletion of neutrophils by the application of 1A8 (reduction of neutrophils: $70\% \pm 3.7\%$, $p < 0.05$), deficiency of Nox2 (= gp91phox), as well as blocking ROS production or their function by the administration of apocynin or N-acetylcysteine (NAC) (Schulz et al., 2014; Tobar et al., 2010), respectively, blocked mast cell degranulation to a similar degree as observed in GPIb α -deficient mice (Figure 5A). To investigate whether neutrophil-derived ROS are responsible for mast cell degranulation, we created chimeric mice by transplanting bone marrow from Nox2 $^{−/−}$ mice to wild-type mice (control $^{Nox2^{−/−}}$) and vice versa (Nox2 $^{−/−}$ control). Compared to their corresponding control (control control), control $^{Nox2^{−/−}}$ showed a significant reduction in perfusion recovery as well as mast cell degranulation, whereas Nox2 $^{−/−}$ control revealed a significant improvement in collateral formation as compared to control (Nox2 $^{−/−}$ Nox2 $^{−/−}$) (Figures 5D and 5E). To confirm that mast cells become activated by ROS derived from neutrophils, neutropenic mice were challenged with C48/80 to induce mast cell degranulation. While neutrophil depletion impaired perfusion recovery after fal, the induction of mast cell degranulation completely restored the phenotype (Figure 5F).

DISCUSSION

In this study, we show that natural bypass growth is a matter of innate immunity, and we highlight the central role of mast cells in orchestrating leukocyte function in this process. In addition, we deciphered the mechanisms responsible for the translation of increased fluid shear stress to the activation of perivascular mast cells (Figure 6).

Mast cells were found to reside in the perivascular space of growing collaterals (Wolf et al., 1998). However, their function in arteriogenesis has never been investigated. Moreover, the mechanism by which perivascular mast cells become activated by increased mechanical load, such as fluid shear stress, has not been resolved up to now. We demonstrate that this is mediated by platelets and neutrophils and that neutrophil-derived ROS are the driving force for mast cell activation.

Fluid shear stress, which stimulates arteriogenesis, is well described to induce the adherence of platelets to ECs, a process mediated by the interaction of the platelet receptor GPIb α with the endothelial vWF (Sadler, 2002). We recently demonstrated that platelet receptor GPIb α is essential for the transient interaction of platelets to collateral endothelium, PNA formation, and extravasation of leukocytes during arteriogenesis (Chandraratne et al., 2015). Here we show that platelet receptor GPIb α is particularly relevant for neutrophil extravasation. We demonstrate that PNA formation through platelet P-selectin and neutrophil PSGL-1 is associated with uPA release to the neutrophil cell surface, paving the way for leukocyte infiltration. Moreover, we found that PNA formation is a prerequisite for neutrophil Nox2-dependent superoxide anion release.

As the deficiency or inhibition of uPA resulted in diminished neutrophil extravasation and mast cell degranulation, it is fair to deduce that the activation of neutrophils through interaction with platelets not only drives extravasation of these cells via uPA but also promotes mast cell activation via the release of neutrophil superoxide anions. This conclusion is endorsed by

our findings showing (1) a rescue of the impaired reperfusion recovery and mast cell degranulation observed in Nox2^{-/-} mice by the transplantation of bone marrow isolated from wild-type mice, and (2) restored perfusion in neutropenic mice by the induction of mast cell degranulation. These *in vivo* data are affirmed by *in vitro* findings showing that ROS stimulate mast cell activation (Gan et al., 2015) as well as by our results showing that activated neutrophils induce mast cell degranulation (Figure S7F). Together, these data indicate that the intravascular, shear stress-dependent activation of platelets and PNA formation triggers the production of effectors, such as ROS, that serve to transmit the locally initiated signal to proximal perivascular sites where mast cell degranulation is initiated.

Interestingly enough, platelet activation, uPA-mediated neutrophil extravasation, as well as mast cell activation recently were shown to contribute to reperfusion injury due to revascularization or organ transplantation (Chang et al., 2014; Egashira et al., 2013; Köhler et al., 2011; Reichel et al., 2011; Yang et al., 2014). In addition, allergic contact dermatitis was reported to strongly depend on mast cells, neutrophils, and neutrophil-derived ROS (Weber et al., 2015). Thus, the mechanisms identified in this study for mast cell activation under arteriogenic conditions appear to have a strong and more general impact, not just on pathogenesis and control of cardiovascular diseases, and they will contribute to the understanding of mast cell-dependent pathways in sterile inflammation/innate immunity.

In our study, we found mast cells to specifically degranulate around growing collateral arteries. Additional pharmacological activation of mast cells with C48/80 greatly enhanced perfusion recovery and, hence, arteriogenesis. Stabilizing mast cells with cromolyn showed the opposite effect and blocked the positive effect of C48/80 as well as dipA. Mast cell-deficient Mcpt5-Cre⁺ R-DTA mice showed no reduced perfusion recovery upon fal, neither was it improved by C48/80 treatment nor impaired by cromolyn. These data suggest that these transgenic mice were capable of compensating the lack of mast cells in the process of arteriogenesis and that cromolyn as well as C48/80 specifically and decisively influenced the action of mast cells in the process of collateral artery growth in wild-type mice.

TNF- α is a major determinant in neutrophil recruitment, as evidenced in many experimental settings (Griffin et al., 2012; Malaviya et al., 1996). Our results demonstrate that inhibition of mast cell degranulation strongly reduced the elevated plasma levels of TNF- α observed upon the induction of arteriogenesis. C48/80 treatment, in contrast, resulted in an increased number of neutrophils, especially at day 1 after fal (Figure S3C). These data indicate that neutrophils are likely to be recruited by mast cells in a positive feedback mechanism. Our data are in line with previous results showing mast cells to be essential for elevated TNF- α levels and neutrophil recruitment (Malaviya et al., 1996; Sun et al., 2007). TNF- α also has been implicated in MCP-1 production (Murao et al., 2000), relevant for monocyte recruitment (Ito et al., 1997). In our study, boosting mast cell activation by C48/80 resulted in increased levels of macrophages and T cells, particularly at day 3 after fal. Recruitment of perivascular macrophages supplying growth factors to growing blood vessels (Arras et al., 1998) was demonstrated to be essential for arterio-

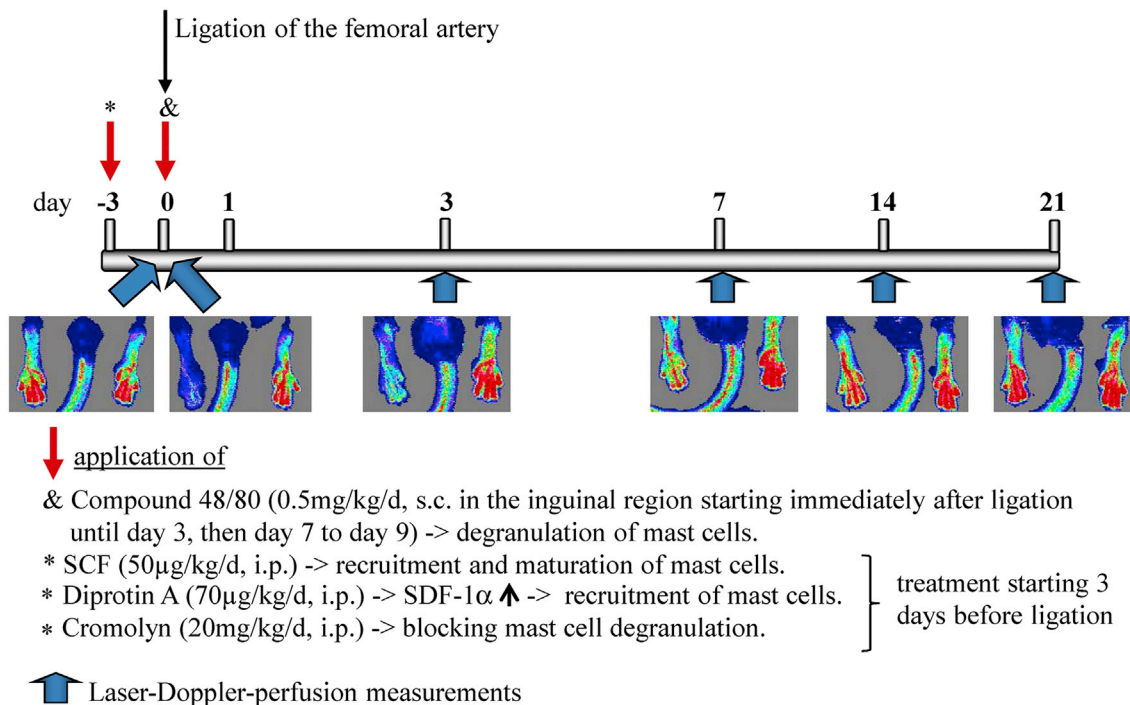
genesis (Heil et al., 2002; Hoefer et al., 2004; Ito et al., 1997), whereas T cells have been described to contribute to macrophage recruitment (Stabile et al., 2003). Hence, mast cells indirectly promoted arteriogenesis by amplifying the inflammatory reaction, thus providing macrophage-derived growth factors supporting vascular cell proliferation. In addition, mast cells may directly contribute to vascular cell proliferation as shown by our *in vitro* results.

In a more translational approach, we administrated dipA, which again increased perfusion recovery. Platelets, which transiently adhere to the endothelium of growing collaterals in the early phase of arteriogenesis (Chandraratne et al., 2015), are a rich source of SDF-1 α . Platelet activation enhances surface expression and release of SDF-1 α (Chatterjee and Gawaz, 2013), which results in recruitment of CXCR-4 $^+$ cells at the site of inflammation. The administration of dipA, blocking DPPIV activity and, hence, SDF-1 α degradation, resulted in a drastic increase in the number of c-kit $^+$ mast cells together with a significantly improved perfusion recovery.

Combined treatment of mice with C48/80 and dipA showed additive effects in terms of perfusion recovery and leukocyte recruitment, and it protected tissue from severe ischemic damage by effectively promoting arteriogenesis. Although we found that leukocytes, which express the SDF-1 α receptor CXCR-4 as well, are recruited upon dipA treatment, a substantial increase in leukocyte recruitment occurred not earlier than upon treatment with dipA in combination with C48/80 (Figure 2D), arguing for the relevance of mast cells in this process.

Mast cells express the SDF-1 α receptor CXCR-4 as well as the SCF receptor c-kit. Both ligands have been addressed in many experimental as well as clinical settings to recruit stem cells aiming at promoting neovascularization. Since it has been demonstrated previously that bone marrow-derived stem cells do not differentiate to ECs or SMCs and, hence, do not contribute to vascularization, i.e., arteriogenesis and angiogenesis (Ziegelhoeffer et al., 2004), our results may shed a different light on the nature of c-kit $^+$ /CXCR-4 $^+$ stem cells recruited to sites of neovascularization. Diverse studies could not demonstrate the presence of recruited stem cells at sites of (neo-) vascularization despite a functional improvement. In this context it might be of particular interest to mention that extensively degranulated mast cells cannot be identified anymore as individual cells in tissue (McGowen et al., 2009). A huge number of publications are available attributing mast cells an essential role in tumor angiogenesis; however, little information is available on the role of mast cells under other pathological or physiological conditions and results are contradictory.

Much effort has been made to find new therapeutic options to treat patients with vascular occlusive diseases. Here we show that promoting mast cell recruitment concomitant with mast cell activation promotes the growth of natural arteriolar bypasses to such an extent that distal tissue is preserved from severe ischemic damage. Local administration of C48/80 showed no systemic side effects in our study, and mast cell activators as well as drugs that inhibit DPPIV are used in clinical applications (Rukwied et al., 2000; Yanai, 2014). Recent clinical studies showed no major adverse cardiovascular events in patients with type 2 diabetes treated with DPPIV inhibitors

**Figure 7. Study Protocol**

Treatment protocol of mice with C48/80, SCF, dipA, or cromolyn with the indicated time points of laser Doppler perfusion measurements. Tissue for qRT-PCR was harvested at 12 hr, for protein analyses at 24 hr, for flow cytometry analyses at days 1 and 3, and for histology or immunohistology at 2 hr, 12 hr, 24 hr, 3 days, or 7 days after fal (right leg) or sham operation (left leg).

(White et al., 2013) and evidenced a lower risk for hospitalization for heart failure (Fadini et al., 2015), although there might be differences depending on the DPPIV inhibitor used. Therefore, SDF-1 α , which recently has been shown in an animal model to promote vascular outward remodeling when locally released (Krieger et al., 2016), or DPPIV inhibitors alone or in combination with locally applied mast cell-activating factors may represent therapeutic approaches to treat affected patients non-invasively.

Collectively, our data show that mast cells play a central role in arteriogenesis by converting signals derived from upstream platelets and neutrophils in actions that specifically support the process of collateral artery growth. Pharmacological induction of mast cell recruitment and degranulation effectively promotes arteriogenesis, thereby protecting tissue from severe ischemic damage, and may thus constitute a therapeutic approach to treat patients with vascular occlusive diseases.

EXPERIMENTAL PROCEDURES

Murine Hindlimb Model of Arteriogenesis and Bone Marrow Transplantation

Animal care and all experimental procedures were performed in strict accordance to the German and NIH animal legislation guidelines and were approved by the Bavarian Animal Care and Use Committee (GZ. 55.2-1-54-2532-73-12). Ligation of the right femoral artery was induced in 8- to 10-week-old male SV129/S6 mice (Charles River Laboratories) treated with the indicated substances (for protocol see Figure 7 and the *Supplemental Experimental Proce-*

dures); in bone marrow-transplanted mice; in Mcpt5-Cre⁺ R-DTA, Nox2^{-/-}, uPA^{-/-}, and IL4-R/Iba mice; and in corresponding wild-type littermates, respectively, as previously described (Limbourg et al., 2009). The left side was sham operated and served as control. For Laser-Doppler perfusion measurements, bone marrow transplantation, and further information, see the *Supplemental Experimental Procedures*.

SDF-1 α , TNF- α , and MCP-1 Quantifications

SDF-1 α protein levels in serum and collaterals were analyzed using a mouse SDF-1 α ELISA kit (ELM-SDF1alpha-001-1, RayBiotech). MCP-1 and TNF- α protein levels were analyzed with MCP-1 and TNF- α ELISA ready-SET-go (REF 88-7391-22 and REF 88-7324-88, eBioscience), respectively, following the manufacturer's protocol. Plasma was collected from heparinized blood after centrifugation at 2,300 \times g at 4°C for 20 min. Tissue was homogenized with 200 μ l of cell lysis buffer (25 mM Tris [pH 7.5], 1% Triton X-100, 0.5 mM EDTA, 150 mM NaCl, 10 mM NaF, and 1% PMSF), treated five times for 2 s with ultrasound, and centrifuged as described above. For qRT-PCR analyses of MCP-1, see the *Supplemental Experimental Procedures*.

MMP Activity Assay

MMP activity in collateral samples was analyzed with SensoLyte 520 Generic MMP Assay Kit (Anaspec). Briefly, collaterals were homogenized in assay buffer with 0.1% (v/v) Triton X-100, centrifuged, and supernatants were incubated for 2 hr with 4-aminophenylmercuric acetate (APMA) at 37°C, following the manufacturer's protocol. Fluorescence signal was measured at excitation/emission = 490/520 nm for 1 hr (Infinite 200, S/N 711003634, TECAN). Data were normalized to the reference standard curve.

Histology and Immunohistology

Paraffin-embedded issue samples were isolated at the indicated time points. After deparaffinization and antigen retrieval using Target Retrieval Solution

(S1699, Dako), sections were stained for CD31 (DIA-310, Dianova, dilution 1:150), Ki67 (M7249, Dako, dilution 1:100), or CD45 (550539, BD Pharmingen, dilution 1:600), respectively. For detection of the immunoreaction, the Vectastain ABC-Kit Elite Rat IgG (PK6104, Vector Laboratories) was used. DAB+ (K3468, Dako) served as chromogen for CD31 and ACE (00-1122, Invitrogen) for Ki67 and CD45 staining. Giemsa and H&E staining were performed according to standard procedures. The luminal diameter of collateral arterioles was measured in at least three different sites of an individual arteriole. Cryopreserved tissue samples were stained with an antibody against c-kit (14-1172-85, eBioscience, dilution 1:100) and secondary antibody donkey anti-rat Cy3 (AC189C, Millipore, dilution 1:300); FGF-2 (ab106245, Abcam, dilution 1:100) and secondary antibody donkey anti-rabbit AF488 (A21206, MoBiTec, dilution 1:100); or PDGF-BB (ab16829, Abcam, dilution 1:100) and secondary antibody donkey anti-rabbit AF488 (A21206, MoBiTec, dilution 1:100), respectively, and viewed with a confocal microscope (Leica SP5).

Flow Cytometry Analyses of Muscle Tissue

For flow cytometry analysis, adductor muscles were digested with 1 mg/ml collagenase II (Biochrom) in PBS/1% BSA at 37°C for 90 min. The suspension was then filtered with PBS/2% BSA through a 70-μm cell strainer (BD Falcon), spun for 10 min at 160 × g, and the pellet was finally resuspended in 100 μl PBS/2% BSA. Surface staining was conducted using CD 45 rat anti-mouse APC-Cy7 (557659, clone 30-F11, BD Biosciences), F4/80 rat anti-mouse eFluor 450 (48-4801, clone BM8, eBioscience), CD 115 rat anti-mouse APC (17-1152, clone AFS98, eBioscience), CD 11b rat anti-mouse fluorescein isothiocyanate (FITC) (11-0112, clone m1/70, eBioscience), GR-1 rat anti-mouse PE (553128, clone RB6-8C5, BD Biosciences), c-kit (CD117) rat anti-mouse PerCP/Cy5.5 (105823, clone 2B8, BioLegend), and CD3 rat anti-mouse eFlour 450 (48-0032, clone 17A2, eBioscience). Rat isotype controls were as follows: IgG2b APC-Cy7 (552773, clone A95-1, BD Biosciences), IgG2a eFluor 450 (48-4321, clone eBR2a, eBioscience), IgG2a APC (17-4321, clone eBR2a, eBioscience), IgG 1 FITC (11-4301, clone eBRG1, eBioscience), IgG2b PE (553989, clone A95-1, BD Biosciences), and IgG2a PerCP/Cy5.5 (45-4321, clone eBR2a, eBioscience). Becton Dickinson fluorescence-activated cell sorting (FACS) lysing solution was used to fix and lyse the samples according to the manufacturer's protocol. Samples were measured using Gallios flow cytometer and analyzed with Kaluza Software (both from Beckman Coulter Genomics).

In Vitro Analyses

For protocols of the in vitro analyses, see the Supplemental Experimental Procedures.

Statistical Analysis

Comparisons between groups were calculated by unpaired Student's t test unless otherwise stated. Results were considered to be statistically significant at *p ≤ 0.05. Data are represented as means ± SEM. Statistical analyses were performed with GraphPad software PRISM6.

SUPPLEMENTAL INFORMATION

Supplemental Information includes Supplemental Experimental Procedures and seven figures and can be found with this article online at <http://dx.doi.org/10.1016/j.celrep.2016.07.040>.

AUTHOR CONTRIBUTIONS

O.C., E.C.K., T.L., J.-I.P., M.R., and M.L. performed in vivo measurements and histological analyses. Y.H. and H.M. conducted in vitro analyses on platelets and neutrophils. A.C.-M. and S.F. performed qRT-PCR, MMP activity assay, and protein analyses. A.M. conducted in vitro proliferation assays, K.T. performed immunohistology, and A.R.M.K. helped with FACS analyses. G.A. helped with histology data analysis. S.M.K., B.N., B.W., C.A.R., and K.T.P. participated in scientific discussions and drafting of the manuscript. E.D. performed experimental design, data analysis, conducted scientific direction, and wrote the manuscript.

ACKNOWLEDGMENTS

This work was supported by the Fritz-Bender-Stiftung (E.D.), the Deutscher Akademischer Austauschdienst (DAAD) (E.D.), the Münchener Universitätsgesellschaft (E.D.), the v. Behring-Röntgen-Foundation (S.F. and K.T.P.), and the Deutsche Forschungsgemeinschaft (SFB 914/TP A02 [B.W.] and /TP B03 [C.A.R.]). The authors are thankful to N. Weissmann, Justus-Liebig-University, for the Nox2-/- mice; S. Massberg, Ludwig-Maximilians-University, for IL4-R/Iba mice; D. Vestweber, Max Planck Institute for Molecular Biomedicine, for PSGL-1-/- and P-selectin -/- mice; A. Roers for Mcpt5-Cre R-DTA mice; and C. Csapo, M.-P. Wu, J. Truong, S. Tannert Otto, S. Schaefer, A. Heier, A. Sendelthofer, and Tobias Haering for technical assistance.

Received: December 25, 2015

Revised: June 23, 2016

Accepted: July 17, 2016

Published: August 11, 2016

REFERENCES

- Arras, M., Ito, W.D., Scholz, D., Winkler, B., Schaper, J., and Schaper, W. (1998). Monocyte activation in angiogenesis and collateral growth in the rabbit hindlimb. *J. Clin. Invest.* 101, 40–50.
- Cai, W., Vosschulte, R., Afsah-Hedjri, A., Koltai, S., Kocsis, E., Scholz, D., Kostin, S., Schaper, W., and Schaper, J. (2000). Altered balance between extracellular proteolysis and antiproteolysis is associated with adaptive coronary arteriogenesis. *J. Mol. Cell. Cardiol.* 32, 997–1011.
- Cao, R., Bräkenhielm, E., Pawliuk, R., Wariaro, D., Post, M.J., Wahlberg, E., Leboulch, P., and Cao, Y. (2003). Angiogenic synergism, vascular stability and improvement of hind-limb ischemia by a combination of PDGF-BB and FGF-2. *Nat. Med.* 9, 604–613.
- Chandraratne, S., von Breuhl, M.L., Pagel, J.I., Stark, K., Kleinert, E., Konrad, I., Farschtschi, S., Coletti, R., Gärtnner, F., Chillo, O., et al. (2015). Critical role of platelet glycoprotein Ibα in arterial remodeling. *Arterioscler. Thromb. Vasc. Biol.* 35, 589–597.
- Chang, J.C., Leung, J., Tang, T., Holzknecht, Z.E., Hartwig, M.G., Duane Davis, R., Parker, W., Abraham, S.N., and Lin, S.S. (2014). Cromolyn ameliorates acute and chronic injury in a rat lung transplant model. *Journal Heart Lung Transplant.* 33, 749–757.
- Chatterjee, M., and Gawaz, M. (2013). Platelet-derived CXCL12 (SDF-1α): basic mechanisms and clinical implications. *J. Thromb. Haemost.* 11, 1954–1967.
- Deindl, E., and Schaper, W. (2005). The art of arteriogenesis. *Cell Biochem. Biophys.* 43, 1–15.
- Deindl, E., Ziegelhöffer, T., Kanse, S.M., Fernandez, B., Neubauer, E., Carmeliet, P., Preissner, K.T., and Schaper, W. (2003). Receptor-independent role of the urokinase-type plasminogen activator during arteriogenesis. *FASEB J.* 17, 1174–1176.
- Egashira, Y., Suzuki, Y., Azuma, Y., Takagi, T., Mishiro, K., Sugitani, S., Tsuruma, K., Shimazawa, M., Yoshimura, S., Kashimoto, M., et al. (2013). The growth factor progranulin attenuates neuronal injury induced by cerebral ischemia-reperfusion through the suppression of neutrophil recruitment. *J. Neuroinflammation* 10, 105.
- Fadini, G.P., Avogaro, A., Degli Esposti, L., Russo, P., Saragoni, S., Buda, S., Rosano, G., Pecorelli, S., and Pani, L.; OsMed Health-DB Network (2015). Risk of hospitalization for heart failure in patients with type 2 diabetes newly treated with DPP-4 inhibitors or other oral glucose-lowering medications: a retrospective registry study on 127,555 patients from the Nationwide OsMed Health-DB Database. *Eur. Heart J.* 36, 2454–2462.
- Gan, X., Xing, D., Su, G., Li, S., Luo, C., Irwin, M.G., Xia, Z., Li, H., and Hei, Z. (2015). Propofol attenuates small intestinal ischemia reperfusion injury through inhibiting NADPH oxidase mediated mast cell activation. *Oxid. Med. Cell. Longev.* 2015, 167014.
- Griffin, G.K., Newton, G., Tarrio, M.L., Bu, D.X., Maganto-Garcia, E., Azcutia, V., Alcaide, P., Grable, N., Luscinskas, F.W., Croce, K.J., and Lichtman,

- A.H. (2012). IL-17 and TNF- α sustain neutrophil recruitment during inflammation through synergistic effects on endothelial activation. *J. Immunol.* 188, 6287–6299.
- Grundmann, S., Hoefer, I., Ulusans, S., van Royen, N., Schirmer, S.H., Ozaki, C.K., Bode, C., Piek, J.J., and Buschmann, I. (2005). Anti-tumor necrosis factor-alpha therapies attenuate adaptive arteriogenesis in the rabbit. *Am. J. Physiol. Heart Circ. Physiol.* 289, H1497–H1505.
- Heil, M., Ziegelhoeffer, T., Pipp, F., Kostin, S., Martin, S., Clauss, M., and Schaper, W. (2002). Blood monocyte concentration is critical for enhancement of collateral artery growth. *Am. J. Physiol. Heart Circ. Physiol.* 283, H2411–H2419.
- Hiromatsu, Y., and Toda, S. (2003). Mast cells and angiogenesis. *Microsc. Res. Tech.* 60, 64–69.
- Hoefer, I.E., van Royen, N., Rectenwald, J.E., Deindl, E., Hua, J., Jost, M., Grundmann, S., Voskuil, M., Ozaki, C.K., Piek, J.J., and Buschmann, I.R. (2004). Arteriogenesis proceeds via ICAM-1/Mac-1-mediated mechanisms. *Circ. Res.* 94, 1179–1185.
- Ito, W.D., Arras, M., Winkler, B., Scholz, D., Schaper, J., and Schaper, W. (1997). Monocyte chemoattractant protein-1 increases collateral and peripheral conductance after femoral artery occlusion. *Circ. Res.* 80, 829–837.
- Köhler, D., Straub, A., Weissmüller, T., Faigle, M., Bender, S., Lehmann, R., Wendel, H.P., Kurz, J., Walter, U., Zacharowski, K., and Rosenberger, P. (2011). Phosphorylation of vasodilator-stimulated phosphoprotein prevents platelet-neutrophil complex formation and dampens myocardial ischemia-reperfusion injury. *Circulation* 123, 2579–2590.
- Kovanen, P.T. (2007). Mast cells: multipotent local effector cells in atherosclerosis. *Immunol. Rev.* 217, 105–122.
- Krieger, J.R., Ogle, M.E., McFaline-Figueroa, J., Segar, C.E., Temenoff, J.S., and Botchwey, E.A. (2016). Spatially localized recruitment of anti-inflammatory monocytes by SDF-1 α -releasing hydrogels enhances microvascular network remodeling. *Biomaterials* 77, 280–290.
- Limbourg, A., Korff, T., Napp, L.C., Schaper, W., Drexler, H., and Limbourg, F.P. (2009). Evaluation of postnatal arteriogenesis and angiogenesis in a mouse model of hind-limb ischemia. *Nat. Protoc.* 4, 1737–1746.
- Maggi, L., Capone, M., Giudici, F., Santarasci, V., Querci, V., Liotta, F., Ficari, F., Maggi, E., Tonelli, F., Annunziato, F., and Cosmi, L. (2013). CD4+CD161+ T lymphocytes infiltrate Crohn's disease-associated perianal fistulas and are reduced by anti-TNF- α local therapy. *Int. Arch. Allergy Immunol.* 161, 81–86.
- Malaviya, R., Ikeda, T., Ross, E., and Abraham, S.N. (1996). Mast cell modulation of neutrophil influx and bacterial clearance at sites of infection through TNF-alpha. *Nature* 381, 77–80.
- McGowen, A.L., Hale, L.P., Shelburne, C.P., Abraham, S.N., and Staats, H.F. (2009). The mast cell activator compound 48/80 is safe and effective when used as an adjuvant for intradermal immunization with *Bacillus anthracis* protective antigen. *Vaccine* 27, 3544–3552.
- Murao, K., Ohyama, T., Imachi, H., Ishida, T., Cao, W.M., Namihira, H., Sato, M., Wong, N.C., and Takahara, J. (2000). TNF-alpha stimulation of MCP-1 expression is mediated by the Akt/PKB signal transduction pathway in vascular endothelial cells. *Biochem. Biophys. Res. Commun.* 276, 791–796.
- Oliveira, S.H., and Lukacs, N.W. (2003). Stem cell factor: a hemopoietic cytokine with important targets in asthma. *Curr. Drug Targets Inflamm. Allergy* 2, 313–318.
- Page, C., and Pitchford, S. (2013). Neutrophil and platelet complexes and their relevance to neutrophil recruitment and activation. *Int. Immunopharmacol.* 17, 1176–1184.
- Pipp, F., Boehm, S., Cai, W.J., Adili, F., Ziegler, B., Karanovic, G., Ritter, R., Balzer, J., Scheler, C., Schaper, W., and Schmitz-Rixen, T. (2004). Elevated fluid shear stress enhances postocclusive collateral artery growth and gene expression in the pig hind limb. *Arterioscler. Thromb. Vasc. Biol.* 24, 1664–1668.
- Rao, K.N., and Brown, M.A. (2008). Mast cells: multifaceted immune cells with diverse roles in health and disease. *Ann. N Y Acad. Sci.* 1143, 83–104.
- Reichel, C.A., Uhl, B., Lerchenberger, M., Puhr-Westerheide, D., Rehberg, M., Liebl, J., Khandoga, A., Schmalix, W., Zahler, S., Deindl, E., et al. (2011). Urokinase-type plasminogen activator promotes paracellular transmigration of neutrophils via Mac-1, but independently of urokinase-type plasminogen activator receptor. *Circulation* 124, 1848–1859.
- Rudijanto, A. (2007). The role of vascular smooth muscle cells on the pathogenesis of atherosclerosis. *Acta Med. Indones.* 39, 86–93.
- Rukwied, R., Lischetzki, G., McGlone, F., Heyer, G., and Schmelz, M. (2000). Mast cell mediators other than histamine induce pruritus in atopic dermatitis patients: a dermal microdialysis study. *Br. J. Dermatol.* 142, 1114–1120.
- Sadler, J.E. (2002). A new name in thrombosis, ADAMTS13. *Proc. Natl. Acad. Sci. USA* 99, 11552–11554.
- Schulz, R., Murzabekova, G., Egemnazarov, B., Kraut, S., Eisele, H.J., Dumitrescu, R., Heitmann, J., Seimetz, M., Witzenrath, M., Ghofrani, H.A., et al. (2014). Arterial hypertension in a murine model of sleep apnea: role of NADPH oxidase 2. *J. Hypertens.* 32, 300–305.
- Stabile, E., Burnett, M.S., Watkins, C., Kinnaird, T., Bachis, A., la Sala, A., Miller, J.M., Shou, M., Epstein, S.E., and Fuchs, S. (2003). Impaired arteriogenic response to acute hindlimb ischemia in CD4-knockout mice. *Circulation* 108, 205–210.
- Stabile, E., Kinnaird, T., la Sala, A., Hanson, S.K., Watkins, C., Campia, U., Shou, M., Zbinden, S., Fuchs, S., Kornfeld, H., et al. (2006). CD8+ T lymphocytes regulate the arteriogenic response to ischemia by infiltrating the site of collateral vessel development and recruiting CD4+ mononuclear cells through the expression of interleukin-16. *Circulation* 113, 118–124.
- Sun, J., Sukhova, G.K., Wolters, P.J., Yang, M., Kitamoto, S., Libby, P., MacFarlane, L.A., Mallen-St Clair, J., and Shi, G.P. (2007). Mast cells promote atherosclerosis by releasing proinflammatory cytokines. *Nat. Med.* 13, 719–724.
- Tobar, N., Villar, V., and Santibanez, J.F. (2010). ROS-NFkappaB mediates TGF-beta1-induced expression of urokinase-type plasminogen activator, matrix metalloproteinase-9 and cell invasion. *Mol. Cell. Biochem.* 340, 195–202.
- Weber, F.C., Nemeth, T., Csepregi, J.Z., Dudeck, A., Roers, A., Ozsvari, B., Oswald, E., Puskas, L.G., Jakob, T., Mocsai, A., and Martin, S.F. (2015). Neutrophils are required for both the sensitization and elicitation phase of contact hypersensitivity. *J. Exp. Med.* 212, 15–22.
- White, W.B., Cannon, C.P., Heller, S.R., Nissen, S.E., Bergenstal, R.M., Bakris, G.L., Perez, A.T., Fleck, P.R., Mehta, C.R., Kupfer, S., et al.; EXAMINE Investigators (2013). Alogliptin after acute coronary syndrome in patients with type 2 diabetes. *N. Engl. J. Med.* 369, 1327–1335.
- Wolf, C., Cai, W.J., Vosschulte, R., Koltai, S., Mousavipour, D., Scholz, D., Af-sah-Hedjri, A., Schaper, W., and Schaper, J. (1998). Vascular remodeling and altered protein expression during growth of coronary collateral arteries. *J. Mol. Cell. Cardiol.* 30, 2291–2305.
- Yanai, H. (2014). Dipeptidyl peptidase-4 inhibitor sitagliptin significantly reduced hepatitis C virus replication in a diabetic patient with chronic hepatitis C virus infection. *Hepatobiliary Pancreat. Dis. Int.* 13, 556.
- Yang, M.Q., Ma, Y.Y., Tao, S.F., Ding, J., Rao, L.H., Jiang, H., and Li, J.Y. (2014). Mast cell degranulation promotes ischemia-reperfusion injury in rat liver. *J. Surg. Res.* 186, 170–178.
- Zaruba, M.M., Theiss, H.D., Vallaster, M., Mehl, U., Brunner, S., David, R., Fischer, R., Krieg, L., Hirsch, E., Huber, B., et al. (2009). Synergy between CD26/DPP-IV inhibition and G-CSF improves cardiac function after acute myocardial infarction. *Cell Stem Cell* 4, 313–323.
- Ziegelhoeffer, T., Fernandez, B., Kostin, S., Heil, M., Voswinckel, R., Helisch, A., and Schaper, W. (2004). Bone marrow-derived cells do not incorporate into the adult growing vasculature. *Circ. Res.* 94, 230–238.

Supplemental Information

**Perivascular Mast Cells Govern Shear
Stress-Induced Arteriogenesis
by Orchestrating Leukocyte Function**

Omary Chillo, Eike Christian Kleinert, Thomas Lautz, Manuel Lasch, Judith-Irina Pagel, Yvonn Heun, Kerstin Troidl, Silvia Fischer, Amelia Caballero-Martinez, Annika Mauer, Angela R.M. Kurz, Gerald Assmann, Markus Rehberg, Sandip M. Kanse, Bernhard Nieswandt, Barbara Walzog, Christoph A. Reichel, Hanna Mannell, Klaus T. Preissner, and Elisabeth Deindl

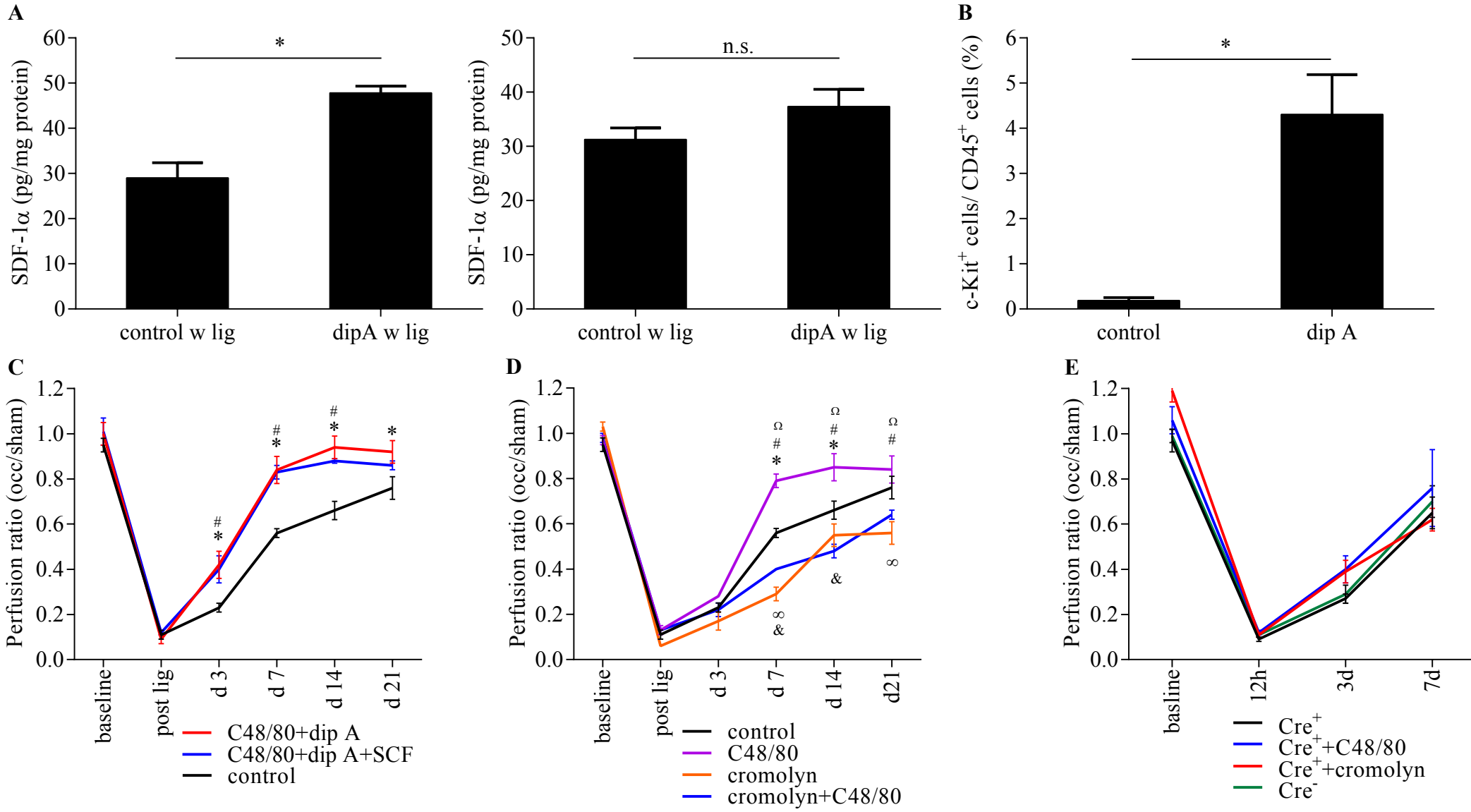


Figure S1. Related to Figure 1. Pharmaceutical recruitment and activation of mast cells promotes arteriogenesis

(A) SDF-1 α levels were measured to investigate the effectiveness of diprotin A treatment. The SDF-1 α levels in collateral arteries (left panel) or sera (right panel) of mice isolated 24h after fal and saline treatment (control w lig), or 24h after fal and diprotin A treatment (dipA w lig) were assessed by ELISA. n=3 in triplicates. (B) Flow cytometry analyses of CD45 $^+$ /c-kit $^+$ cells in adductor muscles of mice at day 1 after fal and saline (control) or dipA treatment. n=6. (C, D, E) Laser Doppler perfusion measurements following fal (right leg) and sham operation (left leg). Color-coded lines indicate treatment of mice (control = saline). Statistical analysis ($P < 0.05$) was performed between different groups (n=6 per group) using repeated measures two-way ANOVA with subsequent multiple comparisons by Bonferroni test. (C) Treatment of mice with C48/80+dipA+SCF showed no additive effects compared to C48/80+dipA treatment. The control and internal control (C48/80+dipA) are identical to Figure 1D. *C48/80+dipA vs control; #C48/80+dipA+SCF vs control. (D) Cromolyn treatment abolished the positive effect of C48/80. The control and internal controls (C48/80, cromolyn) are identical to Figure 1D. *C48/80 vs control; #C48/80 vs cromolyn; Ω C48/80 vs cromolyn+C48/80; &cromolyn vs control; &cromolyn+C48/80 vs control. (E) Perfusion recovery of mast cell deficient Mcpt5-Cre $^+$ R-DTA mice (Cre $^+$) was neither influenced by C48/80 treatment nor by cromolyn treatment. Control mice: Cre $^-$. Data are means \pm SEM.

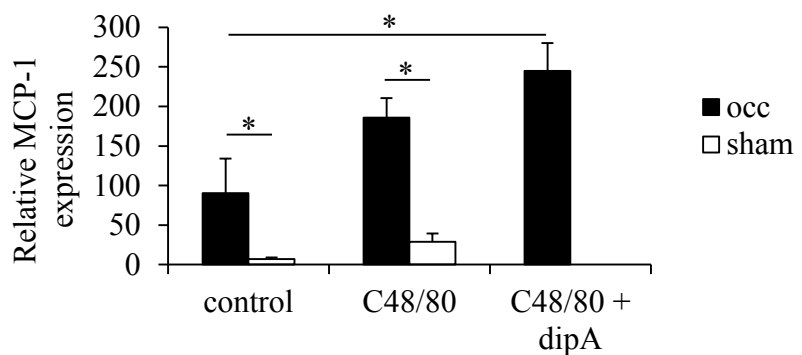


Figure S2. Related to Figure 2. MCP-1 mRNA levels

mRNA expression level of MCP-1 in collaterals of mice treated with saline (control), C48/80, or C48/80 and dipA (C48/80+dipA), 12h after fal (occ) or sham operation, as measured by qRT-PCR. Data are means \pm SEM; n=3 in triplicates. Statistical significances ($*P \leq 0.05$) are from two-way ANOVA with subsequent Newman-Keuls test.

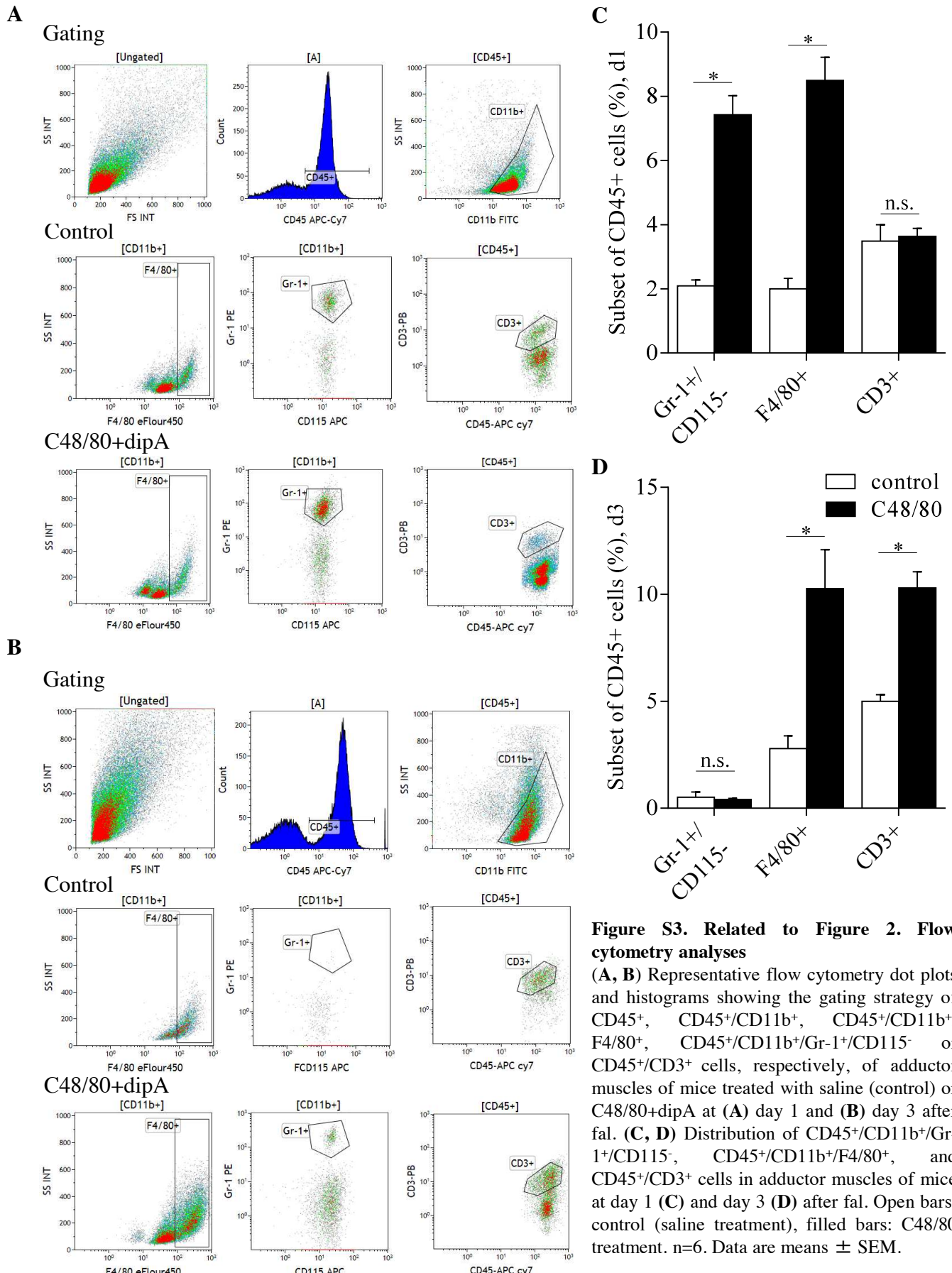


Figure S3. Related to Figure 2. Flow cytometry analyses

(A, B) Representative flow cytometry dot plots and histograms showing the gating strategy of CD45+, CD45+/CD11b+, CD45+/CD11b+/F4/80+, CD45+/CD11b+/Gr-1+/CD115⁻ or CD45+/CD3^x cells, respectively, of adductor muscles of mice treated with saline (control) or C48/80+dipA at (A) day 1 and (B) day 3 after fal. (C, D) Distribution of CD45+/CD11b+/Gr-1+/CD115⁻, CD45+/CD11b+/F4/80⁺, and CD45+/CD3^x cells in adductor muscles of mice at day 1 (C) and day 3 (D) after fal. Open bars: control (saline treatment), filled bars: C48/80 treatment. n=6. Data are means ± SEM.

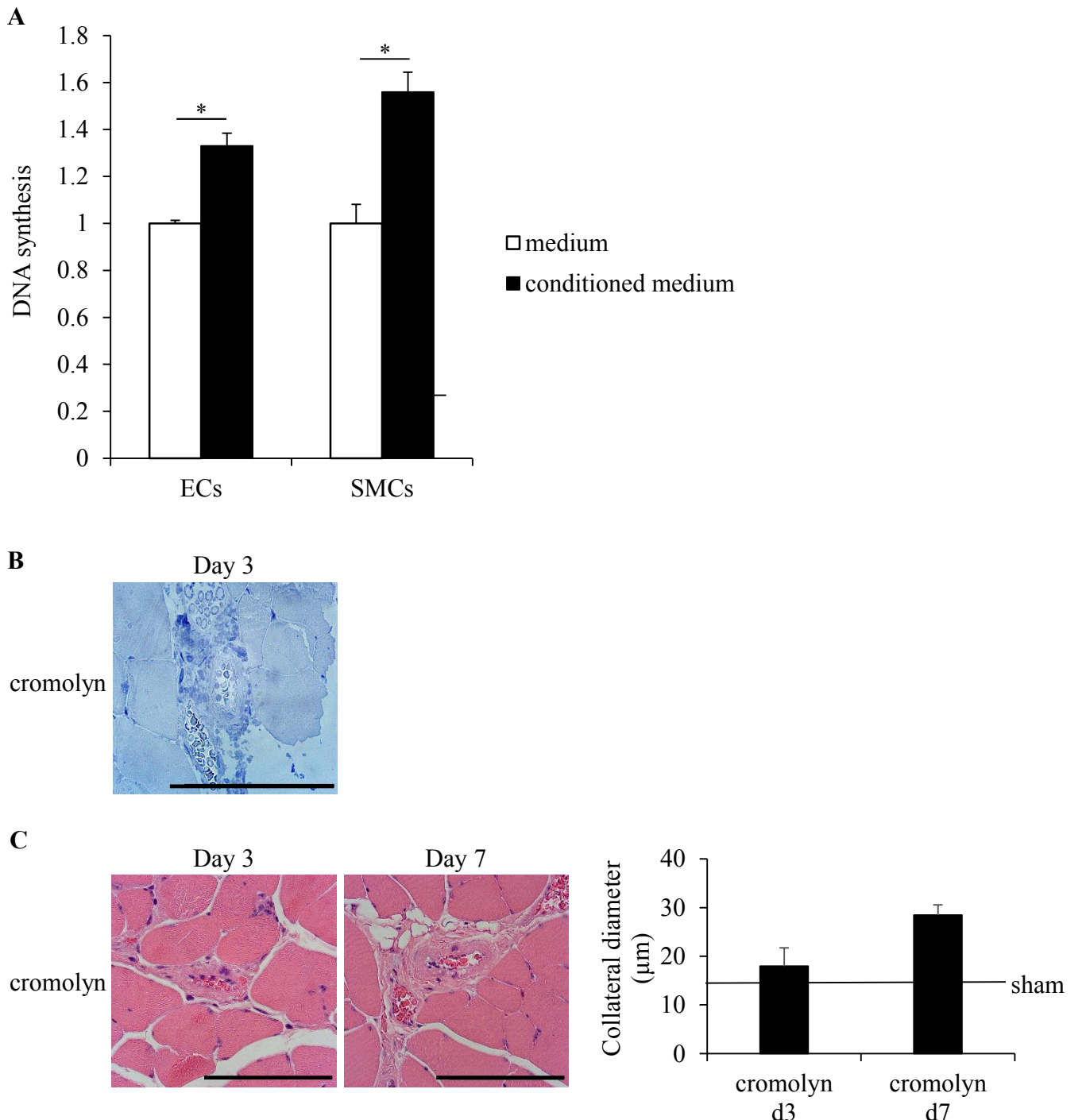


Figure S4. Related to Figure 3. In vitro proliferation assay and histological analyses

(A) Influence of mast cell degranulation factors on in vitro proliferation of primary murine endothelial (ECs) and smooth muscle cells (SMCs), measured by detection of DNA synthesis. Medium: supernatant of mast cells without induction of degranulation (control, number was defined as 1); conditioned medium: supernatant of degranulated mast cells. Data are means \pm SEM; n=3 in triplicates. (B) Immuno-staining of cromolyn treated mice showed no Ki67⁺ cells (stained in brown) in collaterals of mice 3 days after fal. Scale bar = 100mm. (C) Left: representative images of HE staining of collaterals of mice treated with cromolyn at day 3 or day 7 after fal. Scale bar = 100mm. Right: for measurement of luminal diameter 3 animals with 3 collaterals each were analyzed. Data are means \pm SEM

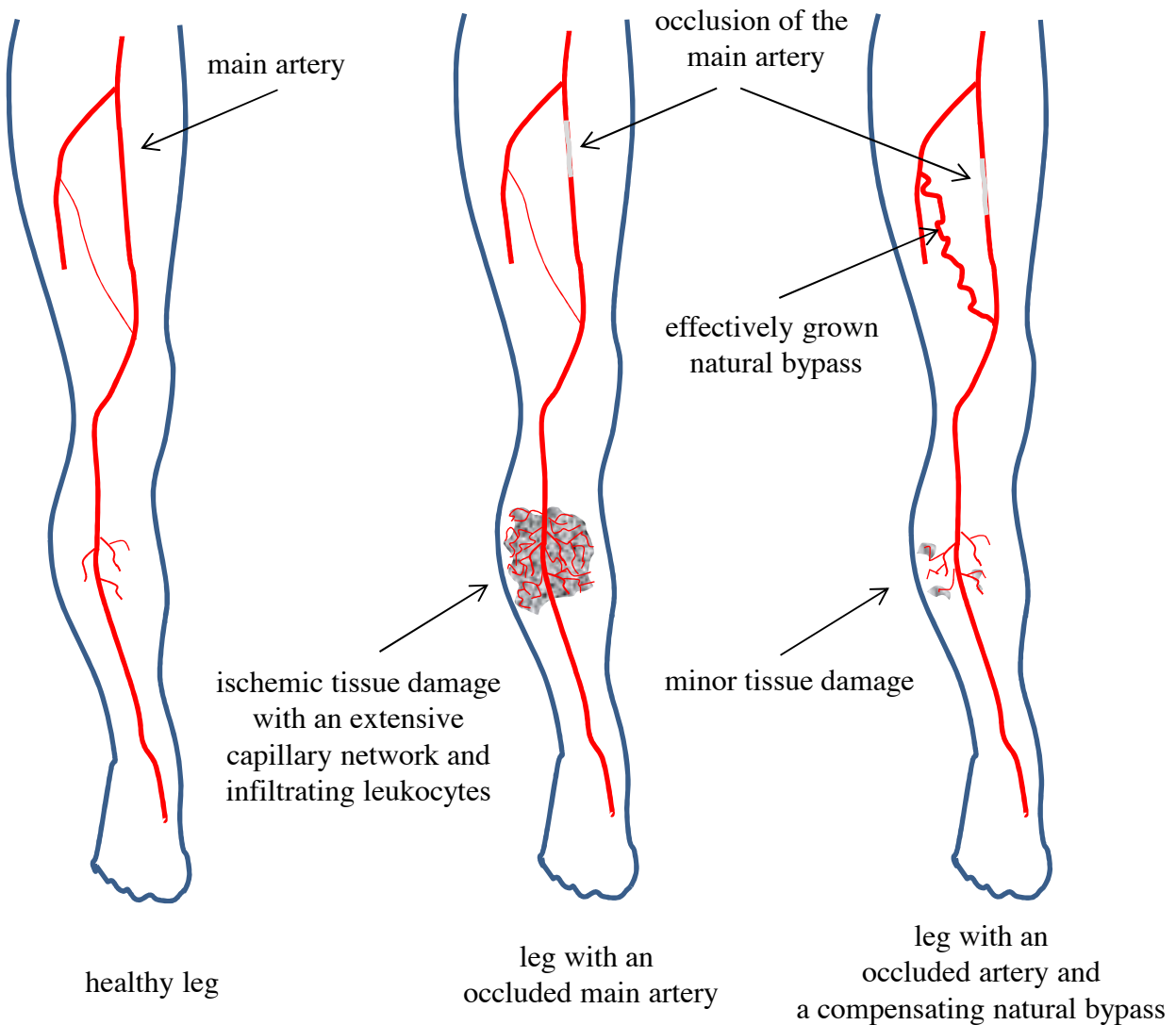


Figure S5. Related to Figure 4. Natural bypasses protect tissue from ischemic damage

Arteries have the function to transport oxygenated blood through the body. In the legs, the femoral artery of the upper leg is the main artery being responsible for blood supply to the lower leg (left). Upon occlusion of the femoral artery, the lower limb suffers from reduced blood supply resulting in tissue fibrosis and gangrene formation. This is associated with a strong infiltration of leukocytes and extensive capillary sprouting in order to remove cellular debris (middle). However, in case of effective collateral artery growth compensating for the loss of the occluded main artery, sufficient blood is transported to the lower leg by naturally grown bypasses preventing severe tissue damage. Accordingly, there is a reduced infiltration of leukocytes and capillary sprouting (right).

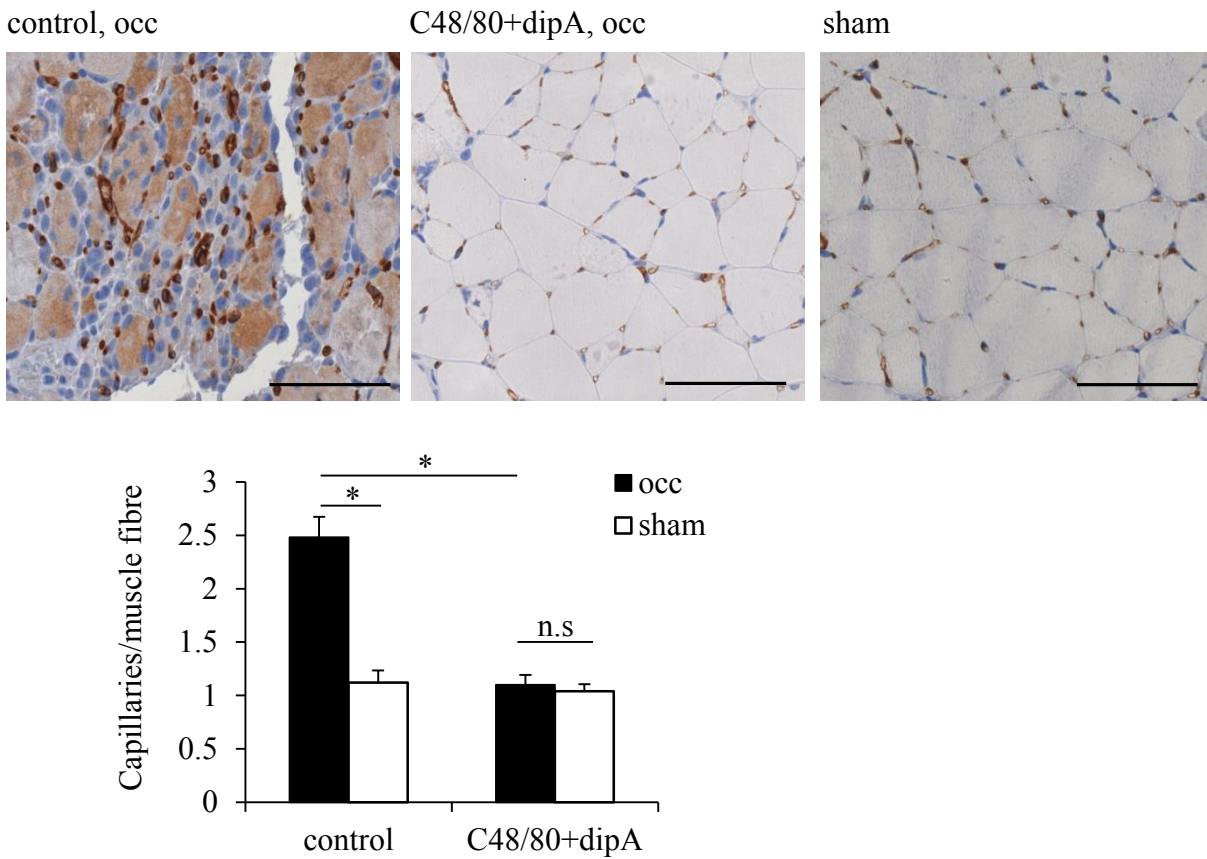


Figure S6. Related to Figure 4. Capillary/muscle fibre ratio

Upper panel: representative CD31 staining (ECs appear in brown) of the m. gastrocnemius of sham operated mice (sham) or mice treated with saline (control, occ) or C48/80+dipA (C48/80+dipA, occ) 3 days after fal. Scale bar = 100mm. Lower panel: for quantification of the capillary/muscle fibre ratio in gastrocnemius muscles high power fields of 6 slices from 3 individual experiments were analyzed. Data are means \pm SEM. Significances are from two-way ANOVA with subsequent Newman-Keuls test.

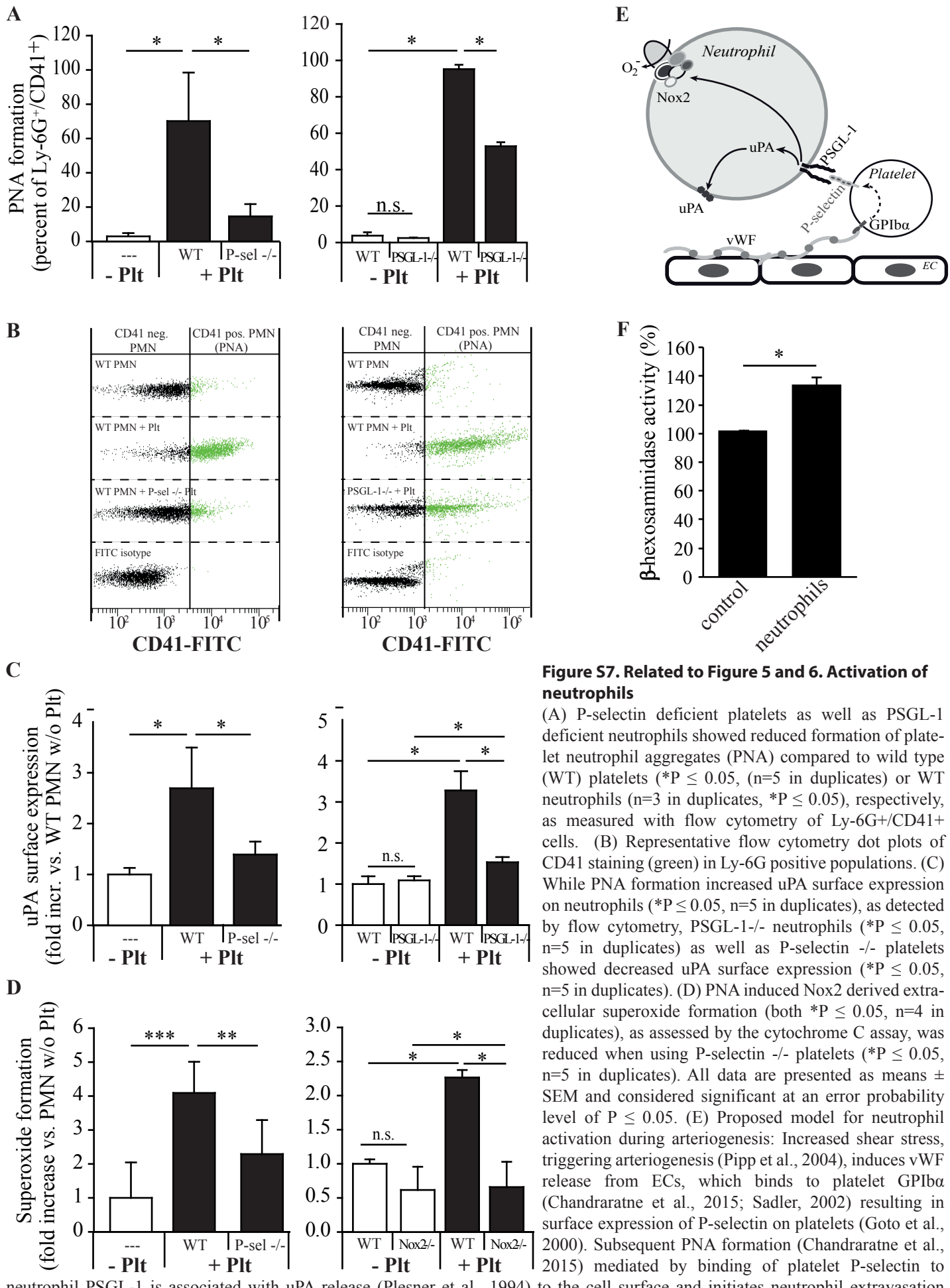


Figure S7. Related to Figure 5 and 6. Activation of neutrophils

(A) P-selectin deficient platelets as well as PSGL-1 deficient neutrophils showed reduced formation of platelet neutrophil aggregates (PNA) compared to wild type (WT) platelets (* $P \leq 0.05$, ($n=5$ in duplicates) or WT neutrophils ($n=3$ in duplicates, * $P \leq 0.05$), respectively, as measured with flow cytometry of Ly-6G⁺/CD41⁺ cells. (B) Representative flow cytometry dot plots of CD41 staining (green) in Ly-6G positive populations. (C) While PNA formation increased uPA surface expression on neutrophils (* $P \leq 0.05$, $n=5$ in duplicates), as detected by flow cytometry, PSGL-1^{-/-} neutrophils (* $P \leq 0.05$, $n=5$ in duplicates) as well as P-selectin ^{-/-} platelets showed decreased uPA surface expression (* $P \leq 0.05$, $n=5$ in duplicates). (D) PNA induced Nox2 derived extracellular superoxide formation (both * $P \leq 0.05$, $n=4$ in duplicates), as assessed by the cytochrome C assay, was reduced when using P-selectin ^{-/-} platelets (* $P \leq 0.05$, $n=5$ in duplicates). All data are presented as means \pm SEM and considered significant at an error probability level of $P \leq 0.05$. (E) Proposed model for neutrophil activation during arteriogenesis: Increased shear stress, triggering arteriogenesis (Pipp et al., 2004), induces vWF release from ECs, which binds to platelet GPIba (Chandraratne et al., 2015; Sadler, 2002) resulting in surface expression of P-selectin on platelets (Goto et al., 2000). Subsequent PNA formation (Chandraratne et al., 2015) mediated by binding of platelet P-selectin to neutrophil PSGL-1 is associated with uPA release (Plesner et al., 1994) to the cell surface and initiates neutrophil extravasation together with EC uPA (Reichel et al., 2011). (F) Co-culture of mast cells and activated neutrophils increased β -hexosaminidase activity, indicative for mast cell degranulation. The activity of control mast cells was set to 100 %. (* $P \leq 0.05$, $n=3$ in duplicates).

Supplemental Experimental Procedures

Murine hindlimb model of arteriogenesis

Ligation of the right femoral artery was induced in 8-10 weeks old mast cell deficient ($\text{Mcpt5-Cre}^+ \text{ R-DTA}$) (Dudeck et al., 2011), GPI α deficient (IL4-R/Iba mice) (Chandraratne et al., 2015), Nox2 deficient (Schulz et al., 2013), uPA deficient mice (Deindl et al., 2003) or corresponding wild type littermates as previously described (Limbourg et al., 2009). The left side was sham operated and served as control. SV129/S6 mice receiving the same surgical procedure were treated with Compound 48/80 to boost mast cell degranulation (McGowen et al., 2009), Diprotin A to boost mast cell recruitment (Juremalm et al., 2000; Zaruba et al., 2009), cromolyn to block mast cell degranulation (Vincent et al., 2013) (all from Sigma Aldrich) or SCF to boost mast cell maturation and activation (Oliveira and Lukacs, 2003) (Immuno Tools) as shown and described in Figure 7. 10 μl of uPA inhibitor UK122 (150mg/kg dissolved in DMSO, i.v., Santa Cruz) or solvent was given 1h before fal. The GPI α -inhibiting Fab fragment or the specific control isotype Fab (Chandraratne et al., 2015) was administered immediately before ligation (150mg/kg, i.v.). Apocynin (Schulz et al., 2013) (50mg/kg/d) (Santa Cruz Biotechnology) or N-acetylcysteine (Tobar et al., 2010) (1g/kg/d) (Sigma Aldrich), respectively, was administered in drinking water starting 3 days before ligation. Neutropenia was induced by administration of neutrophil depleting antibody 1A8 (Drechsler et al., 2010) (100mg/kg, i.p.) (BioXcell) 2 days before ligation and again immediately after fal. Blinded analysis was performed when evaluating tissue samples from these experiments.

Laser Doppler perfusion measurements

Laser Doppler perfusion measurements and calculations of left leg to right leg ratio were performed as previously described (Limbourg et al., 2009; Pagel et al., 2012) using the Laser Doppler Imaging technique (MoorLDI 5061 and Moor Software Version 3.01, from Moor Instruments).

Bone marrow transplantation

For the bone marrow transplantation, 3 x 10 6 bone marrow cells of C57BL/6-Ly5.1 mice were injected into the tail vein of lethally irradiated (twice 600rads) Nox2-/- mice and vice versa. After 6 weeks, when a stable chimerism was guaranteed with flow cytometry analysis of CD45.1 and CD45.2 cell counts, the mice were used for femoral artery ligation and laser Doppler perfusion measurements. Furthermore, Nox2-/- mice received Nox2-/- bone marrow cells and C57BL/6-Ly5.1 mice received C57BL/6-Ly5.1 bone marrow cells, in order to rule out the possible influence of the transplantation on the experiments.

qRT-PCR analyses

Total RNA from collaterals was extracted with Trizol (Life technologies) and DNA digested with DNase I (Promega). 250ng of total RNA was reverse transcribed with the 1st Strand cDNA synthesis kit (Roche), and cDNA was diluted 1:5 in RNase free water. Quantitative PCR was performed with 1 μl diluted cDNA using Power Sybr Green master mix (Life technologies) following manufacturer's protocol and as previously described (Pagel et al., 2012) in a StepOnePlus light cycler (Life technologies). Specific amplification was controlled by melt curve analyses and expression level of MCP-1 was related to the expression levels of the 18S rRNA. On each template three independent qRT-PCR reactions were performed. The primer sequences were as follows: Egr-1, forward, 5'-CGAACAAACCTATGAGCACCTG-3', reverse, 5'-CAGAGGAAGACGATGAAGCAGC-3'; 18S rRNA, forward, 5'-GGACAGGATTGACAGATTGATAG-3', 5'-CTCGTTCGTTATCGGAATTAAC-3'.

Isolation of bone marrow mononuclear cells

C57Bl6J (4-6) mice of 8-12 weeks were sacrificed by cervical dislocation: intact femurs and tibias were removed, and bone marrow cells were harvested by repeated flushing with minimal essential medium. Cells were cultured as described previously (Stassen et al., 2003). Characterization of cells was performed by flow cytometry analysis using anti-mouse c-kit antibody (CD117 from Invitrogen).

Endothelial cells

Mouse coronary endothelial cells were purchased from CellBiologics and cultured as described (CellBiologics Inc.).

Vascular smooth muscle cells

Mouse vascular SMCs were isolated as described earlier (Kanse et al., 1997) and cultivated in Iscove's modified medium containing 10% (v/v) heat-inactivated fetal calf serum, 10U/ml penicillin, 10g/ml streptomycin, and 2mM L-glutamine.

Cell proliferation assay

Cell proliferation was determined by a colorimetric immunoassay, which based on the uptake of BrdU during DNA synthesis and the quantitative binding of a monoclonal anti-BrdU antibody (Roche Diagnostics). Cells were cultivated in a 96-well microtiterplate. Subsequently, supernatants derived from mast cells treated for 1h with ionomycin (1µM, Sigma) or solvent were diluted in serum-free medium to a total volume of 100µl/well. After an incubation period of three days BrdU-incorporation was determined.

Isolation of murine neutrophils and platelets

Murine bone marrow cells were harvested from tibias and femurs of PSGL-1^{-/-}, Nox2^{-/-}, or corresponding wild type mice, respectively, and cultured as previously described (Walzog et al., 1999). Prior to experiments, neutrophils were washed and resuspended in Hank's solution supplemented with 0.25% BSA and 0.1% glucose. Platelet rich plasma from citrated whole blood (wild type or P-selectin deficient mice) was obtained by centrifugation at 200g for 5min. Platelets were pelleted (450g, 10min) and resuspended in a buffer containing 138mM NaCl, 2.7mM KCl, 12mM NaHCO₃, 0.4mM NaH₂PO₄, 1mM MgCl₂, 5mM D-glucose, 5mM Hepes, pH 7.35. Neutrophil and platelet concentrations were measured in a Beckman Coulter (FL/USA) and adjusted to concentrations of 1x10³/µl or 2x10⁵/µl, respectively.

Platelet-neutrophil interaction *in vitro*

For flow cytometry or superoxide anion detection neutrophils were incubated with platelets in an 1:200 ratio at 37°C for 10 or 30min, respectively. PNA formation or surface uPA on neutrophils was measured by flow cytometry (FACS Canto II, BD Biosciences) by incubating cells with FITC-labeled rat anti-mouse CD41 antibody (Cat# 11-0411-81, eBioscience), the corresponding rat isotype control IgG1 FITC (Cat# 11-4301-81, eBioscience), anti-uPA rabbit polyclonal antibody (H140, Cat# sc14019, Santa Cruz; labelled with Alexa fluor 488 labeling kit, life technologies), or the rabbit polyclonal isotype control (Cat# CTL-4112, Biolegend), respectively. Co-staining with an APC-labelled anti-Ly-6G antibody (Cat# 17-5931-81, eBioscience) was performed to identify the neutrophil population. To detect superoxide anion release neutrophil suspensions (Hank's solution, 0.25% BSA, 0.1% glucose) were supplemented with 0.5mg/ml cytochrome C (Sigma) prior to incubation with platelets. Supernatants were transferred to a 96-well plate and absorbance was measured at 550nm. To exclude reduction from radicals others than superoxide anions, samples supplemented with 200U/ml superoxide dismutase (SOD; Roche) were measured in parallel and values were subtracted from values without SOD.

Co-culture of mast cells and neutrophils

300 µl of human mast cells (HMC-1) were seeded into a 24 well plate (2 x 10⁶ cells/ml) in RPMI medium without FCS. After 2 hours filter inserts with a pore size of 0.4 µm (BD Biosciences) containing either 100 µl of RPMI or 100 µl of freshly isolated human neutrophils (500000 cells) were placed above the mast cells. To activate neutrophils, phorbol 12-myristate 13-acetate (PMA, Sigma-Aldrich) was added to the neutrophils and as a control also to medium-containing filter inserts.

After 3 hours, filter inserts containing medium or neutrophils were removed and supernatants of HMC-1 were used for β-hexosaminidase assay. In brief, supernatants were incubated with 26 mM citrate buffer (pH4.5) and 2.3 mg/ml p-nitrophenyl N-acetyl-α-D-glucosaminide for 90 min at 37 °C. The reaction was stopped by adding 0.4 mM glycine (pH 10.7), and the absorbance was measured at 405 and 570 nm using a multiplate reader.

References

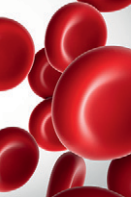
- Deindl, E., Ziegelhoeffer, T., Kans, S.M., Fernandez, B., Neubauer, E., Carmeliet, P., Preissner, K., and Schaper, W. (2003). Receptor-independent role of the urokinase-type plasminogen activator during arteriogenesis. *FASEB J* 17, 1096/fj.01-0563fje.
- Drechsler, M., Megens, R.T., van Zandvoort, M., Weber, C., and Soehnlein, O. (2010). Hyperlipidemia-triggered neutrophilia promotes early atherosclerosis. *Circulation* 122, 1837-1845.
- Dudeck, A., Dudeck, J., Scholten, J., Petzold, A., Surianarayanan, S., Kohler, A., Peschke, K., Vohringer, D., Waskow, C., Krieg, T., et al. (2011). Mast cells are key promoters of contact allergy that mediate the adjuvant effects of haptens. *Immunity* 34, 973-984.
- Goto, S., Ichikawa, N., Lee, M., Goto, M., Sakai, H., Kim, J.J., Yoshida, M., Handa, M., Ikeda, Y., and Handa, S. (2000). Platelet surface P-selectin molecules increased after exposing platelet to a high shear flow. *International angiology : a journal of the International Union of Angiology* 19, 147-151.
- Juremalm, M., Hjertson, M., Olsson, N., Harvima, I., Nilsson, K., and Nilsson, G. (2000). The chemokine receptor CXCR4 is expressed within the mast cell lineage and its ligand stromal cell-derived factor-1alpha acts as a mast cell chemotaxin. *European journal of immunology* 30, 3614-3622.

- Kanse, S.M., Benzakour, O., Kanthou, C., Kost, C., Lijnen, H.R., and Preissner, K.T. (1997). Induction of vascular SMC proliferation by urokinase indicates a novel mechanism of action in vasoproliferative disorders. *Arterioscler Thromb Vasc Biol* 17, 2848-2854.
- McGowen, A.L., Hale, L.P., Shelburne, C.P., Abraham, S.N., and Staats, H.F. (2009). The mast cell activator compound 48/80 is safe and effective when used as an adjuvant for intradermal immunization with *Bacillus anthracis* protective antigen. *Vaccine* 27, 3544-3552.
- Plesner, T., Ploug, M., Ellis, V., Ronne, E., Hoyer-Hansen, G., Wittrup, M., Pedersen, T.L., Tscherning, T., Dano, K., and Hansen, N.E. (1994). The receptor for urokinase-type plasminogen activator and urokinase is translocated from two distinct intracellular compartments to the plasma membrane on stimulation of human neutrophils. *Blood* 83, 808-815.
- Stassen, M., Muller, C., Richter, C., Neudorfl, C., Hultner, L., Bhakdi, S., Walev, I., and Schmitt, E. (2003). The streptococcal exotoxin streptolysin O activates mast cells to produce tumor necrosis factor alpha by p38 mitogen-activated protein kinase- and protein kinase C-dependent pathways. *Infect Immun* 71, 6171-6177.
- Vincent, L., Vang, D., Nguyen, J., Gupta, M., Luk, K., Ericson, M.E., Simone, D.A., and Gupta, K. (2013). Mast cell activation contributes to sickle cell pathobiology and pain in mice. *Blood* 122, 1853-1862.
- Walzog, B., Weinmann, P., Jeblonski, F., Scharffetter-Kochanek, K., Bommert, K., and Gaehtgens, P. (1999). A role for beta(2) integrins (CD11/CD18) in the regulation of cytokine gene expression of polymorphonuclear neutrophils during the inflammatory response. *FASEB J* 13, 1855-1865.

X. Veröffentlichung 2

Lasch, M., Kleinert, E. C., Meister, S., Kumaraswami, K., Buchheim, J. I., Grantzow, T., Fleming, I., Randi, A. M., Sperandio, M., Preissner K. T. & Deindl, E. (2019). Extracellular RNA released due to shear stress controls natural bypass growth by mediating mechanotransduction in mice. *Blood*, 134(17), 1469-1479.

<https://doi.org/10.1182/blood.2019001392>



VASCULAR BIOLOGY

Extracellular RNA released due to shear stress controls natural bypass growth by mediating mechanotransduction in mice

Manuel Lasch,^{1,2} Eike Christian Kleinert,¹ Sarah Meister,^{3,4} Konda Kumaraswami,¹ Judith-Irina Buchheim,^{1,5} Tobias Grantzow,¹ Thomas Lautz,¹ Sofia Salpisti,⁶ Silvia Fischer,⁶ Kerstin Troidl,^{7,8} Ingrid Fleming,⁹ Anna M. Randi,¹⁰ Markus Sperandio,¹ Klaus T. Preissner,⁶ and Elisabeth Deindl¹¹

¹Walter Brendel Centre of Experimental Medicine, University Hospital, ²Department of Otorhinolaryngology, Head and Neck Surgery, University Hospital, ³Institut für Laboratoriumsmedizin, ⁴Department of Obstetrics and Gynaecology, and ⁵Laboratory of Translational Research "Stress and Immunity," Department of Anaesthesiology, University Hospital, Ludwig Maximilian University of Munich, Munich, Germany; ⁶Institute for Biochemistry, Medical School, Justus-Liebig-Universität, Giessen, Germany; ⁷Department of Pharmacology, Max Planck Institute for Heart and Lung Research, Bad Nauheim, Germany; ⁸Department of Vascular and Endovascular Surgery, University Hospital Frankfurt, Frankfurt am Main, Germany; ⁹Institute for Vascular Signalling, Vascular Research Centre, Goethe University, Frankfurt am Main, Germany; and ¹⁰National Heart and Lung Institute, Hammersmith Hospital, Imperial College London, London, United Kingdom

KEY POINTS

- Shear stress–induced release of RNA from endothelial cells is crucial for initiation of arteriogenesis by controlling mechanotransduction.
- Extracellular RNA is essential for VWF release from endothelial cells initiating the inflammatory process driving arteriogenesis.

Fluid shear stress in the vasculature is the driving force for natural bypass growth, a fundamental endogenous mechanism to counteract the detrimental consequences of vascular occlusive disease, such as stroke or myocardial infarction. This process, referred to as "arteriogenesis," relies on local recruitment of leukocytes, which supply growth factors to preexisting collateral arterioles enabling them to grow. Although several mechanosensing proteins have been identified, the series of mechanotransduction events resulting in local leukocyte recruitment is not understood. In a mouse model of arteriogenesis (femoral artery ligation), we found that endothelial cells release RNA in response to increased fluid shear stress and that administration of RNase inhibitor blocking plasma RNases improved perfusion recovery. In contrast, treatment with bovine pancreatic RNase A or human recombinant RNase1 interfered with leukocyte recruitment and collateral artery growth. Our results indicated that extracellular RNA (eRNA) regulated leukocyte recruitment by engaging vascular endothelial growth factor receptor 2 (VEGFR2), which was confirmed by intravital microscopic studies in a murine cremaster model of inflammation. Moreover, we found that release of von Willebrand factor (VWF) as a result of shear stress is dependent on VEGFR2. Blocking VEGFR2, RNase application, or VWF deficiency interfered with platelet–neutrophil aggregate formation, which is essential for initiating the inflammatory process in arteriogenesis. Taken together, the results show that eRNA is released from endothelial cells in response to shear stress. We demonstrate this extracellular nucleic acid as a critical mediator of mechanotransduction by inducing the liberation of VWF, thereby initiating the multistep inflammatory process responsible for arteriogenesis. (Blood. 2019;134(17):1469-1479)

Introduction

Vascular occlusive diseases are the leading cause of morbidity and mortality worldwide. Interestingly, the human body has an endogenous mechanism that can compensate for the loss of an artery. Preexisting arteriolar connections can grow to form a natural bypass, thereby substituting for the occluded vessel.¹ Accordingly, much effort has been spent to unravel the molecular mechanisms of this process, called "arteriogenesis," to enable clinicians to promote this process in patients suffering from myocardial infarction, stroke, or peripheral artery disease (PAD). If successful, this would lead to a substitution for invasive treatments, such as percutaneous luminal angioplasty, bypass surgery, or even heart transplantation.

Intensive research over the last years revealed that arteriogenesis relies on a local inflammatory process that is triggered by fluid shear stress.² Upon narrowing or occlusion of a feeding artery, blood flow is redirected into preexisting arteriolar connections. In these vessels, the subsequently increased fluid shear stress causes an activation of the endothelium, followed by an inflammatory cascade initiated by platelet receptor glycoprotein 1ba (GPIba) and platelet–neutrophil aggregate (PNA) formation.³⁻⁵ Finally, perivascular-recruited macrophages promote collateral artery growth by a cytokine burst to restore blood flow.⁶

A mechanosensory complex consisting of platelet endothelial cell adhesion molecule-1 (PECAM-1), the cell–cell adhesion

receptor vascular endothelial cell (EC) cadherin, and vascular endothelial growth factor receptor 2 (VEGFR2) has been identified by in vitro studies, and results were confirmed in aortas of mice at sites of disturbed blood flow prone to leukocyte recruitment and atherosclerosis.⁷ However, the mechanisms of mechanosensing of ECs are still incompletely understood.⁸ Other investigators have shown that, in response to shear stress, ECs release ATP, which activates the G proteins Gq and G11-coupled purinergic P2Y₂ receptors, which are relevant for tyrosine phosphorylation of PECAM-1.⁹ Subsequently, PECAM-1, which forms a complex with vascular EC cadherin, recruits VEGFR2. Although the direct blockade of VEGFR2 or antibodies directed against vascular endothelial growth factor A (VEGFA) strongly interferes with arteriogenesis, the process is only marginally, if at all, promoted by additional doses of VEGFA (for an overview see Jazwa et al¹⁰), because endogenous VEGFA levels are not rate limiting in arteriogenesis.¹¹ However, for proper arteriogenesis to occur, enhanced VEGFR2 signaling is required. This is mediated by the non-tyrosine kinase coreceptor neuropilin 1 (NRP-1),¹² which is capable of binding the VEGRA₁₆₅ isoform of VEGFA, thereby increasing the local plasma membrane concentration of VEGFA and promoting its binding to VEGFR2.¹³⁻¹⁵ Interestingly, recent in vitro studies from our group pointed to a role for heparin or extracellular RNA (eRNA) in NRP-1-mediated activation of VEGFR2.¹⁶

Nucleic acids, which can be released upon cellular damage, are not inert molecules but trigger diverse biological reactions. For example, they are involved in innate immune reactions related to bacterial killing by neutrophil extracellular traps,¹⁷ as well as thrombus and edema formation.^{18,19} Recently, we were able to demonstrate that eRNA promotes leukocyte recruitment and extravasation in a murine cremaster model of inflammation, identifying eRNA as a proinflammatory factor.²⁰ Arteriogenesis is a matter of innate immunity that involves recruitment of neutrophils, followed by mast cell activation and recruitment of T cells and macrophages.⁴ Whether eRNA plays a role in arteriogenesis has never been investigated, and it was the topic of the present study.

Materials and methods

Quantification of eRNA and LDH in vitro

Bovine aortic ECs (BAECs) were isolated from bovine aorta, as described,²¹ and cultured in Dulbecco's modified Eagle medium containing 10% (volume-to-volume ratio) fetal calf serum. To determine the release of cellular RNA, confluent BAECs were washed twice with phosphate buffered saline (pH 7.4) and maintained under static conditions or exposed to shear stress (12 dyn/cm²) in fetal calf serum-free medium for 60 minutes in a temperature-controlled cone-plate viscosimeter, as previously described.²² Cell supernatants were removed and centrifuged for 5 minutes at 200g to remove cells and cell debris. RNA was isolated using a Master Pure RNA purification kit (Epicentre Biotechnologies, Madison, WI) and quantified using Quant-iT Technology (Invitrogen). Lactate dehydrogenase (LDH) was determined in cell supernatants by measuring its activity using a detection kit (Roche Diagnostics, Basel, Switzerland).

Animals and treatments

All experiments were performed in strict accordance with the German animal legislation guidelines and were approved by the Bavarian Animal Care and Use Committee. Mice were housed in

a temperature-controlled room on a 12-hour light-dark cycle and were fed a standard laboratory diet. Our investigations were performed with wild-type C57BL/6J mice (Charles River Laboratories, Sulzfeld, Germany), which also served as controls for our studies on intercellular adhesion molecule 1 (ICAM-1)-deficient mice (*ICAM1^{tm1Jgr}*),²³ which were a generous gift from C. Scheiermann (Walter Brendel Centre of Experimental Medicine), and von Willebrand factor (VWF)-deficient mice (B6.129S2-Vwf^{tm1Wgr/J}).²⁴ Because C57BL/6J mice show a high spontaneous blood flow recovery rate, for RNase inhibitor treatment we used SV129 mice (Charles River Laboratories), which show a relatively reduced perfusion recovery.²⁵

C57BL/6J mice were treated IV with bovine RNase A (Thermo Fisher Scientific, Waltham, MA), active or inactive human RNase1 (both manufactured by ProteoGenix, Schiltigheim, France), or DNase (Promega, Madison, WI), at a dose of 50 µg/kg, dissolved in saline starting 30 minutes before femoral artery ligation (FAL) and then every other day until the end of the experiment. To inhibit VEGFR2, mice were treated intraperitoneally with semaxanib (Hycultec, Beutelsbach, Germany), 25 mg/kg per day dissolved in dimethyl sulfoxide (DMSO), starting 1 day before the surgical procedure. The highly selective blocking antibody of VEGFR2, DC101 (Bio X Cell, West Lebanon, NH), was administered equally to semaxanib, at a dose of 20 mg/kg dissolved in saline. SV129 mice were treated IV with 20 U RNase inhibitor (Thermo Fisher Scientific) dissolved in saline immediately after ligation and then daily until day 3 after ligation. To block mast cell degranulation, mice were treated intraperitoneally with cromolyn (Sigma-Aldrich, St. Louis, MO), 20 mg/kg per day dissolved in DMSO, starting 3 days before ligation. The control groups of all experimental set-ups were treated with the appropriate solvent.

Additional methods

For a detailed description of FAL, Laser-Doppler perfusion measurements, tissue sampling, histology, immunohistology, flow cytometry analyses, white blood cell counts, and intravital microscopy of the cremaster muscle please see supplemental Material and methods (available on the Blood Web site).

Statistical analyses

Statistical analyses were calculated with GraphPad Prism 6 (GraphPad Software, La Jolla, CA). Data are mean ± standard error of the mean (SEM). Statistical analyses were conducted as indicated in the figure legends. Results were considered statistically significant at $P < .05$.

Results

Fluid shear stress induces the release of eRNA

Collateral artery growth is locally induced by increased fluid shear stress in arterioles bypassing a stenosed vessel. Because arteriogenesis is not associated with cell damage at sites of vessel growth, we wanted to investigate whether fluid shear stress might trigger the release of RNA from ECs. Indeed, the application of shear stress to primary ECs in culture resulted in significantly increased levels of eRNA in cell supernatant (Figure 1A). Because increased eRNA levels were not associated with increased LDH activity (Figure 1B), these data indicate that the eRNA was liberated from ECs as a result active release and not cell damage.

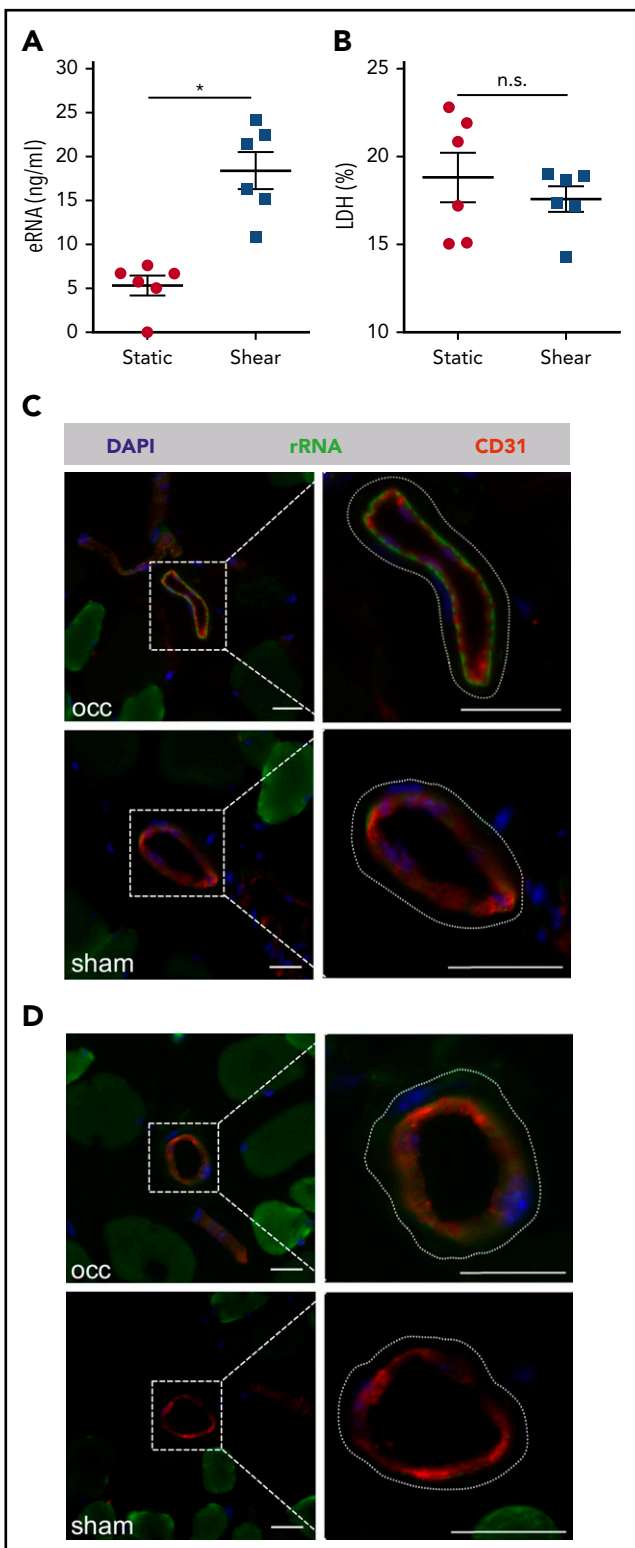


Figure 1. In vitro and in vivo analysis of eRNA release. (A) eRNA levels were measured in supernatant of BAECs, with or without shear conditions of 12 dyn/cm² for 60 minutes. (B) The levels of LDH (expressed as percentage of total) were measured in the same supernatants of the BAECs, exposed to shear or under static conditions. Data are mean \pm SEM; n = 6 per group. (C-D) Representative fluorescent immunohistological pictures of collaterals of mice 30 minutes after induction of arteriogenesis (occ) or sham operation. To visualize collaterals, tissue samples were stained with an antibody against CD31 (red) depicting ECs. Nuclei were counterstained with 4',6-diamidino-2-phenylindole. The dashed lines in the magnified

To investigate whether fluid shear stress might also be associated with release of eRNA in vivo, a fluorescently labeled antibody directed against ribosomal RNA was administered IV immediately after induction of arteriogenesis by FAL, making use of the general property of antibodies not to enter cells. Immunohistological analyses of cross-sections of adductor muscles containing growing collaterals isolated 30 minutes after the experimental procedure revealed decoration of the EC layer with eRNA at its basolateral surface, an observation that was not made in resting collaterals from the contralateral sham-operated side (Figure 1C) or from control-treated animals (Figure 1D).

RNase, but not DNase or inactive RNase, treatment interferes with arteriogenesis

To investigate whether extracellular nucleic acids might play a role in arteriogenesis, mice were treated with bovine RNase A or DNase using the FAL model. Following induction of arteriogenesis, RNase A but not DNase treatment provoked a significant reduction in perfusion recovery in comparison with saline-treated control mice (Figure 2A). In this context, it is important to mention that treatment of animals with RNase has no toxic side effect (even when overdosed 20-fold), as demonstrated by our previous in vivo studies.^{26,27} To examine whether the reduction in perfusion recovery was due to eRNA degradation by RNase or to an unknown function of RNase, mice were treated with recombinant human active or inactive RNase1 (which is the counterpart of bovine RNase A), respectively. Again, perfusion recovery was reduced in mice treated with active RNase1 but not in mice treated with inactive RNase1 (Figure 2B). Moreover, our histological analyses revealed a significant reduction in the luminal diameter of growing collaterals in mice treated with RNase A or active RNase1 but not in mice treated with inactive RNase1 (Figure 2C-D).

Because exogenously administered RNA is rapidly degraded by endogenous RNase in blood²⁸ and is suitable for acute, but not chronic, in vivo experiments, such as arteriogenesis²⁰ (see "Discussion"), mice were treated with RNase inhibitor to fully block any endogenous RNases to protect eRNA against degradation. In vitro RNase inhibitor showed no signs of toxicity to induce the release of LDH (supplemental Figure 1A-C) at concentrations used for the in vivo experiments (10 U/mL). In vivo, the administration of RNase inhibitor significantly increased perfusion recovery after FAL, suggesting that an increase in eRNA bioavailability improves arteriogenesis (supplemental Figure 1D). Together, these results confer a decisive role for eRNA in the process of fluid shear stress–induced arteriogenesis.

RNase treatment interferes with neutrophil extravasation and mast cell activation

To investigate whether eRNA plays a role in the previously identified pathway of perivascular macrophage accumulation during collateral artery growth,⁴ we investigated leukocyte recruitment and mast cell activation in the process of arteriogenesis.

Figure 1 (continued) images (right panels) delineate the outer border of the vessels of the smooth muscle cells. A specific signal for the IV applied fluorescently labeled antibody against ribosomal RNA (green) was found at the abluminal side of ECs of growing collaterals (occ, upper panel), but not of resting collaterals (sham, lower panel) (C), or control mice (D). Scale bars, 20 μ m. *P < .05, unpaired Student t test. n.s., not significant.

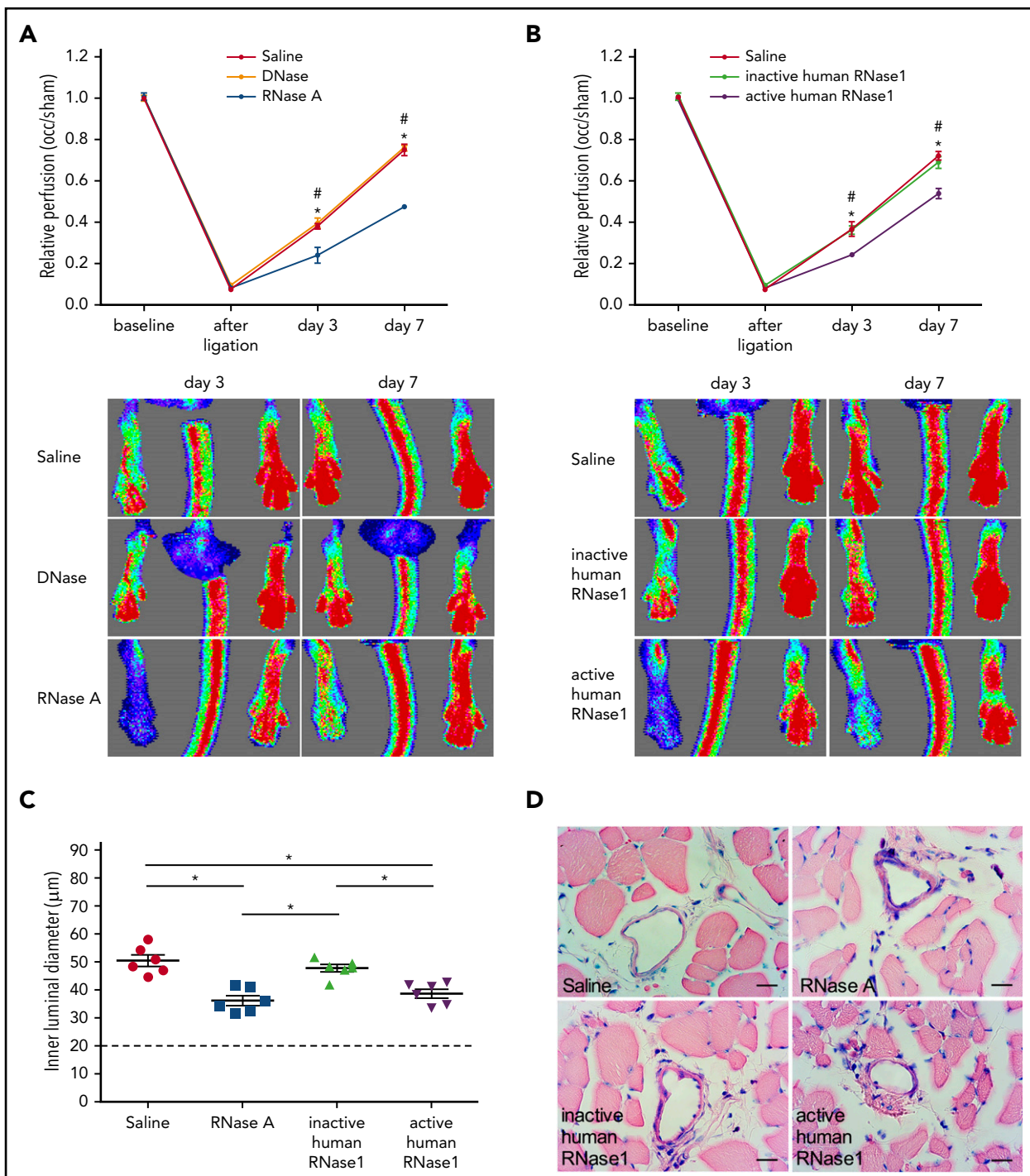


Figure 2. RNase treatment decreases perfusion recovery and vessel growth. (A-B) Laser Doppler perfusion measurements (upper panels) and corresponding flux images (lower panels) of mice treated as indicated. The perfusion was calculated using occluded/sham (right to left) ratios before the surgical procedure, immediately after the surgical procedure, and at days 3 and 7 after surgery ($n = 6$). Representative flux images are shown for days 3 and 7. (C) The dot plots show the inner luminal diameter of mice treated with saline, RNase A, or recombinant inactive or active human RNase1 7 days after the surgical procedure ($n = 6$ per group). Data are mean \pm SEM. The dashed horizontal line indicates the mean sham value. (D) Representative photomicrographs of Giemsa-stained tissue samples. Scale bars, 20 μm . * $P < .05$; *saline vs RNase A, #DNase vs RNase A, *saline vs active human RNase1, *inactive human RNase1 vs active human RNase1, 2-way analysis of variance (ANOVA) with the Bonferroni multiple-comparison test (A-B) and 1-way ANOVA with the Bonferroni multiple-comparison test (C).

Compared with control, treatment of mice with RNase A or active RNase1 resulted in a significant reduction in the number of infiltrated neutrophils ($\text{CD45}^+/\text{Gr1}^+/\text{CD115}^-$) at day 1 following induction of arteriogenesis (Figure 3A-D). This was accompanied by a reduced number of degranulating mast cells in the

perivascular space of growing collateral arteries and was comparable with treatment using the mast cell stabilizer cromolyn (Figure 3E). In contrast, administration of inactive RNase1 did not have an influence on neutrophil recruitment or on mast cell degranulation (Figure 3C-E), confirming that eRNA plays a role in

neutrophil-related mast cell activation. At day 3 following RNase A treatment, reduced numbers of infiltrated macrophages ($CD45^+/F4/80^+$) were seen, in line with the function of activated and degranulated mast cells in the promotion of perivascular accumulation of macrophages (Figure 3F-H). The parallel analyses of blood samples on day 1 and day 3 revealed that RNase A treatment had no influence on the number of circulating leukocyte subsets (Figure 3I-J). This indicates that RNase treatment exclusively affected perivascular leukocyte recruitment but not their mobilization from the bone marrow.

VWF release from ECs is dependent on eRNA and VEGFR2

It has been shown *in vitro* and *in vivo* that VWF is released from ECs as (ultra-)large multimers under conditions of increased shear stress.^{29,30} VWF provides a major ligand for platelet receptor GPIba, mediating effective platelet adhesion, particularly under high fluid shear stress.^{29,31} In addition to other mechanisms, it is well described that VEGFA induces VWF release from endothelial Weibel-Palade bodies (WPBs) by activating the cognate VEGFR2.³² Therefore, we asked whether VEGFR2 is relevant for VWF release under conditions of increased shear stress during arteriogenesis and whether eRNA might play a role in this process.

Administration of the VEGFR2 inhibitor semaxanib (SU5416) significantly interfered with perfusion recovery and collateral artery growth (Figure 4A-D), confirming previous results.¹⁰ To investigate whether VWF is released from collateral ECs during the process of arteriogenesis, we again took advantage of the properties of antibodies not to be able to enter cells and administered an IV antibody against VWF 30 minutes prior to tissue sampling. Our immunohistological analyses performed on tissue samples isolated 2 hours after the surgical procedure showed that induction of arteriogenesis resulted in the release of VWF from ECs of growing collateral arteries (Figure 4E-F). This release process was almost completely abolished when mice were pretreated with semaxanib, a VEGFR2-blocking antibody (DC101), or RNase A (Figure 4E-F).

eRNA and VEGFR2 play a crucial role in PNA formation

We have previously shown that platelet activation by platelet receptor GPIba, followed by PNA formation, is a prerequisite for mast cell degranulation in the context of arteriogenesis.⁴ In the course of the present study, treatment of mice with RNase A or with the VEGFR2 blocker semaxanib, as well as VWF deficiency, significantly interfered with PNA formation. These data indicate that the process of arteriogenesis is dependent on VWF release mediated by activation of VEGFR2 involving eRNA (Figure 5A-C). Under these experimental conditions, the numbers of peripheral blood neutrophils and platelets were not altered (Figure 5D-E), suggesting that the reduced PNA formation in differently treated mice was not due to a reduced bioavailability of 1 of the PNA components.

eRNA initiates mast cell-mediated macrophage recruitment and vascular cell proliferation

The administration of RNase A or semaxanib, as well as a VWF deficiency, in mice also significantly interfered with mast cell degranulation without influencing mast cell recruitment *per se* (supplemental Figure 2), accounting for an eRNA-induced

signaling pathway of mast cell activation. The treatment of mice with RNase A or semaxanib interfered with perivascular M1-polarized ($CD68^+MRC1^-$) and M2-polarized ($CD68^+MRC1^+$) macrophage accumulation (supplemental Figure 3). Comparable results were obtained with mice that were deficient for ICAM-1 (an endothelial adhesion receptor whose increased expression is dependent on enhanced VEGFR2/NRP-1 signaling³³), which is upregulated during arteriogenesis³⁴ and is relevant for monocyte adhesion during collateral artery growth,³⁵ as well as in mice that were treated with the mast cell degranulation blocker cromolyn (supplemental Figure 3). These latter results are in line with our previous data showing that mast cell activation/degranulation is essential for perivascular macrophage recruitment in arteriogenesis.⁴ Moreover, reduced perivascular macrophage accumulation under the same experimental settings was associated with a reduced proliferation of collateral artery ECs and smooth muscle cells after induction of arteriogenesis (supplemental Figure 4). These findings underline the relevance of leukocytes as a source of growth factors and cytokines for the process of arteriogenesis.^{36,37}

eRNA mediates VEGFR2-induced inflammation

To further confirm our data that eRNA is essential for VEGFR2-promoted inflammation and to investigate the relevance of our findings, an acute murine trauma model (cremaster model) of inflammation was included.²⁰ Intrascrotal injection of RNA induced leukocyte adhesion to a comparable level as did tumor necrosis factor α (TNF- α), which was used as a positive control. The blockade of VEGFR2 by semaxanib significantly interfered with eRNA-induced, but not with TNF- α -promoted, leukocyte adhesion (Figure 6A). Interestingly, when TNF- α was applied the rolling flux fraction was reduced, although not significantly. However, due to as yet unknown reasons this was not the case when eRNA was administered (Figure 6B). Together, our data confirm that eRNA provides its proinflammatory action via VEGFR2 and highlight the relevance of our findings for shear stress-induced arteriogenesis, as well as for acute and chronic inflammatory processes in general. However, our data also point to VEGFR2-independent mechanisms of inflammation because TNF- α -induced leukocyte recruitment was not influenced by VEGFR2 blockage.

Discussion

Arteriogenesis is a fluid shear stress-triggered process that is strongly dependent on local leukocyte recruitment. Previous studies identified several signaling processes that are involved in transducing shear stress-mediated effects. However, how leukocytes are locally recruited to sites of sterile inflammation is not clear. In the present study, we identified several missing links in translating fluid shear stress, the triggering force for arteriogenesis, to leukocyte recruitment, thereby promoting collateral artery growth. This allows us to plot the circle of complex mechanisms of cellular and molecular chain reactions in arteriogenesis (Figure 7). In particular, we show that shear stress triggers the release of RNA from preexisting collateral arteries. eRNA, in turn, acts as a mechanotransducer provoking the release of VWF, which subsequently initiates the local inflammatory cascade mediating collateral artery growth.

Nucleic acids and, in particular, RNA, as a result of its extra-nucleic localization, have been described to be released from

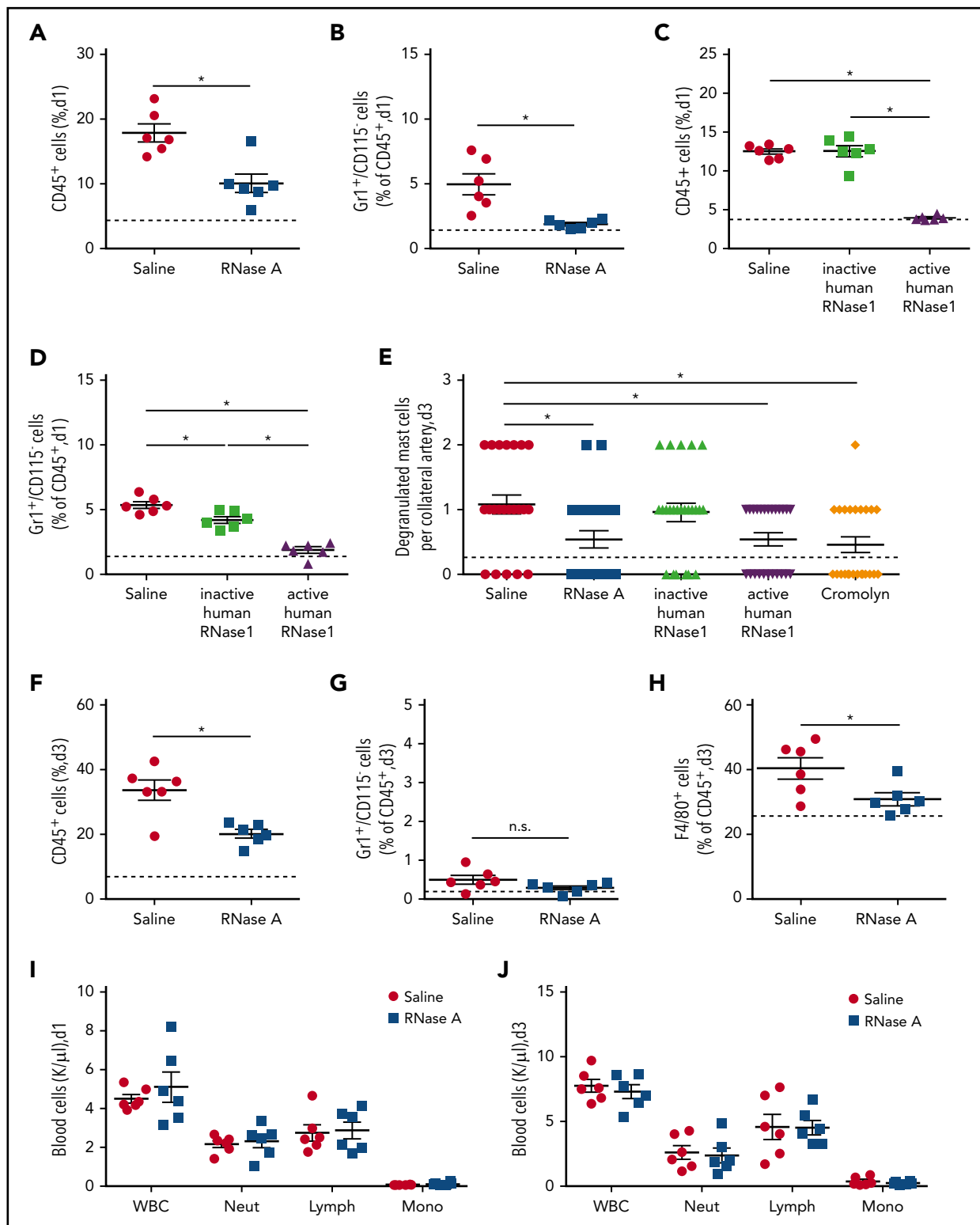


Figure 3. RNase treatment reduces leukocyte infiltration and mast cell degranulation. (A-D,F-H) Quantitative analyses, using flow cytometry, of infiltrated leukocytes in adductor muscles isolated at day 1 or 3 after induction of arteriogenesis via FAL. Scatter plots show the percentages of CD45⁺ cells (A,C,F), CD45⁺/Gr1⁺/CD115⁺ cells (B,D,G), and CD45⁺/F4/80⁺ cells (H) in adductor muscles from mice treated with saline or RNase A (A-B,F-H) or from mice treated with saline, recombinant inactive human RNase1, or recombinant active human RNase1 (C-D). Analyses were performed at day 1 (A-D) and day 3 (F-H) after FAL. (E) The scatter plot shows the number of degranulated mast cells in the perivascular space of growing collaterals at day 3 after induction of arteriogenesis in mice treated with saline, RNase A, recombinant active or inactive human RNase1, or the mast cell stabilizer cromolyn, as evaluated on Giemsa-stained tissue sections. Counts of white blood cell (WBC) populations in blood samples drawn from mice at day 1 (I) or day 3 (J) after induction of arteriogenesis by FAL and saline or RNase A treatment. Data are mean \pm SEM. n = 6 mice per group (A-D,F-J), n > 10 mice per group (E). The dashed horizontal line in the scatter plots indicates the mean sham value. *P < .05, unpaired Student t test (A-B,F-J), 1-way ANOVA with the Bonferroni multiple-comparison test (C-E). Lymph, lymphocytes; Mono, monocytes; Neut, neutrophils.

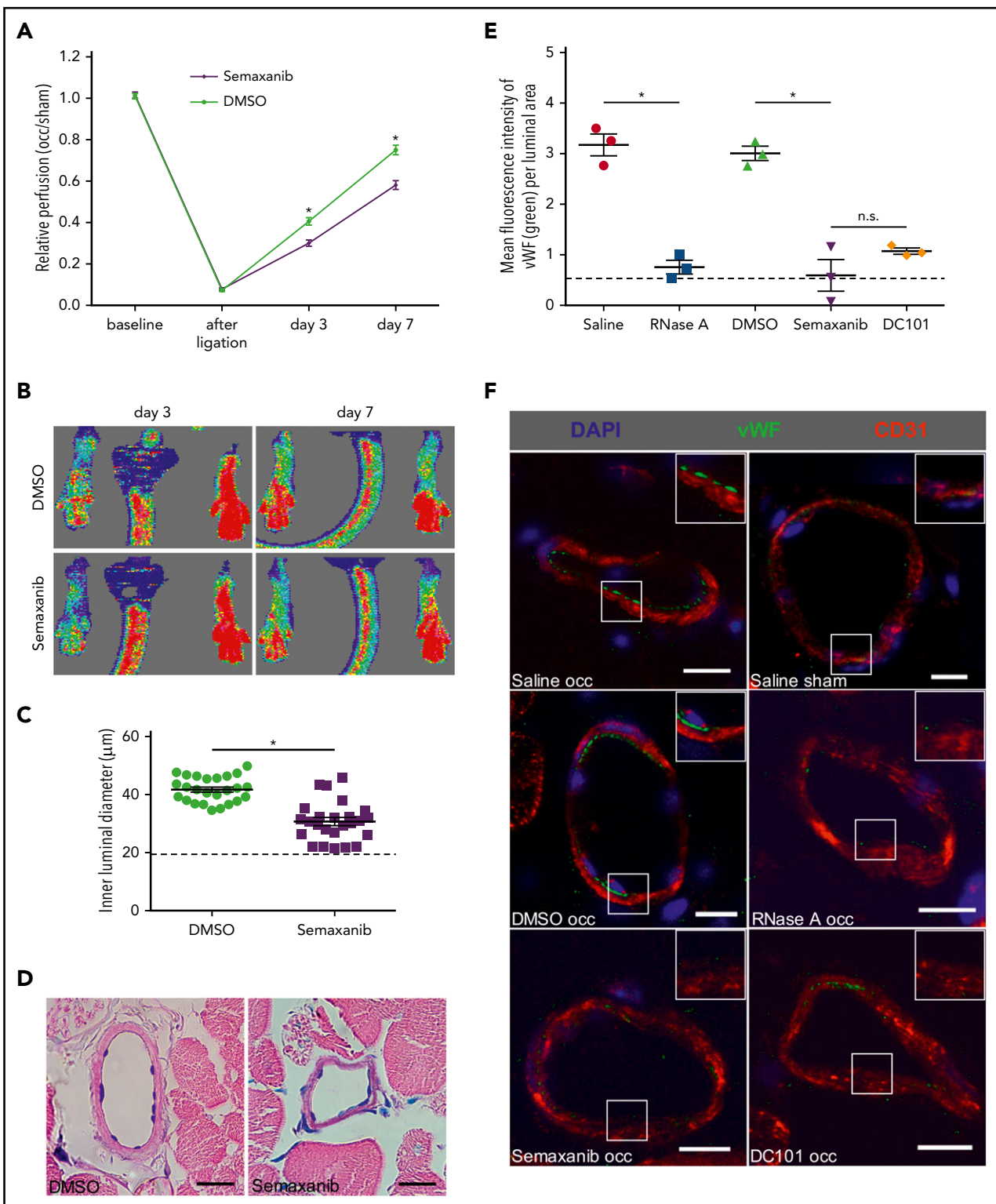


Figure 4. RNase treatment and VEGFR2 blockade interfere with VWF release during arteriogenesis. Laser Doppler perfusion measurements (A) along with corresponding flux images (B) of DMSO (solvent)-treated mice compared with semaxanib-treated mice. The perfusion recovery was calculated by the occluded/sham (right to left) ratio before the surgical procedure, immediately after the surgical procedure, and 3 days and 7 days after ligation. Representative flux images of the Laser Doppler perfusion measurements are shown for day 3 and day 7. The scatter plot shows the inner luminal diameter of mice treated with DMSO or semaxanib 7 days after FAL (C) along with representative Giemsa stains of evaluated tissue samples (D). Scale bars, 20 μm . (E) The scatter plot shows the amount of luminal VWF (as calculated by quantifying the mean green fluorescence intensity per luminal area) in mice treated with saline, DMSO, RNase A, semaxanib, or DC101 (antibody blocking VEGFR2) 2 hours after FAL. (F) Representative immunohistological stains of evaluated collateral arteries. ECs of growing collaterals are strongly decorated with VWF on their luminal surface (green dots; top and middle left panels); this is not visible in the other panels (saline sham, RNase A occ, semaxanib occ, or DC101 occ). Scale bars, 10 μm . Insets show magnifications of collateral arteries in boxes. Data are mean \pm SEM. n = 6 per group (A-B), n > 10 per group (C-D), n = 3 per group (E-F). The dashed horizontal line in the scatter plots indicates the mean sham value. *P < .05, 2-way ANOVA with the Bonferroni multiple-comparison test (A), unpaired Student t test (C), 1-way ANOVA with the Bonferroni multiple-comparison test (E).

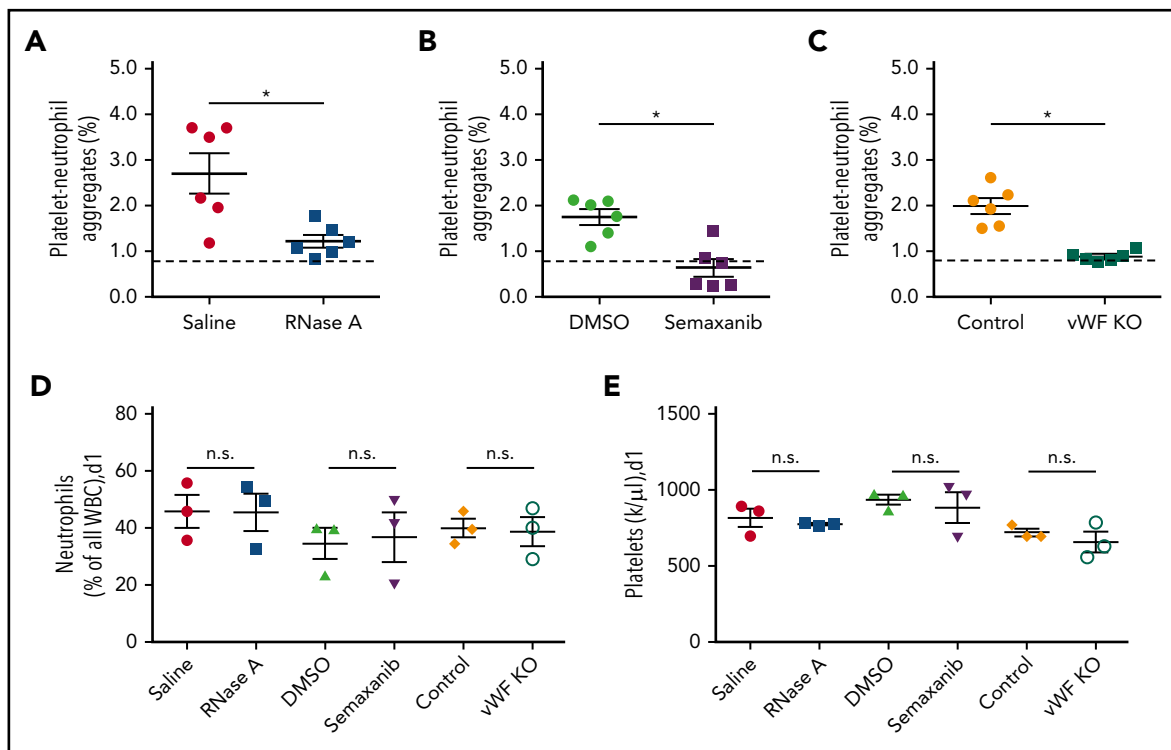


Figure 5. VWF is essential for PNA formation in the process of arteriogenesis. Following induction of arteriogenesis at day 1, whole blood was drawn from wild-type mice treated with saline or RNase A (A) or with DMSO or semaxanib (B) or from VWF-deficient (VWF KO) mice and their respective controls (C) and analyzed using flow cytometry. The scatter plots show the percentage of PNAs relative to the total number of neutrophils. Platelets were detected by a CD41 antibody, and neutrophils were identified by CD11b and Gr-1 antibodies. The dashed horizontal line indicates the mean sham value. For comparison, blood neutrophils (D) and platelets (E) were quantified in wild-type mice treated with saline, RNase A, DMSO, or semaxanib, as well as in VWF-deficient (VWF KO) mice and untreated wild-type mice (Control). Data are mean \pm SEM. n = 6 per group (A-C), n = 3 per group (D-E). *P < .05, unpaired Student t test.

cells as a result of damage.³⁸ However, nucleic acids can be actively released from cells, as shown for neutrophils forming neutrophil extracellular traps.^{17,39} Here, we show that fluid shear stress provides a trigger for the release of eRNA from ECs, although the exact mechanism of liberation remains to be elucidated. Depending on the cell type and the agonist used, eRNA can be released as free RNA or in association with microvesicles^{40,41} (S.F. and K.T.P., unpublished observations). In the case of arteriogenesis, it appears that mainly free ribosomal RNA is released as eRNA from ECs, because this tissue-associated eRNA was stained by a specific antibody or became readily degraded by administered RNase. In contrast, microvesicle-entrapped eRNA would not be recognized by an IV-administered antibody or RNase.⁴⁰ The identified proinflammatory mechanisms that allow eRNA to act as a danger-associated molecular pattern apply for shear stress-induced arteriogenesis, as well as for acute and chronic inflammatory processes in general, as documented previously.^{41,42} In fact, ribosomal RNA makes up >80% of cellular RNA and constitutes the majority of RNA released, once a cell becomes stressed or damaged. In earlier reports, eRNA has been described as a damaging factor in cardiovascular pathologies, and it was demonstrated that administration of RNase1 interfered with the adverse effects of eRNA.^{42,43} In sharp contrast, the present study strongly indicates that endogenous eRNA serves as a potent mechanotransducing and inflammatory factor that is necessary for effective natural bypass growth. Administration of active RNases (bovine pancreatic RNase A or human recombinant RNase1), but not the inactive endonuclease or DNase, strongly

reduced the process of collateral artery growth, pointing to eRNA as a key factor in arteriogenesis. Although one might expect RNase1 to have cytotoxic side effects, RNase1 has been demonstrated to exert its activity exclusively outside of cells.⁴⁴ So far, no distinct receptor for RNase1 has been identified,⁴⁵ and despite the fact that the enzyme might enter cells by endocytosis,⁴⁶ it is rapidly inactivated by the high cytosolic concentrations of RNase inhibitor.^{47,48} In accordance with the function of eRNA as a driving force in arteriogenesis and the counteracting activity of vascular RNases, the bioavailability of eRNA and, hence, the perfusion recovery could be enhanced by administration of RNase inhibitor in the mouse FAL model to abrogate the endogenous RNases and to prevent rapid eRNA degradation.

In a murine cremaster model of inflammation, we recently demonstrated that eRNA promotes leukocyte recruitment and extravasation as strongly as does TNF- α .²⁰ The process of arteriogenesis follows the different steps of a sterile inflammatory pathway. Using the same hindlimb model of arteriogenesis as used here, we demonstrated that arteriogenesis is dependent on activation of the platelet receptor GPIba,³ which results in PNA formation causing extracellular superoxide anion and, hence, reactive oxygen species formation of neutrophils. After extravasation, neutrophil-derived reactive oxygen species activate mast cells, which, in turn, recruit monocytes, which, in the form of perivascular macrophages, promote arteriogenesis by delivering growth factors and cytokines.⁴ The ligands for GPIba are manifold,⁴⁹ and the question about which factor activates the receptor in response to fluid shear stress, resulting in arteriogenesis,

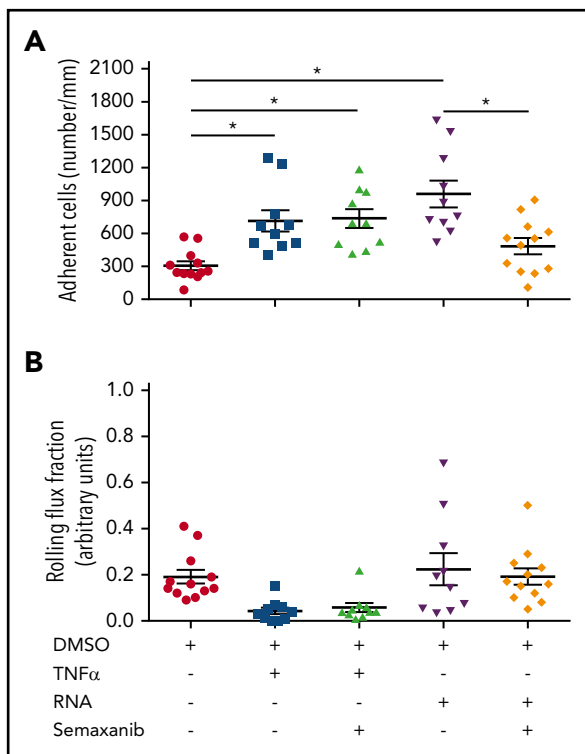


Figure 6. eRNA activates VEGFR2 in a murine cremaster model of inflammation activation. In a cremaster model of inflammation, adherent leukocytes (A) and the rolling flux fraction (B) were investigated using intravital microscopy in venules of mice pretreated with semaxanib blocking VEGFR2 or solvent (DMSO) and stimulated with TNF- α or RNA. Data are mean \pm SEM. n > 10 per group. *P < .05, 1-way ANOVA with the Bonferroni multiple-comparison test.

remained open. Here, we show that deficiency of VWF strikingly interfered with PNA formation without affecting the number of platelets or neutrophils in peripheral blood, identifying VWF as a relevant factor for GPIb α activation.

Interestingly, PNA formation in the arteriogenesis model did not create any prothrombotic situation that would be detrimental for the blood flow reconstitution in growing collaterals. We did not observe any thrombus formation in the growing collaterals, possibly because of the high shear rate-dependent increased production of nitric oxide and prostacyclin in these vessels, thereby blocking platelet aggregation and subsequent fibrin formation.^{5,30,31,50-54} Moreover, under these conditions, ultralarge VWF multimers may become degraded by ADAMTS13,^{30,31,52} resulting in a transient, but not firm, adhesion of platelets to the endothelium of growing collaterals.³ Yet, further investigations are needed to address this issue in more detail.

Shear stress has been closely correlated with VWF release and action.^{29,31} Again, a variety of agonists, among them VEGF and TNF- α , have been described to induce WPB exocytosis; however, the mechanisms relevant for shear stress-triggered release of VWF from WPBs remained to be elucidated.⁵⁵⁻⁵⁷ Our results revealed that blocking VEGFR2 interfered with VWF release and subsequent PNA formation, mast cell activation, leukocyte recruitment, and, finally, the process of arteriogenesis. Similar effects were seen upon treatment of mice with RNase A. It has previously been shown that mutation of Tyr 1175 in the C terminus of VEGFR2 abolished VWF release from ECs in vitro.³² For the

process of arteriogenesis, it was demonstrated that NRP-1, the coreceptor of VEGFA, which is essential for enhancing VEGFR2 signaling, is required for VEGFR2 Tyr 1175 phosphorylation, thereby playing a profound role in the process of collateral artery growth.¹² Moreover, we have shown in vitro that eRNA initiates the binding of VEGFA to NRP-1, thereby increasing the local concentration of VEGFA relevant for proper binding of the cytokine to VEGFR2 and Tyr 1175 phosphorylation.¹⁶ In the present study, we observed an intense immunostaining for eRNA at the abluminal site of ECs in growing collaterals. Although we cannot exclude that eRNA was removed during the process of perfusion fixation of the tissue or as a result of degradation of eRNA by RNases in blood circulation, our data are in line with immunocytochemical data localizing VEGFA at the abluminal plasma membrane of ECs in vivo⁵⁸ and corresponding to the anticipated distribution of VEGFRs and VEGFR2 activity.^{59,60}

To follow these leukocyte-dependent reactions and to provide proof-of-principle data in the context of arteriogenesis, experiments were performed with eRNA in the acute murine cremaster vasculature model of acute inflammation, because in vivo administration of eRNA would not be suitable for chronic experiments, such as the FAL model. Our results showed that blocking VEGFR2 strictly interferes with eRNA-induced, but not with TNF- α -induced, leukocyte recruitment, confirming that the inflammatory properties of eRNA are mediated by VEGFR2. Nevertheless, eRNA is also likely to be involved in TNF- α -related inflammation. We have previously demonstrated that the increased bioavailability of TNF- α in arteriogenesis is dependent on mast cell degranulation,⁴ and our current results suggest that the relevant signal transduction cascade resulting in mast cell degranulation is initiated by eRNA. Finally, it has been described that eRNA liberates TNF- α from macrophages in a TNF- α -converting enzyme-dependent manner.⁴¹ However, eRNA signaling seems to have an even broader relevance for inflammatory

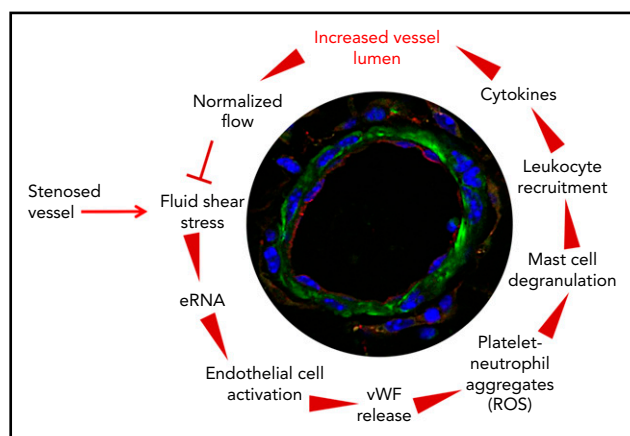


Figure 7. The circle of arteriogenesis. Upon occlusion of a feeding artery, blood flow is redirected in preexisting collaterals circumventing the stenosed artery. Because of the increased blood flow, collaterals experience increased shear stress, which results in release of RNA from ECs. eRNA acts as mechanotransducer provoking EC activation. Activated ECs release VWF from their WPBs, which activates platelets to form PNAs. These, in turn, are essential for mast cell activation, which is a prerequisite for the recruitment of leukocytes that boost vascular cell proliferation and, hence, vessel growth by supplying growth factors and cytokines. When collaterals reached a critical size, allowing them to substitute for the function of the occluded artery, blood flow is normalized, and the collaterals cease to grow.

processes. The facts that P-selectin is concomitantly released with VWF from WPBs and translocated to the cell surface,⁶¹⁻⁶⁴ and that increased expression of ICAM-1 is dependent on enhanced VEGFR2 signaling mediated by engagement of NRP-1³³ suggest that eRNA might also have a function in rolling and firm adhesion of leukocytes. These assumptions are in line with our previous findings on RNA stimulation of cremaster muscle vessels.²⁰

Taken together, our work identified eRNA, released as a result of shear stress, as a relevant factor mediating mechanotransduction and, thereby, initiating the inflammatory response triggering natural bypass growth. However, the discussed mechanisms of eRNA-mediated inflammation are likely to apply to shear stress–driven leukocyte recruitment, as well as to other chronic and acute types of inflammation in which RNA is released because of cell damage, conferring a major role for eRNA in innate immune reactions.

Acknowledgments

The authors thank C. Csapo for technical assistance.

This work was supported by the Lehre@LMU program from the Ludwig Maximilian University of Munich.

REFERENCES

- Faber JE, Chilian WM, Deindl E, van Royen N, Simons M. A brief etymology of the collateral circulation. *Arterioscler Thromb Vasc Biol*. 2014;34(9):1854-1859.
- Pipp F, Boehm S, Cai WJ, et al. Elevated fluid shear stress enhances postocclusive collateral artery growth and gene expression in the pig hind limb. *Arterioscler Thromb Vasc Biol*. 2004;24(9):1664-1668.
- Chandraratne S, von Breuhel ML, Pagel JI, et al. Critical role of platelet glycoprotein ibα in arterial remodeling. *Arterioscler Thromb Vasc Biol*. 2015;35(3):589-597.
- Chillo O, Kleinert EC, Lautz T, et al. Perivascular mast cells govern shear stress-induced arteriogenesis by orchestrating leukocyte function. *Cell Reports*. 2016;16(8):2197-2207.
- Lasch M, Nekolla K, Klemm AH, et al. Estimating hemodynamic shear stress in murine peripheral collateral arteries by two-photon line scanning. *Mol Cell Biochem*. 2019;453(1-2):41-51.
- Arras M, Mohri M, Sack S, Schwarz ER, Schaper J, Schaper W. Macrophages accumulate and release tumor necrosis factor-alpha in the ischemic porcine myocardium. *Circulation*. 1992;86(4):33.
- Tzima E, Irani-Tehrani M, Kiosses WB, et al. A mechanosensory complex that mediates the endothelial cell response to fluid shear stress. *Nature*. 2005;437(7057):426-431.
- Givens C, Tzima E. Endothelial mechano-signaling: does one sensor fit all? *Antioxid Redox Signal*. 2016;25(7):373-388.
- Wang S, Iring A, Strilic B, et al. P2Y₂ and Gq/G₁₁ control blood pressure by mediating endothelial mechanotransduction. *J Clin Invest*. 2015;125(8):3077-3086.
- Jazwa A, Florczyk U, Grochot-Przeczek A, et al. Limb ischemia and vessel regeneration: is there a role for VEGF? *Vascul Pharmacol*. 2016;86:18-30.
- Lautz T, Lasch M, Borgolte J, et al. Midkine controls arteriogenesis by regulating the bioavailability of vascular endothelial growth factor a and the expression of nitric oxide synthase 1 and 3. *EBioMedicine*. 2018;27:237-246.
- Lanahan A, Zhang X, Fantin A, et al. The neuropilin 1 cytoplasmic domain is required for VEGF-A-dependent arteriogenesis. *Dev Cell*. 2013;25(2):156-168.
- Koch S. Neuropilin signalling in angiogenesis. *Biochem Soc Trans*. 2012;40(1):20-25.
- Koch S, Tugues S, Li X, Gualandi L, Claesson-Welsh L. Signal transduction by vascular endothelial growth factor receptors. *Biochem J*. 2011;437(2):169-183.
- Sorkin A, von Zastrow M. Endocytosis and signalling: intertwining molecular networks. *Nat Rev Mol Cell Biol*. 2009;10(9):609-622.
- Fischer S, Nishio M, Peters SC, et al. Signaling mechanism of extracellular RNA in endothelial cells. *FASEB J*. 2009;23(7):2100-2109.
- Brinkmann V, Reichard U, Goosmann C, et al. Neutrophil extracellular traps kill bacteria. *Science*. 2004;303(5663):1532-1535.
- Fischer S, Gerriets T, Wessels C, et al. Extracellular RNA mediates endothelial-cell permeability via vascular endothelial growth factor. *Blood*. 2007;110(7):2457-2465.
- Kannemeier C, Shibamiya A, Nakazawa F, et al. Extracellular RNA constitutes a natural procoagulant cofactor in blood coagulation. *Proc Natl Acad Sci USA*. 2007;104(15):6388-6393.
- Fischer S, Grantzow T, Pagel JI, et al. Extracellular RNA promotes leukocyte recruitment in the vascular system by mobilizing proinflammatory cytokines. *Thromb Haemost*. 2012;108(4):730-741.
- Rosenthal AM, Gotlieb AI. Macrovascular endothelial cells from porcine aorta. In: Piper H, ed. *Cell Culture Techniques in Heart and Vessel Research*, Berlin, Germany: Springer Verlag; 1990:117-129.
- Fleming I, Bauersachs J, Fisslthaler B, Busse R. Ca²⁺-independent activation of the endothelial nitric oxide synthase in response to tyrosine phosphatase inhibitors and fluid shear stress. *Circ Res*. 1998;82(6):686-695.
- Xu H, Gonzalo JA, St Pierre Y, et al. Leukocytosis and resistance to septic shock in intercellular adhesion molecule 1-deficient mice. *J Exp Med*. 1994;180(1):95-109.
- Denis C, Methia N, Frenette PS, et al. A mouse model of severe von Willebrand disease: defects in hemostasis and thrombosis. *Proc Natl Acad Sci USA*. 1998;95(16):9524-9529.
- Helisch A, Wagner S, Khan N, et al. Impact of mouse strain differences in innate hindlimb collateral vasculature. *Arterioscler Thromb Vasc Biol*. 2006;26(3):520-526.
- Kleinert E, Langenmayer MC, Reichart B, et al. Ribonuclease (RNase) prolongs survival of grafts in experimental heart transplantation. *J Am Heart Assoc*. 2016;5(5):e003429.
- Walberer M, Tschnatsch M, Fischer S, et al. RNase therapy assessed by magnetic resonance imaging reduces cerebral edema and infarct size in acute stroke. *Curr Neurovasc Res*. 2009;6(1):12-19.

Authorship

Contribution: M.L., E.C.K., J.-I.B., T.G., and T.L. performed in vivo measurements; M.L., E.C.K., S.M., K.K., and K.T. performed histological analyses; M.L. and E.C.K. performed FACS analyses; S.S., S.F., and I.F. performed in vitro analyses; I.F., A.M.R., M.S., and K.T.P. participated in scientific discussions and drafted and revised the manuscript; and E.D. designed the experiments, analyzed the data, and wrote the manuscript.

Conflict-of interest disclosure: The authors declare no competing financial interests.

ORCID profile: M.S., 0000-0002-7689-3613.

Correspondence: Elisabeth Deindl, Walter Brendel Centre of Experimental Medicine, Marchioninistr 15, 81377 Munich, Germany; e-mail: elisabeth.deindl@med.uni-muenchen.de.

Footnotes

Submitted 1 May 2019; accepted 27 August 2019. Prepublished online as *Blood First Edition paper*, 9 September 2019; DOI 10.1182/blood.2019001392.

The online version of this article contains a data supplement.

The publication costs of this article were defrayed in part by page charge payment. Therefore, and solely to indicate this fact, this article is hereby marked "advertisement" in accordance with 18 USC section 1734.

28. Tsui NB, Ng EK, Lo YM. Stability of endogenous and added RNA in blood specimens, serum, and plasma. *Clin Chem.* 2002;48(10): 1647-1653.
29. Huang J, Roth R, Heuser JE, Sadler JE. Integrin alpha(v)beta(3) on human endothelial cells binds von Willebrand factor strings under fluid shear stress. *Blood.* 2009;113(7):1589-1597.
30. Huck V, Schneider MF, Gorzelanny C, Schneider SW. The various states of von Willebrand factor and their function in physiology and pathophysiology. *Thromb Haemost.* 2014;111(4):598-609.
31. Sadler JE. A new name in thrombosis, ADAMTS13. *Proc Natl Acad Sci USA.* 2002; 99(18):11552-11554.
32. Xiong Y, Huo Y, Chen C, et al. Vascular endothelial growth factor (VEGF) receptor-2 tyrosine 1175 signaling controls VEGF-induced von Willebrand factor release from endothelial cells via phospholipase C-gamma 1- and protein kinase A-dependent pathways. *J Biol Chem.* 2009;284(35):23217-23224.
33. Wang J, Wang S, Li M, et al. The neuropilin-1 inhibitor, ATWLPPR peptide, prevents experimental diabetes-induced retinal injury by preserving vascular integrity and decreasing oxidative stress. *PLoS One.* 2015;10(11): e0142571.
34. Scholz D, Ito W, Fleming I, et al. Ultrastructure and molecular histology of rabbit hind-limb collateral artery growth (arteriogenesis). *Virchows Arch.* 2000;436(3):257-270.
35. Hoefer IE, van Royen N, Rectenwald JE, et al. Arteriogenesis proceeds via ICAM-1/Mac-1-mediated mechanisms. *Circ Res.* 2004;94(9): 1179-1185.
36. Deindl E, Schaper W. The art of arteriogenesis. *Cell Biochem Biophys.* 2005;43(1):1-15.
37. Ito WD, Arras M, Winkler B, Scholz D, Schaper J, Schaper W. Monocyte chemotactic protein-1 increases collateral and peripheral conductance after femoral artery occlusion. *Circ Res.* 1997;80(6):829-837.
38. Deindl E, Fischer S, Preissner KT. New directions in inflammation and immunity: the multi-functional role of the extracellular RNA/RNase system. *Indian J Biochem Biophys.* 2009;46(6): 461-466.
39. Brinkmann V, Zychlinsky A. Beneficial suicide: why neutrophils die to make NETs. *Nat Rev Microbiol.* 2007;5(8):577-582.
40. Elsemüller AK, Tomalla V, Gärtner U, et al. Characterization of mast cell-derived rRNA-containing microvesicles and their inflammatory impact on endothelial cells. *FASEB J.* 2019;33(4):5457-5467.
41. Fischer S, Gesierich S, Griemert B, et al. Extracellular RNA liberates tumor necrosis factor- α to promote tumor cell trafficking and progression. *Cancer Res.* 2013;73(16): 5080-5089.
42. Preissner KT, Herwald H. Extracellular nucleic acids in immunity and cardiovascular responses: between alert and disease. *Thromb Haemost.* 2017;117(7):1272-1282.
43. Kluever AK, Deindl E. Extracellular RNA, a potential drug target for alleviating atherosclerosis, ischemia/reperfusion injury and organ transplantation. *Curr Pharm Biotechnol.* 2018;19(15):1189-1195.
44. Gaur D, Swaminathan S, Batra JK. Interaction of human pancreatic ribonuclease with human ribonuclease inhibitor. Generation of inhibitor-resistant cytotoxic variants. *J Biol Chem.* 2001;276(27):24978-24984.
45. Schirrmann T, Krauss J, Arndt MA, Rybak SM, Dübel S. Targeted therapeutic RNases (ImmunoRNases). *Expert Opin Biol Ther.* 2009;9(1):79-95.
46. Haigis MC, Raines RT. Secretory ribonucleases are internalized by a dynamin-independent endocytic pathway. *J Cell Sci.* 2003;116(Pt 2): 313-324.
47. Haigis MC, Kurten EL, Raines RT. Ribonuclease inhibitor as an intracellular sentry. *Nucleic Acids Res.* 2003;31(3): 1024-1032.
48. Leland PA, Schultz LW, Kim BM, Raines RT. Ribonuclease A variants with potent cytotoxic activity. *Proc Natl Acad Sci USA.* 1998;95(18): 10407-10412.
49. Bergmeier W, Piffath CL, Goerge T, et al. The role of platelet adhesion receptor GPIbalpha far exceeds that of its main ligand, von Willebrand factor, in arterial thrombosis. *Proc Natl Acad Sci USA.* 2006;103(45): 16900-16905.
50. Fisslthaler B, Dimmeler S, Hermann C, Busse R, Fleming I. Phosphorylation and activation of the endothelial nitric oxide synthase by fluid shear stress. *Acta Physiol Scand.* 2000;168(1): 81-88.
51. Keh D, Gerlach M, Kürer I, et al. The effects of nitric oxide (NO) on platelet membrane receptor expression during activation with human alpha-thrombin. *Blood Coagul Fibrinolysis.* 1996;7(6):615-624.
52. Shim K, Anderson PJ, Tuley EA, Wiswall E, Sadler JE. Platelet-VWF complexes are preferred substrates of ADAMTS13 under fluid shear stress. *Blood.* 2008;111(2):651-657.
53. Troidl K, Tribulova S, Cai WJ, et al. Effects of endogenous nitric oxide and of DETA NONOate in arteriogenesis. *J Cardiovasc Pharmacol.* 2010;55(2):153-160.
54. Wen L, Feil S, Wolters M, et al. A shear-dependent NO-cGMP-cGKI cascade in platelets acts as an auto-regulatory brake of thrombosis [published correction appears in *Nat Commun.* 2018;9(1):4969]. *Nat Commun.* 2018;9(1):4301.
55. Bernardo A, Ball C, Nolasco L, Moake JF, Dong JF. Effects of inflammatory cytokines on the release and cleavage of the endothelial cell-derived ultralarge von Willebrand factor multimers under flow. *Blood.* 2004;104(1): 100-106.
56. Matsushita K, Yamakuchi M, Morrell CN, et al. Vascular endothelial growth factor regulation of Weibel-Palade-body exocytosis. *Blood.* 2005;105(1):207-214.
57. Rondaij MG, Bierings R, Kragt A, van Mourik JA, Voorberg J. Dynamics and plasticity of Weibel-Palade bodies in endothelial cells. *Arterioscler Thromb Vasc Biol.* 2006;26(5): 1002-1007.
58. Qu-Hong, Nagy JA, Senger DR, Dvorak HF, Dvorak AM. Ultrastructural localization of vascular permeability factor/vascular endothelial growth factor (VPF/VEGF) to the abluminal plasma membrane and vesiculovacuolar organelles of tumor microvascular endothelium. *J Histochem Cytochem.* 1995;43(4):381-389.
59. Li S, Kim M, Hu YL, et al. Fluid shear stress activation of focal adhesion kinase. Linking to mitogen-activated protein kinases. *J Biol Chem.* 1997;272(48):30455-30462.
60. Zhao L, Zhang MM, Ng KY. Effects of vascular permeability factor on the permeability of cultured endothelial cells from brain capillaries. *J Cardiovasc Pharmacol.* 1998;32(1):1-4.
61. Bonfanti R, Furie BC, Furie B, Wagner DD. PADGEM (GMP140) is a component of Weibel-Palade bodies of human endothelial cells. *Blood.* 1989;73(5):1109-1112.
62. Denis CV, André P, Saffaripour S, Wagner DD. Defect in regulated secretion of P-selectin affects leukocyte recruitment in von Willebrand factor-deficient mice. *Proc Natl Acad Sci USA.* 2001;98(7):4072-4077.
63. Mayadas TN, Johnson RC, Rayburn H, Hynes RO, Wagner DD. Leukocyte rolling and extravasation are severely compromised in P selectin-deficient mice. *Cell.* 1993;74(3): 541-554.
64. Stenberg PE, McEver RP, Shuman MA, Jacques YV, Bainton DF. A platelet alpha-granule membrane protein (GMP-140) is expressed on the plasma membrane after activation. *J Cell Biol.* 1985;101(3):880-886.

Supplemental Information

Extracellular RNA released due to shear stress controls natural bypass growth by mediating mechanotransduction

Manuel Lasch^{1,2}, Eike Christian Kleinert¹, Sarah Meister^{3,4}, Konda Kumaraswami¹, Judith-Irina Buchheim^{1,5}, Tobias Grantzow¹, Thomas Lautz¹, Sofia Salpisti⁶, Silvia Fischer⁶, Kerstin Troidl^{7,8}, Ingrid Fleming⁹, Anna M. Randi¹⁰, Markus Sperandio¹, Klaus T. Preissner⁶, Elisabeth Deindl¹

¹Walter-Brendel-Centre of Experimental Medicine, University Hospital, LMU Munich, 81377 Munich, Germany

²Department of Otorhinolaryngology, Head & Neck Surgery, University Hospital, LMU Munich, 81377 Munich, Germany

³Institut für Laboratoriumsmedizin, LMU Munich, 81377 München, Germany

⁴Department of Obstetrics and Gynaecology, LMU Munich, 81377 Munich, Germany

⁵Laboratory of Translational Research “Stress & Immunity”, Department of Anaesthesiology, University Hospital, LMU Munich, 81377 Munich, Germany

⁶Institute for Biochemistry, Medical School, Justus-Liebig-Universität, 35392 Giessen, Germany

⁷Department of Pharmacology, Max-Planck-Institute for Heart and Lung Research, Ludwigstrasse 43, 61231 Bad Nauheim, Germany

⁸Department of Vascular and Endovascular Surgery, University Hospital Frankfurt, Theodor-Stern-Kai 7, 60590 Frankfurt, Germany

⁹Institute for Vascular Signalling, Vascular Research Centre, Goethe University, 60596 Frankfurt am Main, Germany

¹⁰National Heart and Lung Institute, Hammersmith Hospital, Imperial College London, London, United Kingdom

Supplemental information includes 7 figures and supplemental methods

Correspondence

Elisabeth Deindl
Walter-Brendel-Centre of Experimental Medicine
Marchioninistr. 15, D-81377 Munich, Germany
e-mail: Elisabeth.Deindl@med.uni-muenchen.de

SUPPLEMENTAL MATERIAL AND METHODS

Femoral artery ligation, Laser-Doppler perfusion measurements and tissue sampling

Arteriogenesis was induced in 6-8 weeks old male mice by unilateral femoral artery ligation (FAL) of the right femoral artery while the left femoral artery was sham operated (sham) as previously described.^{1,2} For every surgical procedure mice were anesthetized with a combination of fentanyl (0.05 mg/kg, CuraMED Pharma, Karlsruhe, Germany), midazolam (5.0 mg/kg, Ratiopharm GmbH, Ulm, Germany) and medetomidine (0.5 mg/kg, Pfister Pharma, Berlin, Germany). Hindlimb perfusion measurements were performed using the Laser-Doppler Imaging (LDI) technique (Moor LDI 5061 and Moor Software Version 3.01, Moor Instruments, Remagen, Germany) under temperature-controlled conditions from 36 °C to 38 °C. Measurements were performed before ligation (baseline), directly after ligation and 3 or 7 days after FAL. A defined region of interest (ROI) was charted over each hindlimb from the ankle to the toes of each animal and all areas (ROIs) were chosen equal in size (0.50 cm²) for all animals (Supplemental Figure 5). Later, the software processed a flux mean value and the perfusion was calculated by flux means of right-to-left (ligated-to-sham operated) ratios. Prior to tissue sampling for histological analyses mice were perfused with adenosine buffer (1% adenosine (Sigma-Aldrich, St. Louis, MO), 5% bovine serum albumin (BSA, Sigma-Aldrich), dissolved in phosphate buffered saline (PBS, PAN Biotech, Aidenbach, Germany, pH 7.4)) to assure maximal vasodilation³, followed by perfusion with 3% paraformaldehyd (PFA, Merck, Darmstadt, Germany) (for cryopreservation), or 4% PFA (for paraffin embedding) in PBS, pH 7.4.

Histology and immunohistology

For all histological- and immunhistological analyses two superficial collateral arteries of mice were analyzed (Supplemental Figure 6).

eRNA staining: Mice received intravenously Alexa fluor 488 labeled rRNA antibody Y10b (Novus Biological, Centennial, CO, USA) (2mg/kg) immediately after FAL. Mice were sacrificed 30 min after FAL and tissue samples were harvested and cryopreserved. 8-10µm thick cryosections were incubated with anti-CD31-Alexa fluor 647 antibody (BioLegend, San Diego, CA, USA) (dilution 1:50) overnight at 4 °C to stain endothelial cells and counter-stained with 4',6-diamidino-2-phenylindole (DAPI) (Thermo Fisher Scientific, Waltham, MA, USA) (dilution 1:1000) for 20 min at room temperature (RT) to detect nuclei. Images were captured with a Zeiss fluorescent microscope (Carl Zeiss AG, Feldbach, Switzerland) and analyzed by AxioVision software (Carl Zeiss AG).

vWF Staining: Mice were treated intravenously with vWF antibody (Dako Denmark/Agilent Technologies, Santa Clara, CA, USA) (800µg/kg, dissolved in PBS) 30 min before tissue sampling. Two hours after FAL, tissue samples were harvested and cryopreserved. 10 µm thick cryosections were stained with Alexa fluor 488 conjugated secondary antibody (Abcam, Cambridge, United Kingdom) (dilution 1:200) for 1h at RT. For endothelial cell staining the anti-CD31-Alexa fluor 647 antibody (BioLegend) (dilution 1:50) was used followed by DAPI counter-staining. The imaging was done using a LSM 700 laser scanning confocal microscope (Carl Zeiss AG). For a quantitative analysis of vWF the mean luminal fluorescence intensity was measured with ZEN software (Carl Zeiss AG).

Macrophage Staining: Cryosections were stained for MRC1 (Abcam) and CD68 (Abcam) as previously described.⁴ The perivascular macrophages were counted around the two main

superficial collateral arteries using a Leica (DM6 B) fluorescence microscope (Leica Microsystems, Wetzlar, Germany).

Bromodesoxyuridine (BrdU) staining: Mice were treated daily with BrdU (Sigma-Aldrich) (1.25 mg dissolved in 100 µl PBS, i.p.) for 6 consecutive days starting directly after the surgical procedure. Cryosections were incubated for 5 min with 2M HCl in order to denature DNA, and thereafter with an anti-BrdU antibody (Abcam) (dilution 1:50) at 4 °C overnight. This was followed by incubation with Alexa fluor 488 conjugated secondary antibody (Abcam) (dilution 1:200) for 20 min at RT, and an anti-CD31-Alexa fluor 647 antibody (BioLegend) (dilution 1:50), which was used to visualize the endothelial cell layer, followed by DAPI stain. Imaging was done using a Leica (DM6 B) fluorescence microscope (Leica Microsystems). Giemsa staining on paraffin embedded tissue samples was performed according to standard procedures. Slices were analyzed with an Axioscope 40 (Carl Zeiss AG). The inner luminal diameter of the 2 main superficial collateral arteries was determined by measuring the area of the lumen and calculating the diameter of the coextensive circle by AxioVision software (Carl Zeiss AG). Giemsa stained tissue sections were also used to investigate perivascular mast cell accumulation and degradation. Mast cells were counted at 24 h and at day 3 after FAL.

Flow cytometry analyses of digested muscles

Mice were perfused with 3-5 ml saline using an aortic catheter and adductor muscles were isolated. Individual muscles were cut into small pieces with a scissor and digested with collagenase II (Collagenase II, Biochrom GmbH, Berlin, Germany) (2mg/ml, in PBS/1%BSA) at 37 °C for 90 min to 2 hours. The suspensions were then filtered with PBS/1%BSA using a 70 µm cell-restrainer (Greiner Bio-One, Kremsmünster, Austria). After centrifugation (160 x g, 10 min, RT) the cell pellets were washed with PBS/1%BSA and after a second centrifugation, dissolved in PBS/1%BSA. Surface staining was conducted using antibodies against CD45 (dilution 1:100), Gr-1 (dilution 1:200) (both BD Bioscience, San Jose, CA, USA), F4/80 (dilution 1:40), CD11b (dilution 1:100), CD115 (dilution 1:333) (all eBioscience/Thermo Fisher Scientific) for 15 min at RT. The samples were washed with lysing solution (FACS Lysing solution, BD Bioscience), centrifuged (225 x g, 5 min, RT) and the pellets were resolved in PBS/1%BSA for analysis by flow cytometry (Galios Flow Cytometer, Beckman Coulter, CA, USA) using Kaluza Analysis Software (Beckman Coulter) (for gating strategy and representative pictures see Supplemental Figure 7).

Flow cytometry analyses of whole blood

Whole blood collection was performed by cardiac puncture, the blood was anticoagulated with heparin (Ratiopharm GmbH, Ulm, Germany) and immediately diluted with 2 ml lysing solution (BD Bioscience). Thereupon, the blood was centrifuged (300 x g, 5 min, RT). Cell pellets were incubated with antibodies against CD11b (dilution 1:300), CD115 (dilution 1:300), CD41 (dilution 1:400), Gr-1 (dilution 1:800) (all BioLegend), (all diluted in 100µl PBS/1%BSA) for 20 min at 4 °C. The samples were washed with PBS (PAN Biotech) and centrifuged again (300 x g, 5 min, RT). The cell pellet was dissolved in PBS/1%BSA for analysis by flow cytometry (Galios Flow Cytometer, Beckman Coulter) using Kaluza Analysis Software (Beckman Coulter).

White Blood Cell Counts

Blood samples were withdrawn by cardiac puncture and collected in ethylenediaminetetraacetic acid (EDTA)-tubes (SARSTEDT, Nümbrecht, Germany) in order to avoid coagulation. White

blood cell counts were investigated employing a Hematology analyzer Indexx ProCyte Dxt (Indexx Laboratories, Westbrook, ME, USA).

Intravital microscopy of the cremaster muscle

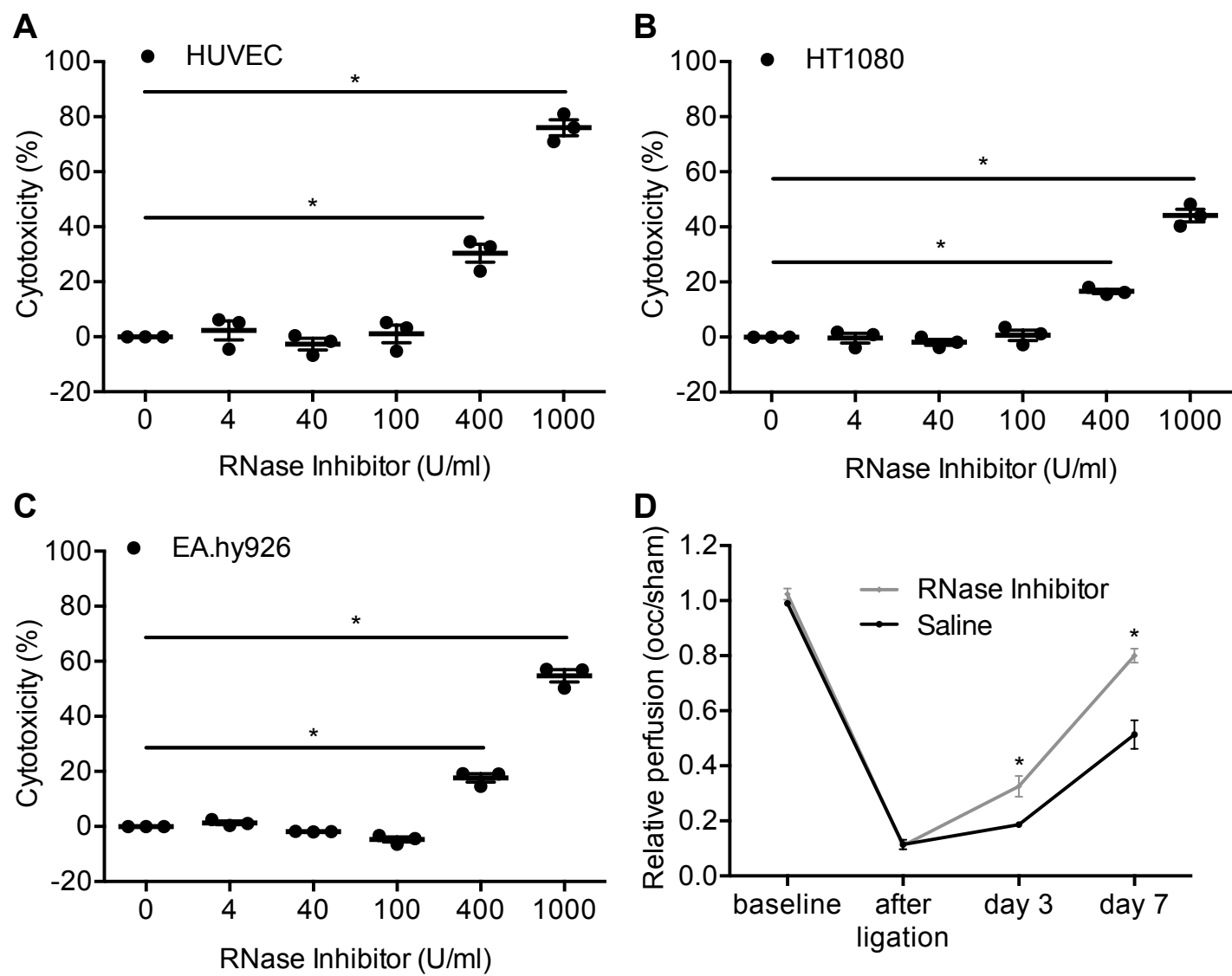
To analyze leukocyte rolling and adhesion, we performed intravital microscopical studies on a murine cremaster model as previously described.⁵ Mice were treated with Semaxanib (4mg/kg i.p.) dissolved in DMSO, or DMSO alone (control) 1 day as well as 3 h before analyses. Two hours before analyses both groups were either treated with TNF α (R&D, Minneapolis, MN, USA) (500 ng, intrascrotal (i.s.)), or 15 μ g of total cellular RNA (i.s.) (isolated from skeletal muscles of another mouse according to the method of Chomczynski and Sacchi)⁶. Mice were anesthetized with a combination of fentanyl (0.0015 mg/kg, CuraMED Pharma, Karlsruhe, Germany), midazolam (0.15 mg/kg, Ratiopharm GmbH, Ulm, Germany) and medetomidine (0.015 mg/kg, Pfister Pharma, Berlin, Germany). Analyses were recorded using a CCD camera system (model CF8/1; Kappa, Gleichen, Germany) on a Panasonic S-VHS video recorder.

Cytotoxicity of Recombinant Ribonuclease Inhibitor

Primary human umbilical vein endothelial cells (HUVEC) were prepared and cultured as described.⁷ The endothelial cell line EA.hy926 and the fibrosarcoma cell line HT1080 were purchased from American Type Culture Collection (ATCC) and cultured as described by the supplier. Cytotoxicity of treatments with Recombinant Ribonuclease Inhibitor (Thermo Fisher Scientific) to cells was determined by measuring the activity of released lactate dehydrogenase (LDH) in cell supernatants. After treatments, cell supernatants were removed, centrifuged for 10 min at 300 g to remove cell debris, and LDH activity was measured by using the detection kit from Roche Diagnostics (Basel, Switzerland). All values were referred to the LDH activity measured after treating cells with 0.1 % (v/v) Triton X100, which was set to 100 %.

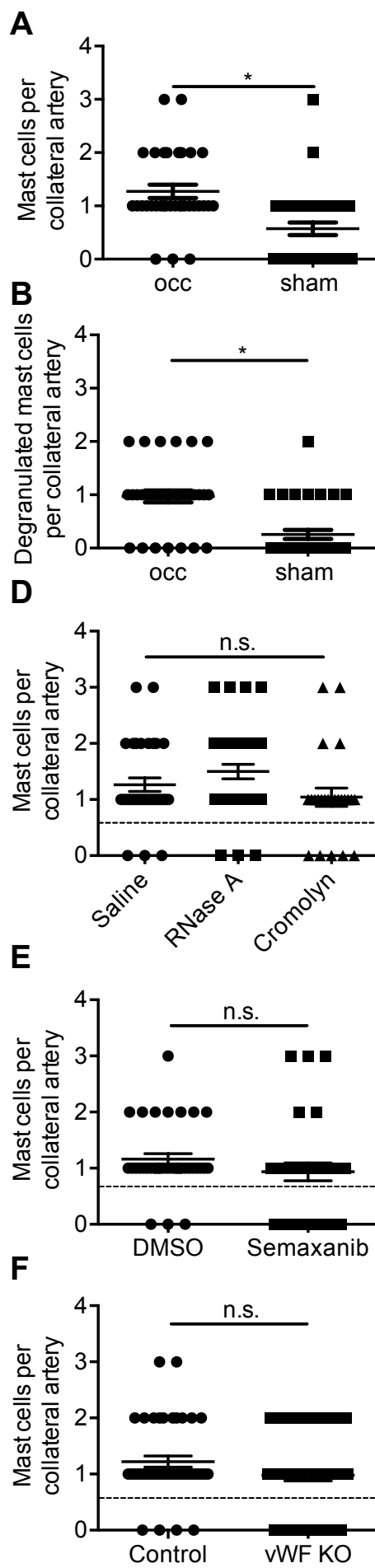
REFERENCES

1. Lasch M, Nekolla K, Klemm AH, et al. Estimating hemodynamic shear stress in murine peripheral collateral arteries by two-photon line scanning. *Mol Cell Biochem* 2018;
2. Limbourg A, Korff T, Napp LC, Schaper W, Drexler H, Limbourg FP. Evaluation of postnatal arteriogenesis and angiogenesis in a mouse model of hind-limb ischemia. *Nat Protoc* 2009; **4**(12): 1737-1746.
3. Lasch M, Caballero-Martinez A, Troidl K, Schloegl I, Lautz T, Deindl E. Arginase inhibition attenuates arteriogenesis and interferes with M2 macrophage accumulation. *Lab Invest* 2016; **96**(8): 830-838.
4. Troidl C, Jung G, Troidl K, Hoffmann J, Mollmann H, Nef H, et al. The temporal and spatial distribution of macrophage subpopulations during arteriogenesis. *Curr Vasc Pharmacol*. 2013; **11**(1):5-12.
5. Fischer S, Grantzow T, Pagel JI, et al. Extracellular RNA promotes leukocyte recruitment in the vascular system by mobilising proinflammatory cytokines. *Thromb Haemost* 2012; **108**(4): 730-741.
6. Chomczynski P, Sacchi N. Single-step method of RNA isolation by acid guanidinium thiocyanate-phenol-chloroform extraction. *Anal Biochem* 1987; **162**: 156-159.
7. Jaffe, E. A., Nachman, R. L., Becker, C. G., and Minick, C. R. Culture of human endothelial cells derived from umbilical veins. Identification by morphologic and immunologic criteria. *J. Clin. Invest.* 1973; **52**, 2745-2756



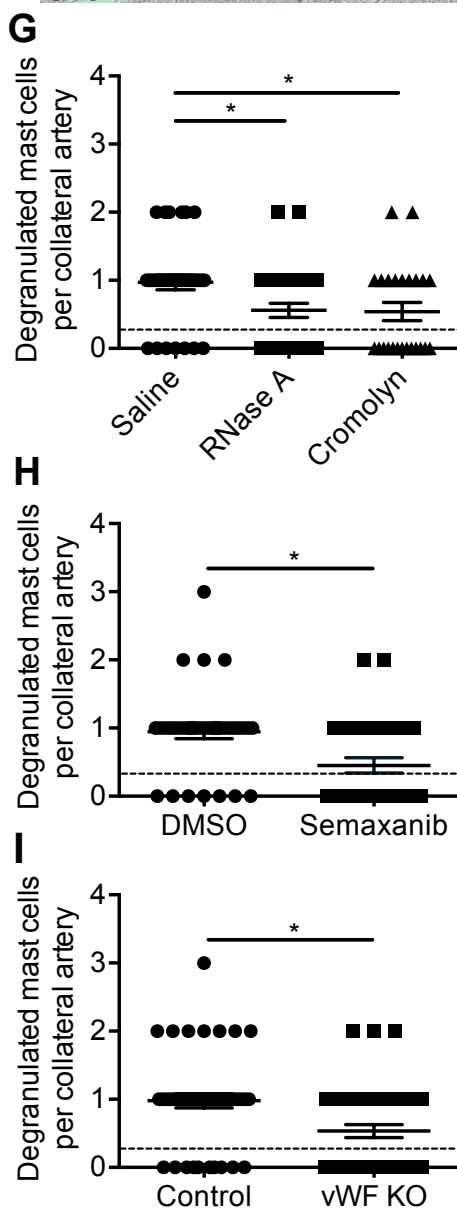
Supplemental Figure 1. RNase Inhibitor Improves Perfusion Recovery

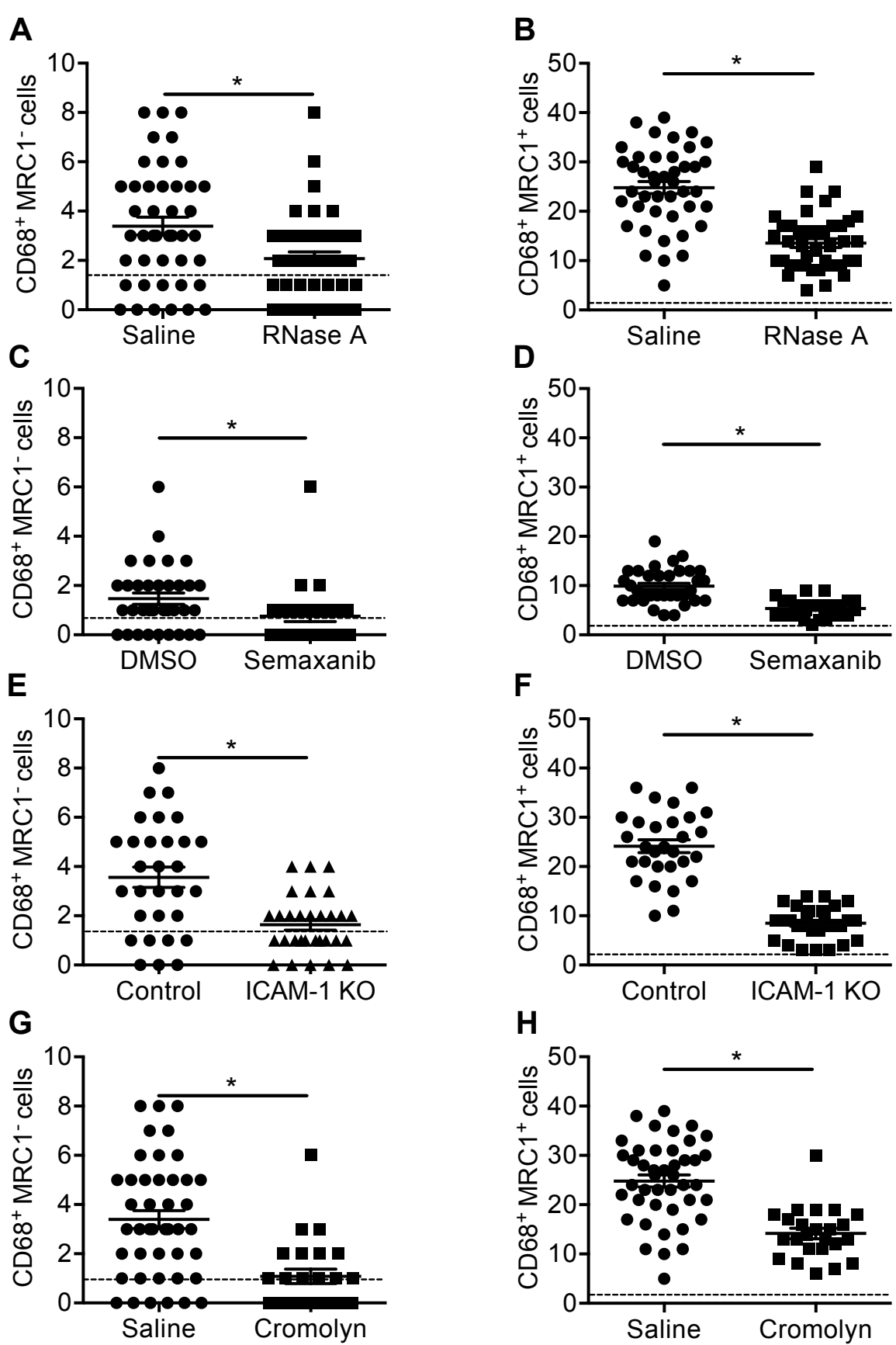
Cytotoxicity tests of RNase Inhibitor: (A) HUVEC, (B) HT1080- or (C) EA.hy926-cells were treated with different concentrations of RNase Inhibitor for 24 h. Afterwards, LDH activity in supernatants was determined and referred to the LDH activity measured after treating cells with 0.1 % Triton X100, which was set to 100 %. Data are means \pm s.e.m, n=3. *P<0.05 (different concentrations vs 0 U/ml RNase Inhibitor group), from one-way ANOVA with Bonferroni's multiple comparison test. (D) Laser Doppler Imaging perfusion measurements of SV129 mice treated with Saline or RNase Inhibitor. The perfusion was calculated by means of occ to sham (right to left) ratios before, immediately after the surgical procedure, and at day 3 and 7 after surgery. Data are means \pm s.e.m., n=5 per group. *P<0.05 (Saline vs RNase Inhibitor treated group), from two-way ANOVA with Bonferroni's multiple comparison test.



Supplemental Figure 2. RNase A as well as Cromolyn and Semaxanib Treatment Inhibit Mast Cell Activation alike vWF-Deficiency

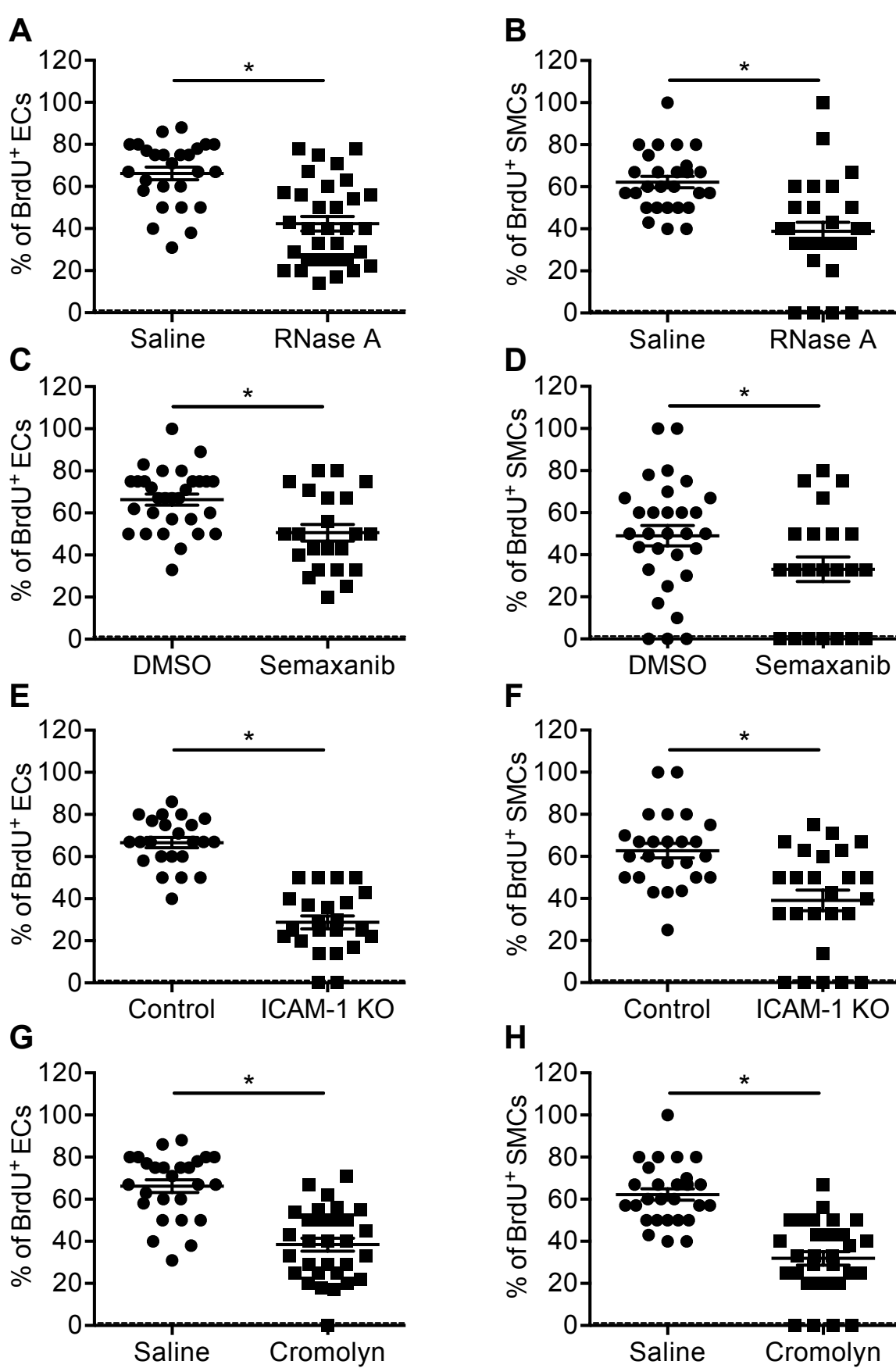
The scatter plots show the number of (A) all perivascular mast cells, or (B) of degranulated perivascular mast cells during the process of arteriogenesis (occ) or in resting collateral arteries (sham) at day one after the procedure. (C) Representative pictures of analyzed Giemsa stained tissue samples. The upper picture (occ) shows a degranulated mast cell (black rectangle, zoom) in the perivascular space of a growing collateral artery; the lower picture (sham) a non-degranulated mast cell (grey rectangle, zoom) next to a resting collateral. Scale bars 20 μ m. The number of all perivascular mast cells and degranulated mast cells was moreover quantified in mice either treated with (D, G) RNase A and Cromolyn, or (E, H) Semaxanib, or (F, I) in mice deficient for vWF, as well as their respective controls (Saline, DMSO or untreated wild-type mice (control)). Data are means \pm s.e.m., n>10 per group. *P<0.05 (occ vs sham group; RNase A vs Cromolyn vs Saline-treated group; Semaxanib vs DMSO-treated group; vWF deficient vs untreated wild-type mice) from (A, B, E, F, H, I) unpaired student's t-test or (D, G) one way ANOVA with Bonferroni's multiple comparison test. (D-I) The dotted line indicates the mean sham value for each scatter plot.





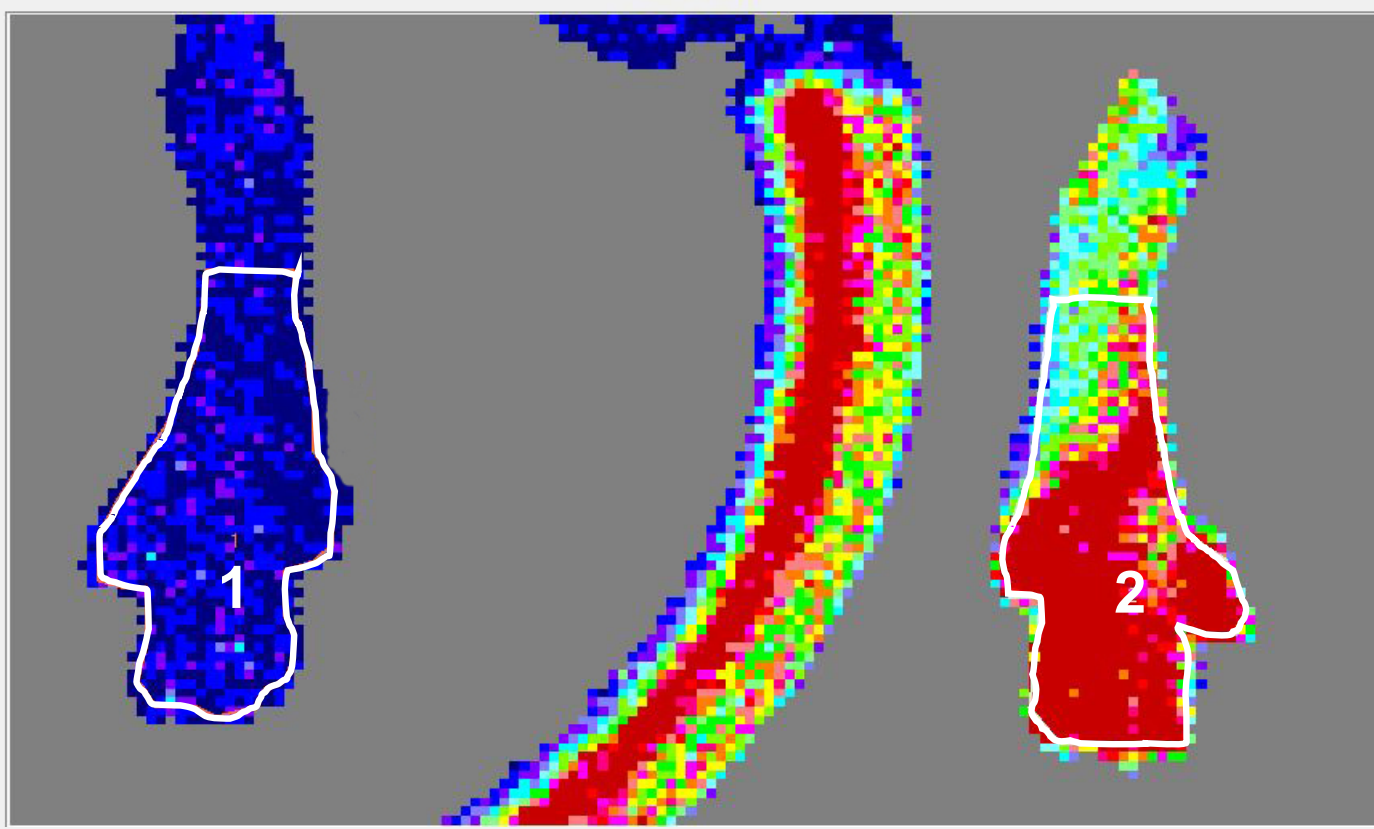
Supplemental Figure 3. RNase A as well as Semaxanib Treatment Interfere with Perivascular Macrophage Accumulation

The scatter plots show the number of perivascular macrophages (CD68⁺ MRC1⁻ and CD68⁺ MRC1⁺) around growing collaterals of mice treated with (A, B) RNase A, or (C, D) Semaxanib, or (E, F) in ICAM-1-deficient mice, or of mice treated with (G, H) Cromolyn, or their respective controls (Saline, DMSO or untreated wild-type mice (control)) at day 7 after induction of arteriogenesis via FAL. Data are means \pm s.e.m., n>10 per group. *P<0.05 (RNase A vs Saline-treated group; Semaxanib vs DMSO-treated group; ICAM-1-deficient mice vs untreated wild-type mice, Cromolyn vs Saline-treated group) from unpaired student's t-test. The dotted line in the scatter plots indicates the mean sham value.



Supplemental Figure 4. RNase A as well as Semaxanib Treatment show Adverse Effects on Vascular Cell Proliferation

The scatter plots show the percentage of proliferating endothelial cells (ECs) and smooth muscle cells (SMCs) in growing collaterals of mice treated with (A, B) RNase A, or (C, D) Semaxanib, or (E, F) in mice deficient for ICAM-1-deficient, or (G, H) Cromolyn treated mice as well as their respective controls (Saline, DMSO or untreated wild-type mice (control)) at day 7 after induction of arteriogenesis via FAL. Data are means \pm s.e.m., n>10 per group. *P<0.05 (RNase A vs Saline-treated group; Semaxanib vs DMSO-treated group; ICAM-1-deficient mice vs untreated wild-type mice, Cromolyn vs Saline-treated group) from unpaired student's t-test. The dotted line in the scatter plots indicates the mean sham value.

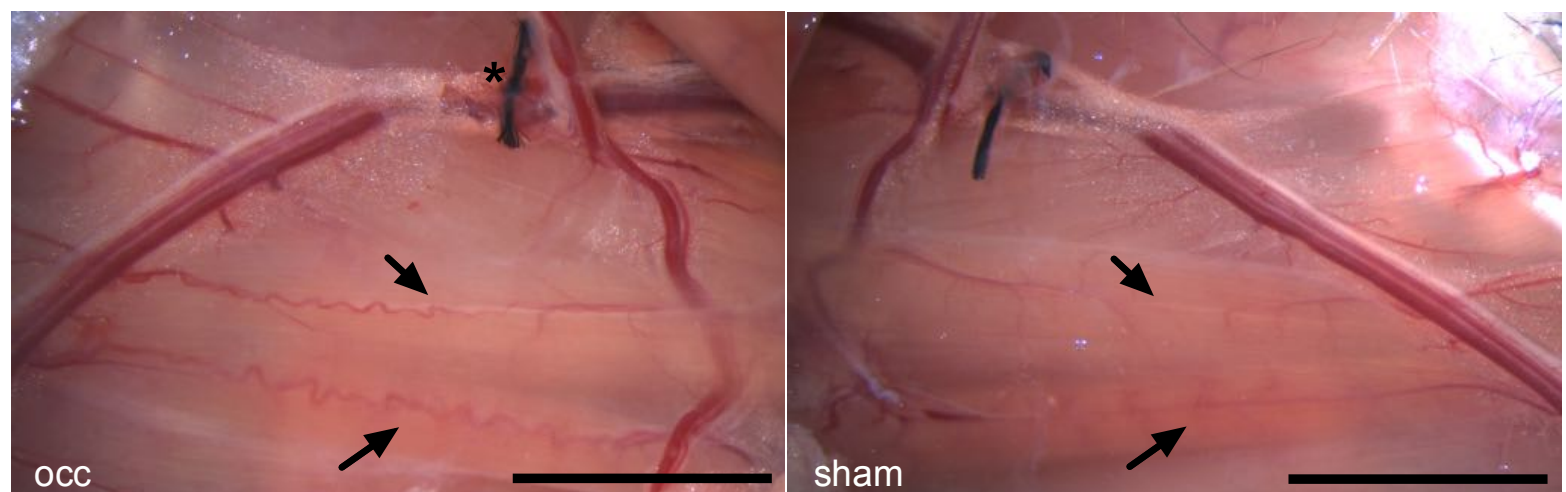


Blood Flow Statistics (Flux - PU)

ROI No	Mean	Std	Median	Min	Max	Total	Valid	Valid %	Area
*Poly 1	54.2	30.9	48	3	221	740	740	100.0	0.50
Poly 2	928.1	469.1	870	162	3484	737	737	100.0	0.50

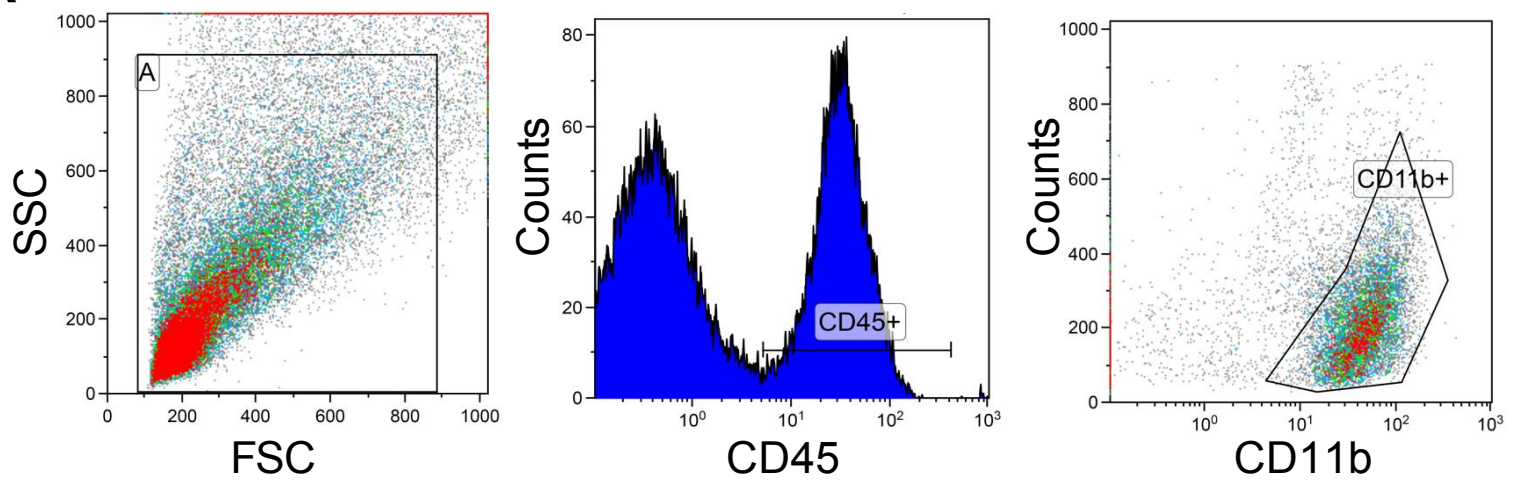
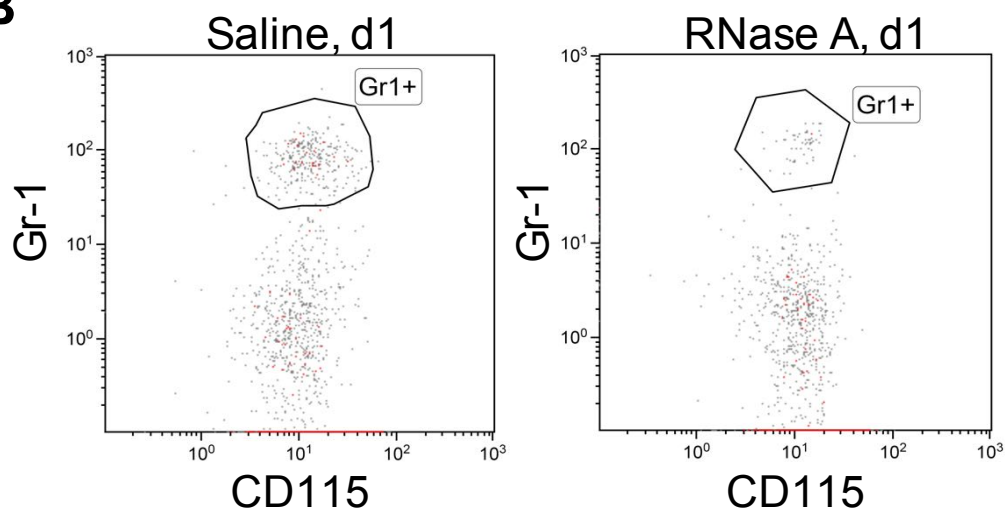
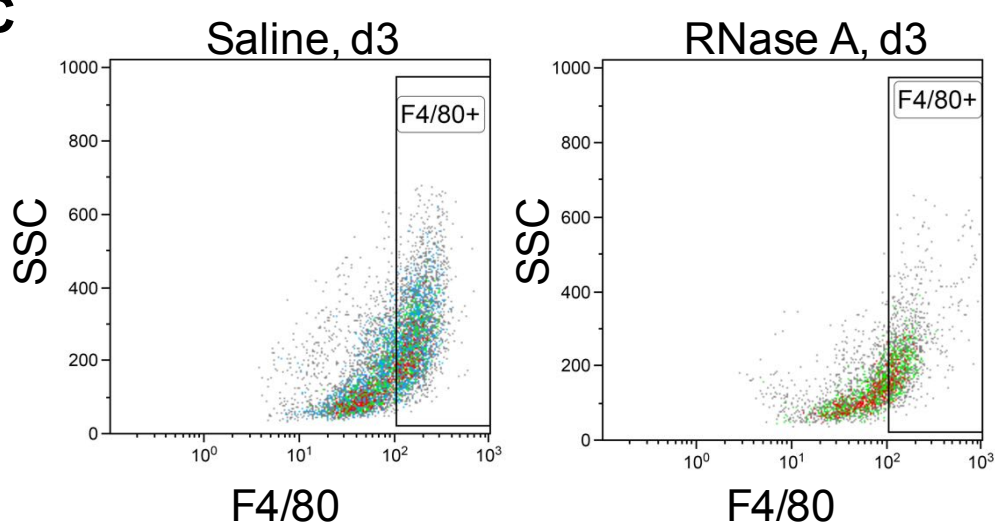
Supplemental Figure 5. Representative Picture of Laser Doppler Imaging (LDI)

The upper panel shows a representative picture of a flux image after ligation (1) of the right leg or sham operation (2) of the left leg. The region of interest (ROI) is marked in white. The lower panel displays the calculated flux statistics by the software.



Supplemental Figure 6. Characteristics of Collateral Vessel Morphology

Photographs of superficial collateral arteries 7 days after femoral artery ligation (FAL, occ, left picture) or sham operation (right picture). Arrows indicate the two growth-induced collaterals of the experimental site (occ) or pre-existing collaterals of the sham-operated site (sham) which connect the arteria femoralis and profunda femoris, and which were investigated by means of (immuno-) histology in the different experimental setups. The ligation (*) of the femoral artery was performed downstream of the profound artery. Scale bars: 5mm.

A**B****C**

Supplemental Figure 7. Flow Cytometry Analyses with Gating Strategy and Representative Pictures

Representative flow cytometry dot plots visualizing the gating strategy of (A) leukocytes (CD45⁺), (B) neutrophils (CD45⁺/CD11b⁺/Gr-1⁺/CD115⁻) and (C) macrophages (CD45⁺/CD11b⁺/F4/80⁺) of adductor muscles of mice treated with Saline or RNase A (B) one day or (C) 3 days after FAL.

XI. Danksagung

An erster Stelle möchte ich meiner Doktormutter und Betreuerin, Frau PD Dr. rer. nat. Elisabeth Deindl, ganz besonders danken. Herzlichen Dank für die Aufnahme und die Möglichkeit in Ihrer Arbeitsgruppe zu forschen, für diese intensiven Erfahrungen und Herausforderungen, die ich dort erleben durfte und die mich in meiner weiteren beruflichen Laufbahn maßgeblich geprägt haben. Danke für alles, was ich bei Ihnen und durch Sie lernen durfte, für den außergewöhnlichen Einblick in die Forschung und Wissenschaft.

Weiter danke ich meiner gesamten Arbeitsgruppe für die Zusammenarbeit und die gegenseitige Unterstützung. Insbesondere möchte ich mich bei Herrn Eike Kleinert, Herrn Thomas Lautz, Frau Amelia Caballero-Martinez und Herrn Konda Kumaraswami bedanken, die mir sämtliche Methoden beigebracht haben und darüber hinaus immer bei Fragen oder Problemen zur Verfügung standen. Zusätzlich möchte ich mich herzlich bei Frau Christine Eder für ihre technische und insbesondere organisatorische, tägliche Hilfe im Institut bedanken.

Mein besonderer Dank gilt meiner Familie und meiner Verlobten, die mich nicht nur während der Doktorarbeit, sondern auch den Großteil meiner Ausbildung unterstützt haben. Mama und Papa, vielen Dank für alles, was ihr mir bisher ermöglicht habt, ohne diese Unterstützung wäre mein Medizinstudium in München und diese Doktorarbeit nicht möglich gewesen. Danke auch dir, Verena, dass du als kleine Schwester immer, egal bei welchen Problemen, für mich da warst. Sarah, Dir danke ich in besonderem Maße für deine permanente fachliche und menschliche Unterstützung als hervorragende Wissenschaftlerin und Partnerin. Deine Hilfe und Zuversicht ermöglichten mir alle Höhen und Tiefen dieser Zeit erfolgreich zu bewältigen.

XII. Abbildungsverzeichnis

Abbildung 1: Angiogenese und Arteriogenese.....	12
Abbildung 2: Freisetzung von vWF.....	23
Abbildung 3: Der Kreislauf der Arteriogenese.....	24